COMPARISON OF CIRCADIAN GENE EXPRESSION AMONG DIFFERENT OSCILLATOR MODELS: IDENTIFICATION OF CRITICAL OUTPUT SIGNALS OF THE SCN PACEMAKER

A Dissertation

by

GUS JOHN MENGER III

Submitted to the Office of Graduate Studies of
Texas A&M University
in partial fulfillment of the requirements for the degree of

DOCTOR OF PHILOSOPHY

May 2007

Major Subject: Biology

COMPARISON OF CIRCADIAN GENE EXPRESSION AMONG DIFFERENT OSCILLATOR MODELS: IDENTIFICATION OF CRITICAL OUTPUT SIGNALS OF THE SCN PACEMAKER

A Dissertation

by

GUS JOHN MENGER III

Submitted to the Office of Graduate Studies of
Texas A&M University
in partial fulfillment of the requirements for the degree of

DOCTOR OF PHILOSOPHY

Approved by:

Chair of Committee,	David Earnest
Committee Members,	Vincent Cassone
	Susan Golden
	Rajesh Miranda
	Mark Zoran
Head of Department,	Vincent Cassone

May 2007

Major Subject: Biology

ABSTRACT

Comparison of Circadian Gene Expression among Different Oscillator Models:

Identification of Critical Output Signals of the SCN Pacemaker.

(May 2007)

Gus John Menger III, B.S., Southwest Texas State University

Chair of Advisory Committee: Dr. David Earnest

Diverse forms of life have evolved 24-hour or circadian timekeeping systems serving to coordinate internal biological events with the daily solar cycle. The generation of circadian rhythms by this timekeeping system ensures that internal processes occur at the appropriate time of day or night in relation to the environmental cycle and to other functionally-affiliated events. For mammals, endogenous oscillations in gene expression are a prevalent feature of oscillatory cells residing in the suprachiasmatic nucleus (SCN) and non-SCN tissues. To determine whether immortalized cells derived from the rat SCN (SCN2.2) retain the intrinsic rhythm-generating properties of the SCN, oscillatory behavior of the SCN2.2 transcriptome was analyzed and compared to that found in the rat SCN *in vivo*. In SCN2.2 cells, 116 unique genes and 46 ESTs or genes of unknown function exhibited circadian fluctuations for 2 cycles. Many (35%) of these rhythmically-regulated genes in SCN2.2 cells also exhibited circadian profiles of mRNA expression in the rat SCN *in vivo*. To screen for output signals that may distinguish oscillatory cells in the mammalian SCN from peripheral-type oscillators, the rhythmic behavior of the transcriptome in forskolin-stimulated NIH/3T3 fibroblasts was analyzed and compared relative to SCN2.2 cells *in vitro* and the rat SCN *in vivo*. Similar to the circadian profiling

of the SCN2.2 and rat SCN transcriptomes, NIH/3T3 fibroblasts exhibited rhythmic fluctuations in the expression of the core clock genes and 323 (2.6%) functionally diverse transcripts. Overlap in rhythmically expressed transcripts among these different oscillator models was limited to the clock genes and four genes that function in metabolism or transcription. Coupled with evidence for the rhythmic regulation of the inducible isoform of nitric oxide synthase (*Nos)* in SCN2.2 cells and the rat SCN but not in fibroblasts, studies examining the effects of antisense oligonucleotide-mediated inhibition of *Nos2* suggest that the gaseous neurotransmitter nitric oxide may play a key role in SCN pacemaker function. Thus, our comparative analysis of circadian gene expression in SCN and non-SCN cells has important implications in the selective analysis of circadian signals involved in the coupling of SCN oscillators and regulation of rhythmicity in downstream cells.

DEDICATION

The accomplishment of this dissertation is a milestone in my life. It is dedicated to my mother and father, Carol and Gus Menger, Jr. and my dear friends Ms. Ann Kinney and Mr. Mike Atkins.

ACKNOWLEDGEMENTS

Many people and organizations have contributed to this manuscript and my training as a graduate student at Texas A&M University. I thank God and Jesus Christ for providing me with the interest to explore the natural world and ask questions. I am thankful to my mother and father, Carol and Gus J. Menger, Jr., for their support and candor before and during my graduate training. My committee members have provided me with a treasure-trove of professional survival skills that will undoubtedly see me through my career. Drs. Susan Golden, Mark Zoran, Vincent Cassone, Rajesh Miranda, and David Earnest have trained my mind to explore the natural world and ask those questions in a manner that is efficient and productive. The Texas A&M University Department of Biology and Biological Clocks programs have engendered rigorous criteria for excellence and fostered a didactic program that has challenged and enhanced my thinking skills, planning skills, and my will to succeed. These organizations have made me a better person and helped me see my scientific endeavors to this milestone. I am thankful to Dr. David Earnest most of all in this regard. Dr. Earnest has had the patience and expertise to sculpt my interest in biology into a skill that has enhanced my outlook of life and my potential success in achieving goals within and outside scientific pursuits. The bulk of this manuscript reflects interpretations and explanations of technical analyses. Many people contributed to the technical workings of this thesis including Drs. Terry Thomas, Tom McKnight, Kim Lu, Phillip Beremand, and Andrew Tag of the Texas A&M Functional Genomics Core and Nichole Neuendorff, Elizabeth Qu, Sang Nahm, and Gregg Allen of the Earnest laboratory. Dr. Allen was, indeed, critical in

establishing much of the foundation for my investigations of the SCN oscillator cells and I look forward to collaborating with him and like minds in the future. Mr. David Reed of the Department of Biology Computing Services also deserves much gratitude in providing computer and software operating systems capable of handling the analytical demands of our microarray studies. Ms. Ann Kinney, for your encouragement and unyielding support of my research interests, I thank you. And, finally, I thank all who have contributed to this work, my training, and financial support not mentioned in this acknowledgement. Of course, I will look back a month, a year, and decades from now, God willing, and recognize so many people aided my success in life and my magnificent experience at Texas A&M University. This dissertation project was funded in part by National Institutes of Health Program Project Grant PO1 NS39546.

TABLE OF CONTENTS

TABLE OF CONTENTS (continued)

TABLE OF CONTENTS (continued)

LIST OF FIGURES

FIGURE Page

LIST OF TABLES

CHAPTER I

INTRODUCTION

OVERVIEW

A universal property of nature is that nothing is constant and most events occur in cycles. A preeminant example of this cyclicity is day and night. On Earth, diverse forms of life have evolved 24-hour or circadian (circa – around; dies – a day) timekeeping systems serving to coordinate internal biological events with the daily solar cycle. The generation of circadian rhythms by this timekeeping system ensures that internal processes occur at the appropriate time of day or night in relation to the environmental cycle and to other related events, both physiological and behavioral. Organisms, including cyanobacteria, fungi, plants, invertebrates, and vertebrates possess circadian timekeeping systems characterized by a common tertiary configuration – 1) input/entrainment pathways, 2) a core clockwork and 3) output pathways. While fundamental elements of the core clockwork have been identified across these diverse organisms, limited information is available on output pathways especially with regard to their functional roles in coordinating rhythmic processes in mammals (**17**). In fact, much remains to be understood about how this circadian timekeeping system communicates time within and among individual cells.

Circadian rhythms – a historical perspective. Some of the earliest circadian rhythms were observed in the movements of flowering plants. By using a kymograph to record the movements of plant leaves via a transducing actuator, Pfeffer (c.1910) first automated recordings of circadian rhythms of movement (**19**). Pfeffer's drum could be rolled

---

This dissertation follows the style of *Physiological Genomics*.

on a sheet of paper to produce a negative image of the actuator needle's tracings through the charcoal. Subsequent to these founding observations, a myriad of processes including behavior, metabolism, neuro-endocrine physiology, neuronal activity, cell division and numerous facets of gene expression (e.g., chromatin modification, mRNA abundance, translation and post-translational regulation) have been shown to exhibit circadian rhythms (**120**, **137, 44, 34, 76**, **63, 158, 96**, **20, 107**, **27**, **86, 132, 33, 163, 70**). These processes exemplify the broad and diverse activities regulated by the circadian timekeeping system and, at the same time, outline the progression to a modern synthesis in our understanding of circadian timekeeping – overt rhythms of physiology and behavior arise from circadian rhythms of gene expression.

Because of their tractability and high degree of fidelity in gauging circadian regulation, analyses of behavior, metabolism and gene expression are frequently employed as indices of circadian timekeeping in mammals (**120, 137, 86, 132, 33**). These processes can offer tangible measurements of circadian timekeeping. For instance, behavioral activity in rodents can be analyzed for several months by means of measuring parameters of wheel-running activity **(Fig. 1)**. Similarly, radioactively-labeled tracers such as 2-deoxyglucose can be used to gauge daily oscillations of metabolism in specific brain tissues and cell cultures. Furthermore, recent advances in technology, specifically the acceleration of mammalian genome sequencing and high-density lithography, have provided scientists with tools to simultaneously analyze the expression of many thousands of genes reproducibly. Thus, behavioral, metabolic, and gene expression processes are useful as indices of circadian timekeeping because these processes can be measured with accuracy and technical reproducibility. Although modern technological

advances have expanded the scope and accuracy of measuring these indices of circadian timekeeping, much of our understanding of mammalian timekeeping is still derived from examinations of the formal properties of the circadian rhythm itself.

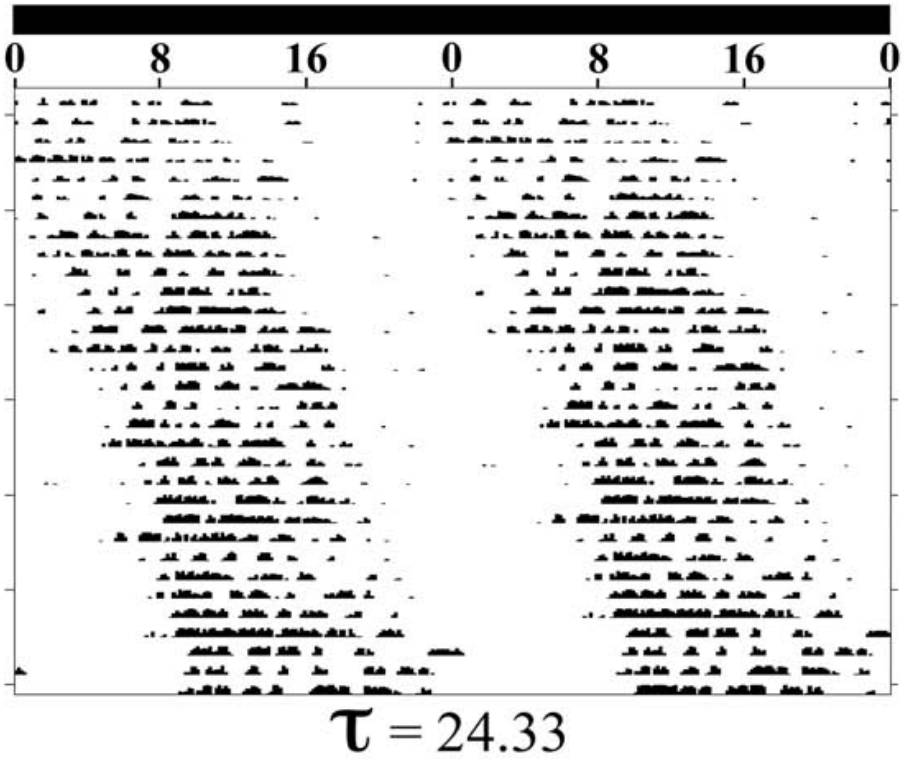

Fig. 1. Circadian wheel-running behavior in rodents. Representative circadian wheel-running activity in an individual Sprague-Dawley rat during exposure to constant darkness across 48 hours. Daily activity bouts are double plotted. The endogenous period of the animal's activity rhythm is 24.33 hours.

Formal properties of circadian rhythms. A cadre of formal properties serves as a benchmark in determining whether a biological oscillation is a bona fide circadian rhythm. By definition, a circadian rhythm must display a period of oscillation approximating a day and persists in the absence of environmental time cues (**57**). Because circadian rhythms oscillate independent of external time cues, the term *free-run* is used to describe the persistent nature of the rhythm (**17**). Entrainment to local environmental time is a second distinctive property of circadian timekeeping. This process provides for the temporal coordination of internal processes with external environmental cycles (**64)**. Generally speaking, entrainment of internal processes can be likened to the Disney icons Cinderella, Snow White and Pooh riding on the outer train at Disney World. The time it takes these entertainment, *and perhaps entrainment*, icons to completely travel around the park (*their period of travel*) is set by the velocity of the train. Now, let's say that Cinderella is riding in the front car, Snow White is in the middle car and Pooh rides in the end car. Because these icons ride in different cars, their positions on the train establish the order in which they will pass by Space Mountain. Cinderella will always pass Space Mountain first and Pooh last. Pooh will also be the last to see an approaching honeycomb. Thus, by boarding the train, the relative positions of Cinderella, Snow White, and Pooh are coordinated with the cycle of the Disney train. Similarly, through entrainment, the period of the circadian timekeeping system is consistently coordinated with the cycle of the external environment. This coordination permits different circadian oscillations to maintain their temporal relationships across the circadian cycle. Just as Cinderella, Snow White and Pooh, are held to their relative positions as they ride the Disney train.

In nature, light-dark cycles entrain circadian rhythms and maintain the temporal relationships among circadian rhythms. Photic signals derived from the light-dark cycle are the predominant *zeitgebers* (translated as "time givers" from German) capable of regulating the period and phase relationships of circadian rhythms (**124**). Every day circadian photoentrainment requires adjustments of circadian rhythms so that their endogenous periods equal the length of the entraining light/dark cycle. These adjustments are mediated through time-dependent phase shifts or discrete changes in the period of the circadian rhythm. The extent of these adjustments is equal to the difference between the circadian period and the length (usually 24 hours) of the entraining photoperiod. In addition to the regulation of the period of circadian rhythms, photoentrainment also entails phase control. Thus, through period and phase control, circadian photoentrainment insures that critical biological processes are coordinated with local environmental time so as to occur during appropriate phases of the light-dark cycle. For mammals, evidence of these features of circadian photoentrainment can be seen in the effects of light on circadian period [Compliance with Aschoff's rule (the circadian period of a nocturnal organism increases with light intensity)], in the effects of light pulses on the phase of circadian rhythms, and in the limits of light to entrain (**12, 124**).

A third feature of circadian timekeeping is that the period of a circadian rhythm is usually temperature compensated. Temperature compensation reflects a general independence of the endogenous circadian period (τ) in relation to changes in ambient temperature (**78**). The steadiness of the intrinsic circadian period (τ) across a range of temperatures is thought to stabilize the phase relations among circadian regulated processes, maintaining temporal precision among these processes. Pittendrigh (**1954**) first

demonstrated temperature compensation in *Drosophila* and this fundamental property has been borne out in numerous species (**123, 121, 38**). It is important to note that temperature compensation, like entrainment, has limits. Nonetheless, it is a beneficial and necessary property for faithful circadian timekeeping as the circadian period can remain true even when an organism encounters cold and warm environments.

The mammalian circadian system. Based on the formal properties of circadian regulation and previous research observations, the mammalian circadian timekeeping system is organized into components comprising input pathways, a master circadian clock, and output pathways **(Fig. 2)**. In mammals, the master clock responsible for coordinating circadian rhythms throughout the body resides in the suprachiasmatic nuclei (SCN) of the anterior hypothalamus, a region of the brain responsible for the regulation of many autonomic body functions (**69**). The SCN circadian clock contains many cell types some of which function as autonomous circadian oscillators called pacemaker cells. These pacemaker cells function with other SCN cells in integrating inputs, entraining to these inputs and transmitting outputs to collectively coordinate circadian rhythms elsewhere in the body (**17**). Photic signals, emanating from the retina, are integrated in a specific region of the SCN, the ventrolateral SCN. These signals are then transmitted to other regions of the SCN, through neuronal and diffusible factors, to facilitate synchrony between the cellular activities of the SCN and the progression of the daily solar cycle. Lastly, through neuronal and diffusible output pathways, SCN pacemaker cells coordinate the physiological and biochemical functions of other cells and tissues throughout the body with the environmental cycle or with other internal rhythms (**76**) **(Fig. 2)**. In summary, SCN pacemaker cells provide critical coordination of steady-state

circadian oscillations of cell function in target tissues. Yet, before SCN cells can coordinate circadian rhythms outside the brain, SCN cells must themselves be entrained.

Input/entrainment pathways. Detailed anatomical examination of the mammalian photoentrainment pathway has revealed mechanistic principles regarding how light governs entrainment of the SCN. Light stimulates irradiance-sensitive ganglion cells in the inner retina. These cells transmit photic signals to the SCN by means of the retinohypothalamic tract (RHT). Specifically, RHT fibers pass through the optic nerve and optic chiasm to form mono-synaptic connections with target cells within the ventrolateral SCN. Retinorecipient cells in the SCN then integrate and disseminate photic information to other cells in the SCN to facilitate entrainment of SCN pacemaker cells. These three basic components, the retina, retinohypothalamic tract (RHT), and retinorecipient cells residing within the ventrolateral region of the SCN, are essential for photoentrainment (**40, 65**) **(Fig. 2)**.

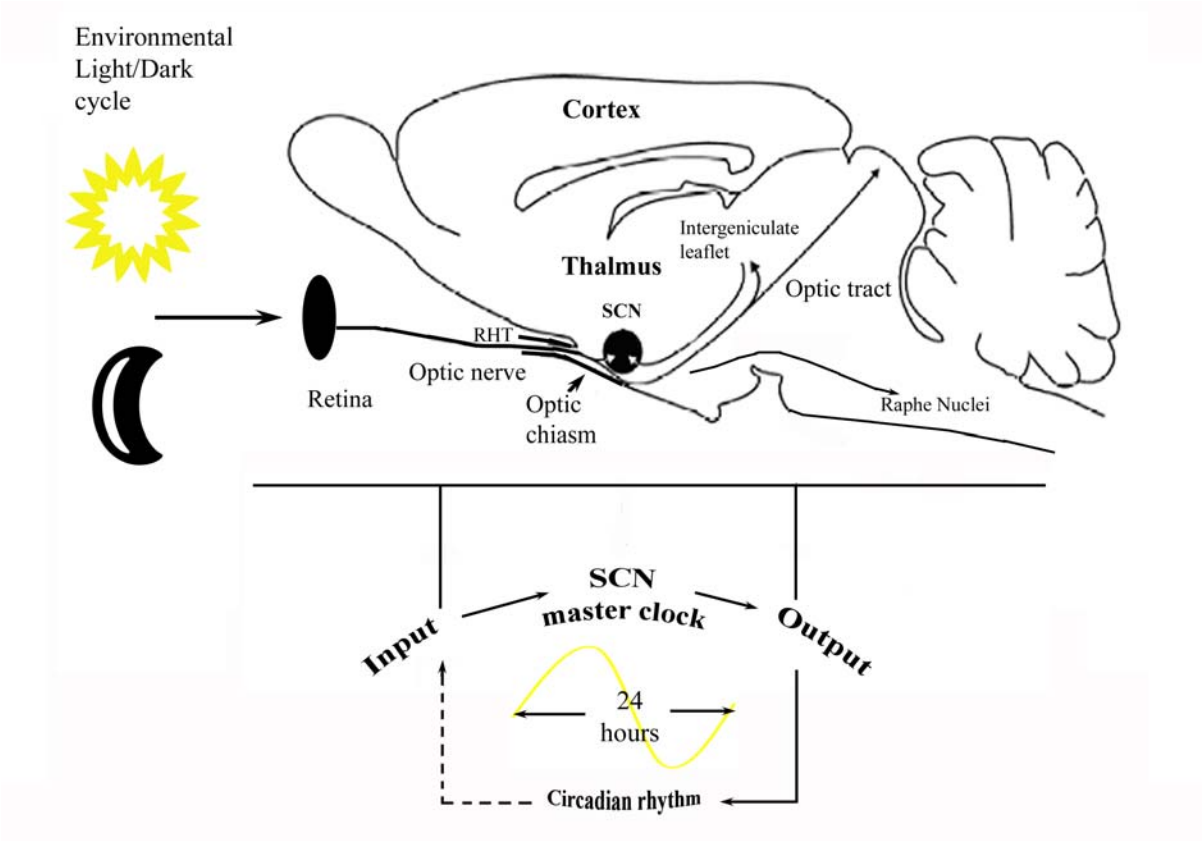

Fig. 2. The mammalian entrainment pathway and circadian timing system. The circadian locus in mammals resides in the suprachiasmatic nuclei (SCN) of the anterior hypothalamus. RHT fibers extending from the retina to the ventrolateral SCN function to transmit entraining signals to the SCN. Environmental signals are also transmitted to the intergeniculate leaflet in the thalamus. The intergeniculate leaflet and the Raphe nuclei indirectly modulate the entrainment of the SCN clock. Signals transmitting temporal information to the SCN clock mechanism function as inputs that synchronize the SCN clock with the external environment. Once entrained, the SCN transmits temporal information to other regions of the brain and body through output pathways. The SCN clock as well as many aspects of physiology affected by SCN outputs exhibit the formal properties of circadian rhythmicity. SCN output pathways, some of which are presumably rhythmically regulated, may feedback to modulate SCN activity. Rat brain drawing adapted from **van Esseveldt *et al*., 2000** (**152, used with permission**).

Retinal ganglion cells are critical. Recent studies support the role of type III ganglion cells as the primary retinal photoreceptors involved in mammalian circadian photoentrainment (**55**). These cells reside in the ganglion cell layer of the inner retina and are distinguished from other ganglion cells in that they are intrinsically light-sensitive and express melanopsin, a photoreceptive molecule similar to the opsins expressed in rod and cone cells (**55**). Primary evidence for the role of melanopsin in mammalian photoentrainment is derived from genetic lesion studies (**115, 134**). Genetic ablation of the melanopsin (*Opn4*) gene in mice significantly impairs their photoentrainment as melanopsin (*Opn4-/-*) mice exhibit a 40% attenuation in their phase shifting responses of circadian locomotor activity in response to light pulses. Because circadian photo-responsiveness is not completely abolished in melanopsin (Opn4)-deficient animals, redundant photoentrainment mechanisms likely exist (**134, 115**). This notion is further supported by two critical observations: 1) in rats, SCN neurons exhibit spectral sensitivities and firing patterns in compliance with the photoreceptive properties of rods and cones and 2) in mice lacking rods and most of their cones, SCN cells still exhibit the expression of the light-induced immediate early gene *c-fos*. (**3**).

The RHT. The RHT is a critical anatomical component in the mammalian timekeeping system. Transection of the RHT at the level of the ventrolateral SCN abolishes circadian photoentrainment (**65**). RHT fibers arise from the retina to innervate the rostral-to-caudal extent of the ventral SCN with the greatest density of contralateral neural connections occurring in the rostral third of the SCN (**1**). The monosynaptic projections of the RHT are thought to arise from melanopsin-containing retinal ganglion cells as transgenic animals expressing the marker gene LacZ in place of melanopsin show

LacZ expression in ganglion cell bodies and their afferent projections to retinorecipient cells in the SCN (**55**). Yet, it is speculated that these and other ganglion cells may project RHT fibers to other regions of the hypothalamus including the subparaventricular zone, preoptic, retrochiasmatic, and tuberal regions as well as the thalamic intergeniculate leaflet (**1, 66, 119**). An important indicator of RHT function is the expression of the immediate early gene *c-fos* in retinorecipient cells of the SCN (**71).** Several types of retinorecipient cells in the ventrolateral SCN express *c-fos* in response to brief light pulses (**22**, **35**).

RHT neurotransmitters. Glutamate and pituitary adenylate cyclase activating peptide (PACAP) are the primary neurotransmitters of the RHT that are responsible in communicating photic signals to SCN cells. Glutamate and PACAP co-localize in RHT fibers that terminate in the retinorecipient field of the SCN where SCN cells express receptors for glutamate (NMDA and AMPA) and PACAP (PAC1) (**52, 99, 41, 51**). Functional evidence for the role of these neurotransmitters in the RHT is supported by the observations that, similar to light, glutamate and PACAP elicit time-dependent phase shifts in circadian rhythms *in vivo* and *in vitro* (**97, 141, 50, 54a**). Furthermore, pharmacological inhibition of glutamate receptors attenuates light-induced expression of *c-fos* in the SCN; similarly, light-induced *c-fos* expression in PAC1-deficient mice is significantly blunted (**51**). Thus, multiple lines of evidence suggest glutamate and PACAP are critically important for light-induced phase shifting of the SCN clock.

Other neurotransmitters involved in mediating mammalian photoentrainment include the gaseous neurotransmitter nitric oxide and the neuromodulator 5-HT (serotonin). Pharmacological inhibition of nitric oxide synthase, the enzyme responsible

for the production of NO, blocks glutamate-mediated phase-resetting action of the SCN clock (**30, 157**). Serotonergic innervation arising from the raphe nuclei has also been shown to influence the communication of the photic signals within the SCN. Serotonin, is thought to play a role in photic regulation of the SCN clock because 5-HT agonists directly induce phase shifts or modulate the resetting action of light (**94a, 89, 126, 130**). Recently, Pickard and co-workers have shown that serotonin can act directly on presynaptic 5-HT_{1B} receptors on RHT fibers (**118**).

The Suprachiasmatic Nucleus. Primary evidence for the circadian clock function of the SCN is derived from seminal lesion studies demonstrating that complete destruction of the bilateral SCN abolishes circadian rhythmicity in several behaviors (**105, 146**). And, transplantation of fetal SCN tissue or immortalized SCN cells restores behavioral rhythmicity in SCN-lesioned hosts (**83, 129, 37, 142**). An interesting feature of SCN tissue is that SCN transplants can pace formal properties of host circadian rhythmicity to match those of the donor SCN (**129, 84**). This was definitively shown by transplanting SCN tissue derived from *Tau* mutant hamsters into wild type hosts such that the 20-hour period of homozygous (*tau/tau*) mutant hamsters was conveyed to host animals (**129**). Thus, the SCN can function as an autonomous timekeeper and as a pacemaker. These observations are intriguing as not all SCN cells are pacemaker cells.

Basic cellular properties of the SCN. Some cells within the SCN display the capacity to exhibit autonomous oscillations of cell function. This feature is resoundingly supported by the observations that individual SCN neurons can exhibit their own unique circadian cycles of electrical activity in the absence of synaptic inputs (**158, 61)**. Further support is derived from studies showing that SCN pacemaker cells exhibit intrinsic

circadian rhythms of cellular metabolism, neuropeptide secretion, and electrical activity that persist in the absence of external inputs *in situ* and *in vitro* (**34, 44, 110, 131, 137**). Interestingly, not all SCN cells exhibit self-sustained oscillations in their endogenous cell functions. Thus, examinations of the morphological, functional, and organizational properties of cells within the SCN will provide insight regarding how a consortium of oscillator and non-oscillator cells functions as a *whole* SCN to coordinate circadian rhythms throughout the body.

The SCN is a bi-laterally symmetrical tissue residing ventral to the third ventricle in the anterior hypothalamus. The mammalian SCN comprises 8,000 - 10,500 neurons, displays a volume of ≈ 0.1 cubic mm, and expresses approximately 25 different neuropeptides and neurochemicals (**69, 1**). At the cellular level, SCN neurons typically show soma characterized by invaginated, sometimes paired nuclei, 2-3 dendrites, and short thin axons in close apposition to other neurons (**69, 1**). Many of these neurons express one or more neuropeptides. Prominent examples of SCN neuropeptides include vasoactive intestinal peptide (VIP), arginine vasopressin (AVP), and gastrin-releasing hormone (GRP). Less prominent neuropeptides include somatostatin, neurotensin, angiotensin II, and galanin (**1**). The functional importance of the neuropeptide VIP in the rhythmic properties of the SCN has been demonstrated in animals deficient in the expression of the VIP receptor VPAC2. Genetic ablation of VPAC2 disrupts the intrinsic rhythms of the SCN and overt circadian rhythms of behavior (**28, 54**). Glial cells are also found throughout the SCN. An interesting observation is that astrocytes that express glial fibrilary acidic protein (GFAP) are predominantly found along side neurons expressing gastrin-releasing hormone in the ventrolateral SCN (**151a**). The importance of this glial

distribution is not known; however, Munekawa and co-workers (**2000**) suggest that in young rats, the developing RHT may promote the establishment of GFAP-containing astroglial cells in the ventrolateral subdivision of the SCN (**108**).

Current research findings indicate that the unique rhythm properties of the SCN are derived in part from its organization (**48**). Several lines of evidence indicate that the SCN is compartmentalized. Neuronal fibers arising from the retina pass through the retino-hypothalamic tract to innervate the ventrolateral region of the SCN. This region houses neurons rich in VIP and GRP and has been called the ventrolateral "core." This core subdivision of the SCN also receives fibers containing neuropeptide Y and 5-HT/serotonin, indicative of projections arising from the intergeniculate leaflet and raphe nuclei, respectively (**1**). In contrast to the SCN core, neurons in the dorsomedial region of the SCN are smaller, more densely packed, and exhibit strong AVP immunoreactivity (**106, 69).** This region has been called the SCN 'shell.' The ventrolateral core and shell subdivisions show distinct properties in the expression of genes, proteins, and rhythms of behavior. For example, in hamsters, a subnucleus of the SCN critically important in the maintenance of circadian behavioral rhythms has also been identified. This region shows the expression of the calcium-binding protein calbindin, a pattern of clock gene expression distinct from either the ventrolateral core or the dorsomedial shell, and is required for the transmission of circadian rhythms of behavior (**48, 161, 85**). Consequently, the organization of pacemaker cells as well as non-pacemaker cells within the SCN likely provide the SCN with its distinctive capacity to transmit temporal cues to other tissues and propagate rhythms of behavior.

Outputs from the SCN. Outputs from the SCN coordinate circadian rhythms of physiology throughout the body and propagate rhythms of behavior (**for review see 69**). These output signals are transmitted by neuronal connections and humoral factors **(Fig.s 2 and 3)**. Neuronal connections extend to both hypothalamic and extra-hypothalamic regions of the brain. Of the hypothalamus, the subparaventricular zone, the preoptic, supraoptic, and ventral medial nuclei are regions receiving SCN innervation (**1**). Extrahypothalamic regions innervated by SCN fibers are less clear because the small diameter of SCN axons makes their tracing difficult (**69, 1**). However, direct or indirect connections with the paraventricular nuclei, lateral septal nuclei, medial forebrain bundle, raphe nuclei, and superior cervical ganglion have been indicated. Furthermore, some subdivisions of the SCN show distinct neuronal projections to specific brain regions (**1**) **(Fig. 3)**. Recently, Abrahamson and Moore (2006) have shown that some of the brain regions targeted by SCN efferents including the subparaventricular zone (SPVZ), the dorsomedial nucleus (DMN), and the posterior hypothalamic area-tuberomammillary nucleus (PHA-TMN) are responsible for transmitting rhythmic waking behavior in rodents (**2**). However, humoral factors secreted from the SCN also function in conveying temporal information to extra-SCN cells in the brain and tissues throughout the body. This notion is supported by two important research observations derived from asking the question if neural connections arising from the SCN were even necessary in transmitting behavioral rhythmicity, i.e. **LeSauter et al., 1996 and Silver et al., 1996** (**84, 143)**. The former two studies demonstrated that transplanted micropunches of SCN tissue ('SCN islands') or SCN tissue encapsulated in a permeable bio-polymer could restore circadian rhythms of behavior in arrhythmic SCN-lesioned animals (**84, 143)**. While these studies

showed neuronal connections were not required for the maintenance of behavioral rhythms, non-neuronal or humoral factors sufficient for the maintenance of these rhythms remained unclear.

Some progress has been made in identifying humoral output signals secreted by the SCN. However, most of these signals show limited roles in propagating circadian rhythms of behavior. Transforming growth factor alpha (TGF-α) is secreted from the SCN and functions in light-mediated suppression of locomotor rhythms (**Weitz and co-workers, 73)**. While no obvious role has been found for TGF-α in transmitting behavioral rhythmicity in constant darkness, genetic ablation of the TGF-α receptor epidermal growth factor receptor (EGFR) does disrupt the precision the 24-hour locomotor rhythm and intracranial administration of TGF-α suppresses activity during the day (**73, 145**). A better understood SCN-specific humoral factor is Prokeneticin 2 (PK2). PK2 has been shown to be an output signal secreted by the SCN and it is necessary to propagate rhythms of behavior. Qualifying PK2 as a bona fide output is the observation that PK2 is not required for the SCN to exhibit intrinsic rhythms of endogenous cell function (**24)**. Prokineticins signal via orphan G-protein linked receptors that regulate calcium mobilization, phosphoinostitide turnover, and activation of MAP Kinase pathways (**24**). Furthermore, *Prokineticin 2*, like *Tgf-α* is rhythmically expressed in the SCN and its receptors are expressed in SCN target tissues (**24**). Thus, the secretory and rhythmic properties of potential SCN output signals can be used to identify candidate substances involved in communicating phase information to sites outside the SCN.

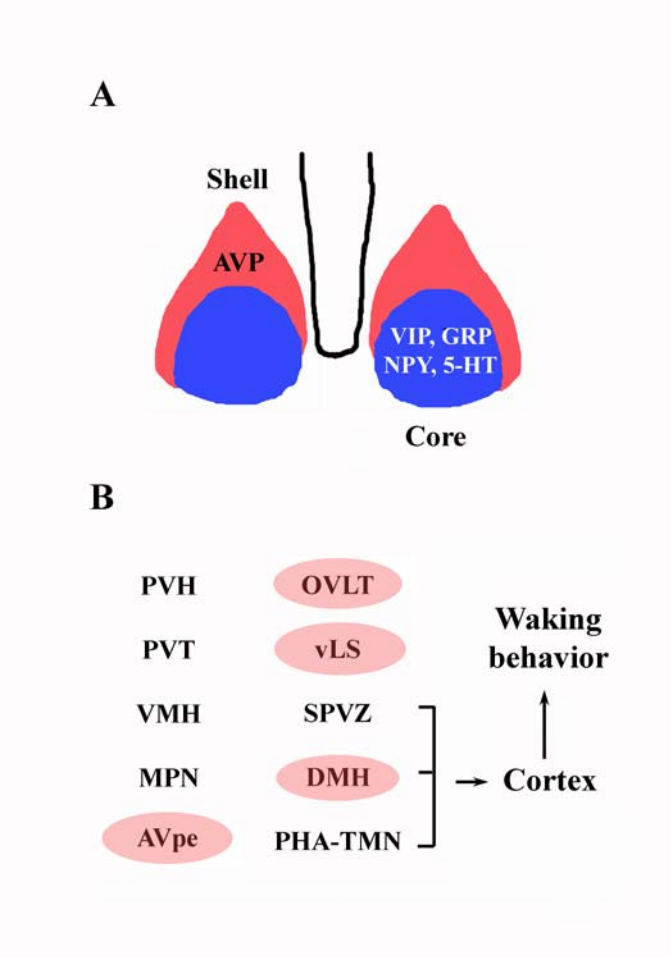

Fig. 3. Organization of the SCN and its prominent projections in the brain. Based upon histological and immunocytochemistry analyses of coronal SCN sections, the SCN exhibits regional distinctions in the morphology of neurons and in the expression of neuropeptides. Tightly packed neurons in the dorsomedial SCN "shell" express predominantly AVP whereas loosely–packed neurons in the ventrolateral "core" express mostly arginine vasopressin; VIP, vasoactive intestinal polypeptide; GRP, gastrin-releasing peptide; NPY, neuropeptide Y; and 5-HT, serotonin (**A**). Based on histological examinations of SCN efferents, the SCN extends projections to several hypothalamic regions and proximal zones including the PVH, paraventricular hypothalamic nucleus; PVT, paraventricular thalamic nucleus; VMH, ventromedial hypothalamic nucleus; MPN, medial preoptic nucleus; paraventricular thalamic nucleus; AVPe, anteroventral periventricular nucleus; OVLT, organum vasculosum lamina terminalis; vLS, ventral lateral septum; SPVZ, subparaventricular zone; DMH, dorsomedial hypothalamic nucleus; and PHA-TMN, posterior hypothalamic area-tuberomammillary nucleus. Acronyms shaded in red indicate projections that arise predominantly from the dorsomedial SCN. Recently, Abrahamson and Moore (**2006**) demonstrated that SCN efferents to the SPVZ regulate rhythms in rest-activity (waking) behavior via projections to the DMH and PHA-TMN, fibers known to extend to the brain cortex (**B**).

Molecular clockworks of the SCN. Recent genetic dissection of the SCN circadian clock has revealed that the molecular core of the timekeeping mechanism consists of mammalian orthologs of the *Drosophila* clock genes. Specifically, *Period1* (*Per1*), *Per*2, *Cryptochrome1* (*Cry1*), *Cry*2, and *Bmal1* (*Mop3*) have been implicated as core elements of the molecular clockworks responsible for the generation of mammalian circadian rhythms based on evidence indicating that mutation or knockout of these genes in mice alters or abolishes the circadian rhythm of activity (**163, 131, 132**). In mammals, these genes form interlocking transcription-translation feedback loops similar to those observed in fungal and fly circadian clocks **(163) (Fig. 4)**. BMAL1 and CLOCK are thought to form heterodimers and activate the transcription of the *Per* and *Cry* genes by binding to the E-box (CACGTG) domains on the promoters of these genes. In the cytoplasm, PER and CRY proteins accumulate, bind to each other as homo- or hetero-dimers, and translocate to the nucleus where they bind to BMAL1:CLOCK to negatively regulate their own transcription. The retinoic-related orphan nuclear receptor gene (ROR-alpha/ Rev-erb alpha) **(148, 113, 125)** is also thought to be involved in mediating the inhibitory effects of Cry and Per on the transcriptional activation of Bmal. The differential expression of core clock genes over the course of the circadian cycle is necessary for appropriately timed progression through the self-sustained feedback loops **(Fig. 4)**. In turn, the circadian clock mechanism coordinates downstream rhythmicity in the expression of other genes controlling diverse biochemical, cellular, and physiological processes within the SCN (**69**). These clock-controlled genes are not essential for normal circadian function, but some presumably couple the clock mechanism to SCN-specific output signals that regulate rhythmicity in other neural substrates or endocrine organs.

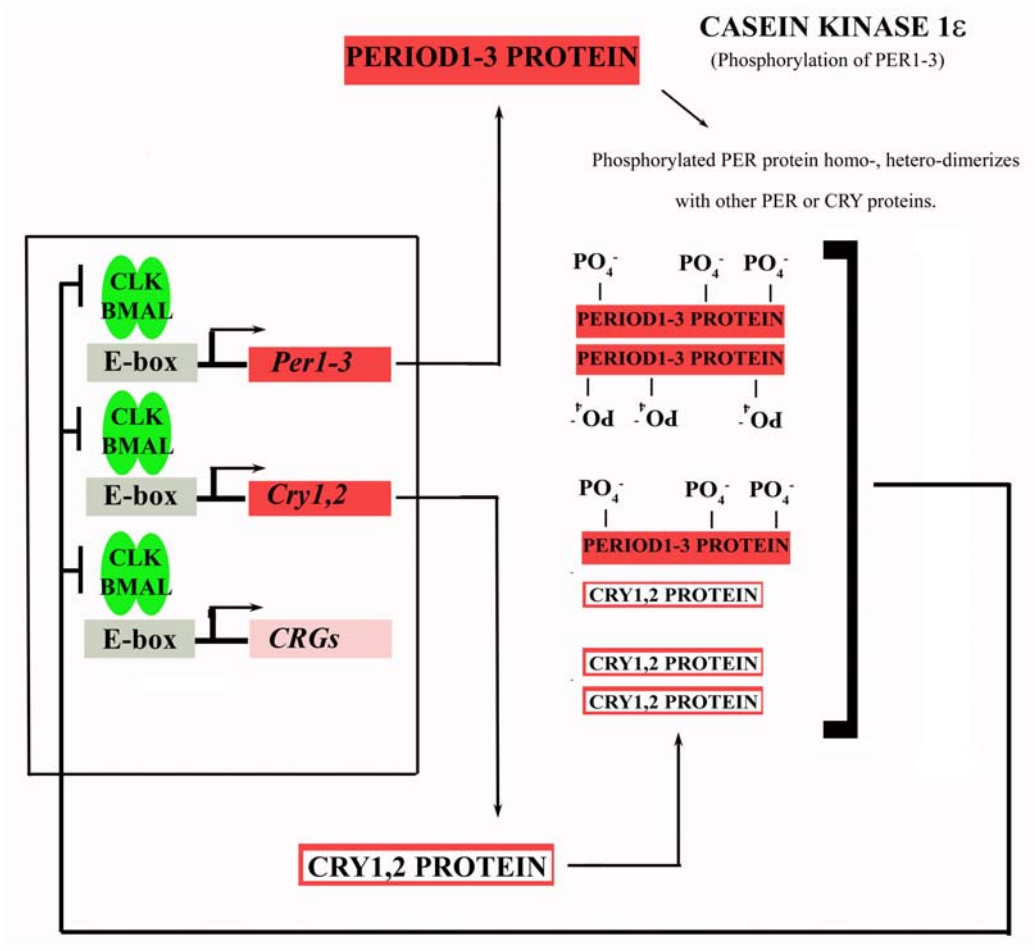

Fig. 4. Molecular clockworks in the SCN. PERIOD proteins, PER1-3, form either homo- or heterodimers with PER or with CRY1 or CRY2 that inhibit the expression of the *per* gene. These dimers enter the nucleus and inhibit the CLK/BMAL1 complex that normally stimulates *per* expression via E-box binding. CRYs can also inhibit *per* transcription without the presence of PER. PER and PER/CRY dimers have a similar negative effect on the expression on CRY and, perhaps, also on other clock-controlled genes (CCGs). Rev-erbα, not pictured, is thought to be a common target of the positive and negative components of the clock mechanism. Rev-erbαis thought to regulate the expression of *Bmal1* (**125**).

Peripheral oscillators. While previous dogma espoused that SCN cells are uniquely capable of generating endogenous molecular rhythms, recent studies demonstrate that many other tissues, e.g. heart, liver, and kidney, or cell lines show circadian oscillations of gene expression (**139, 164, 160, 147, 114, 67**). Studies using *in vitro* models have shown well-matched findings indicating that peripheral or non-SCN cells are also capable of expressing clock gene rhythms. Several fibroblast cell lines including rat-1 and NIH/3T3 fibroblasts show oscillating gene expression for 2-3 cycles when pulsed with a stimulus such as serum shock or forskolin. This molecular rhythmicity in peripheral tissues *in vivo* and in cultured fibroblasts is not restricted to core clock elements, but includes clock-controlled genes such as D-element binding protein (DBP) and Rev-erb α. Recently, circadian oscillations in the expression of the core-clock gene *Per2* have been observed in liver, lung, heart, and other tissues extracted from SCN-lesioned animals (**162**). These findings indicate that a common cellular program for circadian timekeeping is prevalent throughout the body and functional even in the absence of SCN, suggesting the notion that the circadian clockworks provide local time at the cellular level. Despite the similarity in the oscillatory nature of the core clockworks, peripheral oscillators and non-SCN cells do not exhibit functional properties equivalent to the SCN. SCN cells, not fibroblasts, restore circadian behavior when transplanted into arrhythmic SCN-lesioned hosts in vivo and also confer metabolic and molecular oscillations to co-cultured cells via the secretion of an unknown diffusible signal (**8, 10**). Collectively, these findings raise important questions regarding why the molecular clockworks found in SCN cells do not transmit similar pacemaker function to non-SCN cells.

Summary and critical questions. In mammals, the suprachiasmatic nuclei (SCN) of the anterior hypothalamus function as a master clock that regulates overt circadian rhythms throughout the organism (**69**). The SCN clock is also capable of producing self-sustained circadian oscillations in many of its intrinsic molecular and cellular activities. SCN cells are marked by circadian regulation of neuropeptide secretion, cellular metabolism, and electrical activity *in vivo* and *in vitro* (**43**). Although the SCN is vital to the function of the mammalian circadian system, the expression and rhythmic regulation of these core clock genes are not spatially confined to this neural locus. Circadian rhythms in gene expression are a common property of the pacemaker in the mammalian suprachiasmatic nucleus (SCN), oscillators in peripheral tissues, and stimulated fibroblasts *in vitro*. Despite this similarity in the circadian regulation of the canonical clockworks, only SCN cells are capable of functioning as a pacemaker that drives oscillations in co-cultured cells and restores behavioral rhythmicity when transplanted into SCN-lesioned hosts. These observations provoke three critical questions in the field of circadian timing: 1) How are SCN oscillators that comprise the master clockwork in mammals different from (and perhaps similar to) peripheral oscillators?; 2) If cells in peripheral tissues express all the core components of the SCN clockwork, why are peripheral oscillators incapable of generating self-sustained high-amplitude circadian rhythms of cell function and functioning as a pacemaker by communicating rhythmicity to other cells?; and 3) What output signals are used to synchronize multiple autonomous clock neurons in the SCN?

Rationale. Our current knowledge of the molecular organization of the mammalian circadian clockwork is lacking in an understanding of the molecular

substrates that provide the SCN with endogenous rhythms of gene expression and metabolism and the capacity to synchronize rhythms of gene expression in other cells outside the SCN. While peripheral oscillators and non-SCN cells do exhibit molecular oscillations of the canonical clock genes, these cells do not possess functional properties equivalent to the SCN. For instance, oscillations of clock gene expression can be induced via serum-shock in NIH/3T3 fibroblasts but these cells still lack the capacity to rhythmically metabolize glucose (**8, 10**). The most parsimonious explanation is that the SCN circadian clock produces output signals that are distinct from the outputs of peripheral circadian oscillators, albeit similar facets of circadian regulation are expected as the expression of core clock genes is wide spread throughout the body. To explore these issues, we have developed an immortalized line of rat SCN cells (SCN2.2) that retains the endogenous oscillatory and pacemaker properties of the SCN *in vitro* and *in vivo.* SCN2.2 cells are capable of intrinsically generating self-sustained rhythms of metabolism and clock gene expression, of imposing these oscillations on cocultured fibroblasts, and of restoring behavioral rhythmicity when transplanted into SCN-lesioned hosts (**36, 37, 8, 10**). In the absence of other neural and endocrine inputs, the SCN2.2 model may provide a unique opportunity to ultimately examine how the molecular clock imposes oscillatory properties on SCN cellular physiology and downstream oscillators (fibroblasts). In light of these observations, we hypothesize that 1) a major distinction between the circadian properties of SCN2.2 cells and the oscillatory behavior of stimulated fibroblasts is that fibroblasts may not express critical circadian pacemaker outputs found in SCN cells and 2) some of these SCN outputs may also function to synchronize SCN clock neurons.

This thesis describes experiments designed to identify 1) circadian genes – genes that show endogenous rhythmicity in their expression within the suprachiasmatic nucleus (SCN) and 2) pacemaker genes – candidate genes encoding outputs or intrinsic components of the SCN pacemaker.

Will global characterization reveal overlapping patterns of circadian-regulated gene expression in SCN2.2 cells and the rat SCN?

Specific Aim 1. Because SCN2.2 cells display circadian and pacemaker functions characteristic of the rat SCN, **we hypothesized that global characterization of gene expression in the rat SCN and SCN2.2 cells would reveal overlapping patterns of circadian gene regulation.**

Do forskolin-pulsed NIH/3T3 cells exhibit patterns of global gene expression unique to peripheral oscillators when compared to rat SCN and SCN2.2 pacemaker models?

Specific Aim 2. Because, peripheral oscillators lack pacemaker properties but display rhythms of clock gene expression, **we hypothesized that forskolin-pulsed NIH/3T3 cells would exhibit different patterns of clock-controlled gene expression relative to those found in the rat SCN and SCN2.2 cells.** We predicted that functional classifications would reveal some genes with circadian profiles in the rat SCN and SCN2.2 cells, but not NIH/3T3 cells, that may play a role in pacemaker output pathways, especially those genes involved in cellular communication.

Does perturbation of candidate gene expression in SCN2.2 cells alter the capacity of SCN2.2 cells to drive rhythms of clock gene expression and metabolism in NIH/3T3 cells?

Specific Aim 3. We hypothesized that the perturbation of candidate gene(s) identified in Specific Aims 1 and 2 would alter the capacity of SCN2.2 cells to drive rhythms of metabolism and gene expression in NIH/3T3 cells. We predicted that knock-down of a candidate gene will alter the capacity of SCN2.2 cells to convey rhythmic properties to co-cultured NIH/3T3 cells.

CHAPTER II

CIRCADIAN PROFILING OF THE TRANSCRIPTOME IN IMMORTALIZED RAT SCN CELLS*

INTRODUCTION

Many organisms, ranging from cyanobacteria to humans, have evolved circadian clock mechanisms that provide for the rhythmic organization of internal biological processes so as to approximate the 24-hour time course of the daily solar cycle (**45, 120**). In mammals, the master clock responsible for the regulation of circadian rhythms throughout the body is located in the suprachiasmatic nuclei (SCN) of the anterior hypothalamus (**69**). Complete lesions of the SCN abolish circadian rhythmicity in a wide array of molecular, biochemical, endocrine and behavioral processes (**104**) and transplantation of fetal SCN tissue restores behavioral rhythmicity in SCN-lesioned hosts (**129**). Consistent with the timekeeping function of the SCN, many of its cellular activities and functions oscillate independent of environmental or external input. Circadian rhythms of gene expression, cellular metabolism, neuropeptide secretion, and neural activity are intrinsic to the SCN *in vivo* and persist following isolation of SCN cells *in vitro* (**34, 44, 110, 131, 137**).

The SCN clock mechanism consists of interlocked transcription-translation feedback loops in which the gene products of core components rhythmically suppress their own transcription or the expression of other clock genes. *Clock*, *Period1* (*Per1*),

---

*Used with permission. **Menger GJ, Kim L, Thomas T, Cassone VM, and Earnest DJ.** Circadian profiling of the transcriptome in immortalized rat SCN cells. *Physiol Genomics* 21: 370-81, 2005.

*Per*2, *Cryptochrome1* (*Cry1*), *Cry*2, and *Bmal1* (*Mop3*) have been identified as core elements of the molecular clockworks in the SCN based on evidence indicating that mutation or knockout of these genes in mice alters or abolishes circadian behavior (**132**). In turn, these core elements of the molecular clockworks coordinate downstream rhythmicity in the expression of other genes controlling diverse biochemical, cellular and physiological processes within SCN cells. Some of these clock-controlled genes presumably couple the clock mechanism to SCN-specific output signals that regulate rhythmicity in other neural substrates or endocrine organs.

Despite our current understanding of the molecular organization of the mammalian circadian clock, important questions remain with regard to how the core clock mechanism regulates clock-controlled genes in SCN cells and how these genes are configured in biochemical pathways so as to generate SCN outputs that synchronize or coordinate rhythmicity in other cells and tissues. We used an immortalized line of rat SCN cells (SCN2.2) to explore these issues because these cells retain many of the circadian properties of the SCN *in vitro* and *in vivo*. SCN2.2 cells are capable of endogenous, self-sustained rhythmicity, and of functioning as a pacemaker by imposing rhythmic properties upon co-cultured cells and by restoring behavioral rhythmicity when transplanted into SCN-lesioned hosts (**8, 10 36, 37**). In the absence of other neural and endocrine inputs, the SCN2.2 model also provides an opportunity to ultimately examine how the molecular clock imposes oscillatory properties on SCN cellular physiology. Using Affymetrix GeneChips, the transcriptome in SCN2.2 cells collected at 6-hour intervals over two circadian cycles was profiled and then compared to the temporal

patterns of gene expression observed in the rat SCN. This profiling of rhythmic gene expression was used to determine: 1) whether global properties of the rat SCN transcriptome are conserved in SCN2.2 cells; 2) the extent to which the transcriptome is rhythmically regulated by the circadian clock in SCN2.2 cells; and 3) whether rhythmically-regulated genes in SCN2.2 cells show similar patterns of expression in the rat SCN. Bioinformatic tools were applied to characterize the functional distribution of clock-controlled genes in SCN2.2 cells and their configuration within metabolic and signaling pathways.

MATERIALS AND METHODS

***SCN2.2 cultures and RNA extraction*.** For each of three biological replicates, SCN2.2 cells (passages 15 and 16) were seeded on laminin-coated culture dishes (60mm; Corning, Corning, NY) and maintained at 37°C and 5% CO_2 in Minimum Essential Medium (MEM) supplemented with 20% FBS, 3000 µg/ml glucose and 292 µg/ml L-glutamine. At 48-hour intervals, the medium was changed and cultures were split at 1:3 or 1:4. Prior to experimental analysis, cultures were plated on multiple 6-well plates (35mm) coated with poly-D-lysine and laminin. At approximately 24 and 44 hours after plating, the culture medium was changed so as to respectively reduce the FBS concentration to 10% and then to 5%. To facilitate cell cycle and circadian clock synchronization across cultures, cells were subjected to medium replacement and exposed to serum-free medium (Neurobasal medium supplemented with 3000 ug/ml glucose, 292 ug/ml L-glutamine and 1X B-27 serum-free supplement) containing 15µM forskolin (Calbiochem, La Jolla, CA) for 2 hours. Cultures were rinsed and thereafter maintained in serum-free Neurobasal medium with supplements. At the conclusion of the

forskolin treatment, cells were harvested from individual 6-well plates (approximate density = 9.5 x 10^4 cells/cm^2) at 6-hour intervals for 48 hours and total cellular RNA was extracted using RNAeasy Midi-Kit protocols (Qiagen, Valencia, CA). RNA extracts from individual samples were treated with on-column DNase-I digestion and concentrated with sequential ethanol precipitations.

Rat SCN and RNA extractions. Adult male Long-Evans rats (175-200g; N=45) (Harlan Laboratories, Indianapolis, IN) were housed 2-3 per cage and maintained in the vivarium at the Texas A&M University System Health Science Center under a standard 12h light:12h dark photoperiod (LD 12:12; lights-on at 0600 hr). At 1800 hr (circadian time [CT] 12), animals were exposed to constant darkness (DD) and 12 hours later (0600 hr or CT 0), sacrificed under isoflurane anesthesia by decapitation at 6-hr intervals (N=5) for 48 hours using an infrared viewer. After the eyes were removed in the dark, SCN tissue was immediately dissected as described previously (**34**) under dim light, frozen in liquid nitrogen, and stored at –80^{0}C. SCN tissue from individual animals was separately homogenized in TRIzol reagent (Invitrogen, Carlsbad, CA) by aspiration through a 25-gauge needle and then extracted total cellular RNA for all 5 animals at each timepoint was pooled into a single sample. RNA samples were subjected to on-column treatment with DNAse-I to digest genomic DNA and then stored at –80°C.

Affymetrix GeneChip analysis. Prior to microarray analysis, the quality of all SCN2.2 and rat SCN RNA samples was assessed by electrophoresis on 1% agarose gels containing 0.1μg/ml ethidium bromide. Experimental procedures including double stranded cDNA synthesis and biotinylated cRNA preparation were conducted according to protocols described in the Affymetrix GeneChip Expression Analysis Technical

Manual (**82**). Briefly, first strand cDNA was reverse transcribed from 15μg of total RNA using 600U of SuperScript II Reverse Transcriptase (Invitrogen) in a 20μl total volume containing T7-(dT)24 primer, 10mM DTT, 500μM of each dNTP, and 1X first-strand cDNA buffer for 1 hour at 42°C. Second-strand cDNA was synthesized in 1X reaction buffer containing 200μM of each dNTP, 10U DNA ligase, 40U DNA polymerase I, and 2U of RNase H (final volume = 150μl) for 2 hours at 16°C. Samples were then treated with 20U of T4 DNA polymerase for 5 minutes at 16°C and incubated in 10μl of 0.5M EDTA. Double-stranded cDNA was purified with Phase Lock Gel Electrophoresis (Eppendorf Scientific, Inc., Westbury, NY) and phenol/chloroform extraction followed by ethanol precipitation. Biotin-labeled cRNA was subsequently produced using BioArray HighYield RNA Transcript Labeling Kit (Affymetrix, Inc., Santa Clara, CA). Labeled cRNA was spin-purified (Qiagen) and fragmented. To assure the quality of labeling and fragmentation efficiency, unfragmented and fragmented cRNA products were analyzed on an Agilent 2100 bioanalyzer prior to hybridization on arrays. Fragmented biotinylated cRNA (15μg) was hybridized on Affymetrix GeneChip rat U34A arrays at 45°C and 60rpm in a GeneChip Hybridization Oven 640 (Affymetrix, Inc.) for 16 hours.

Following hybridization, arrays were washed and stained using Affymetrix protocols for antibody amplification staining on a GeneChip Fluidics Station 400 in conjunction with Affymetrix Microarray Suit 5.0 software. After a brief wash with a non-stringent buffer, the stained signals on the array were then amplified with a solution containing 3μg/ml anti-streptavidin biotinylated antibody (Vector Laboratories, Burlingame, CA), 1X morpholine ethane sulfonic (MES) buffer, 2mg/ml acetylated BSA,

and 0.1mg/ml normal goat IgG for 10 min followed by a second staining with streptavidin phycoerythrin (SAPE) for 10 min at 25°C. After a final wash with a stringent buffer, the probe array was scanned at the excitation wavelength of 570 nm using an Agilent GeneArray Scanner (Palo Alto, CA).

After scanning, each image was first checked for major chip defects or abnormalities during hybridization as a quality control. Arrays were scanned using a global scaling strategy in which the average absolute signal intensity of all arrays was set to an arbitrary target signal intensity of 500 prior to uploading into GeneSpring 6.1 software (Silicon Genetics, Redwood City, CA).

Data processing and global analyses. GeneChip signal intensity data from three biological replicates of SCN2.2 cells and two technical replicates of the rat SCN derived from separate aliquots of pooled RNA samples were uploaded into GeneSpring 6.1 and filtered in an identical fashion. For each GeneChip probe set, signal intensities were converted to Log base 2 values and then normalized to the 50^{th} percentile of all measurements. Experimental averages of normalized data were calculated for each of 9 time points in SCN2.2 cells and for each of 8 time points in the rat SCN. The data were then sequentially filtered at three levels. To verify gene expression, we filtered the probe sets according to two criteria: 1) detection of a "Present" flag in 55% or more of the time points and 2) a raw signal intensity value of ≥50 which was above the average experimental background signal in 55% or more of the time points. In both SCN2.2 cells and the rat SCN, the temporal profiles of genes surpassing these expression criteria were filtered to isolate those showing stable expression. Stable genes were distinguished by temporal expression profiles that did not differ statistically (Standard correlation value:

p>0.995) from a flat line created with the GeneSpring 6.1"Draw Gene" tool. Finally, cycling genes with a peak-to-trough difference of 1.5-fold or greater and periodicities of 18-30 hours were identified among the remaining transcripts using methods similar to those described previously (**26, 93**). The normalized data were cross-correlated (p>0.90) with cosine waves of specific phase and period using the PRISM software package (GraphPad, San Diego). For SCN2.2 cells, we imposed an additional requirement that circadian-regulated transcripts show at least one pair of non-overlapping standard errors bars between time points with the highest and lowest values. The analytical and amplitude criteria used to identify cycling transcripts in both SCN2.2 cells and the rat SCN are consistent with those applied in recent microarray studies profiling circadian gene expression (**2, 13, 43, 65**). Because our filtering parameters excluded some transcripts that were readily detectable in our and/or other analyses of the rat SCN, we re-analyzed the normalized data using secondary expression criteria that identified genes with a raw signal intensity of ≥50 which was above the average experimental background signal in at least four of the time points in SCN2.2 cells and three or more of the time points in the rat SCN. Microarray data have been deposited in the National Center for Biotechnology Information's (NCBI) Gene Expression Omnibus (GEO) database (Accession Numbers GSE1654 and GSE1673).

Bioinformatics and validation. Because some genes surpassing circadian expression filters were represented by multiple probes on the RG-U34A GeneChip, we used GeneSpring 6.1, GenMAPP 1.0 & 2.0 freeware (**29, 31**) and bioinformatic tools available as links from the National Center for Biotechnology Information (NCBI) (**109, 127**), including Basic Alignment Search Tool (BLAST) (**11**), to identify unique genes

with rhythmic patterns in SCN2.2 cells. To corroborate rhythmicity in SCN2.2 cells, cycling genes were compared with those found in the rat SCN. For a limited set of clock and clock-controlled genes, quantitative PCR (qt-PCR) was also used to validate rhythmic expression in SCN2.2 cells. *Per2*, *Bmal1*, *Nos2*, and the calcium channel subunit *α1C* are primary examples of cycling genes that were validated by qt-PCR. Quantification of relative mRNA abundance was performed using TaqMan or SYBR-Green real-time PCR technology (Applied Biosystems, Inc. [ABI], Foster City, CA). To generate single-strand cDNAs, total cellular RNA (1-2μg) was reverse transcribed using Superscript II (Invitrogen) and a primer mixture of oligo-dTs and random hexamers. Using the cDNA equivalent of 50ng of total RNA, triplicate aliquots of each sample were then PCR amplified in an ABI PRISM 7700 sequence detection system (**56**). The following probes and primers were designed using PrimerExpress software (ABI):

rPer2 forward: 5'-TTCGACTACCTGCATCCAAAAG-3'

rPer2 reverse: 5'-AAGTCCAGTCTTCGCATCGAT-3'

rBmal1 forward: 5'-CCAAGAAAGTATGGACACAGAC-3'

rBmal1 reverse: 5'-GCATTTTTGATCCTTCCTTGGT-3'

rCry1 forward: 5'-CTGGCGTGGAAGTCATCGT-3'

rCry1 reverse: 5'-CTGTCCGCCATTGAGTTCTATG-3'

Id-1 forward: 5'-TGGTCTGTCGGAGCAAAGC-3'

Id-1 reverse: 5'-TCCTTGAGGCGTGAGTAGCA-3'

Nos2 forward: 5'- ACCCGACTGAAGCACTTTGG-3'

Nos2 reverse: 5'-TCGTTGGGAGTGGACGAAG-3'

α1C (*Rob2*) forward: 5'-CCGGAAGCCAGTGCATTTT-3'

α1C (*Rob2*) reverse: 5'-TGGTGAAGATCGTGTCATTGAC-3'

α1C (*Rob2*) probe: 5'-FAM-CCAAACAACAGGTTCCGCCTGCAGT-TAMRA-3'

α1A forward: 5'-GGATGACAACACCGTTCACTTC-3'

α1A reverse: 5'- CCACCCTTTGCGATTTTGAT-3'

α1A probe: 5'-FAM-TGGCTCTGATCCGAACCGCCC-TAMRA-3'

α1G forward: 5'-CCTGCCTGTTGCCGAGAG-3'

α1G reverse: 5'-CAGGAGACGAAACCTTGACTGA-3'

α1G probe: 5'-FAM-CGGCCTATATCTTTCCTC-TAMRA-3'

CypA forward: 5'-TGTGCCAGGGTGGTGACTT-3'

CypA reverse: 5'-TCAAATTTCTCTCCGTAGATGGACTT-3'

To control for differences in sample RNA content, 18S ribosomal RNA (rRNA) was amplified and multiplexed in the same reaction with target genes or amplified in separate cDNA aliquots (50ng) from the same RNA samples using the Ribosomal RNA Control Reagent Kit (VIC Probe, ABI). For normalization of the clock genes, *Per2*, *Bmal1*, and *Cry1*, rRNA or cyclophilin A (*CypA*) mRNA was amplified using the cDNA equivalent of 1ng total RNA. In both multiplex and conventional reactions, the relative mRNA abundance for a given target gene was calculated by normalization to corresponding rRNA or cyclophilin levels in each sample using the comparative C_T method described in the ABI Prism 7700 Sequence Detection System User Bulletin #2 (PE-ABI). Values for the same target gene (amplicon) were adjusted for inter-assay variation according to ABI protocols. Relative abundance of target mRNA was represented as a percentage of the maximal value obtained within an individual experiment.

RESULTS AND DISCUSSION

Global properties. We separately examined temporal regulation of the transcriptome in SCN2.2 cells and in the rat SCN so as to compare global and specific facets of gene expression between these two experimental models. The breadth of gene expression was similar in SCN2.2 cells and the rat SCN. In SCN2.2 cells, 3993 out of the 8,800 probes sets on the rat U34A GeneChip. For mRNA from the rat SCN 2929 probe sets surpassed stringent expression criteria (**Table 1**). Comparison of probe sets detected in both models with those in only the rat SCN indicates that SCN2.2 cells express 83% of the genes detected in the rat SCN (2430 out of 2929). The similarity in the extent and level of common gene expression across these experimental models suggests that SCN2.2 cells retain SCN-like properties with regard to the regulation of genomic activity and the functionality of *in vivo* cellular pathways. In addition, a wide array of genes was regulated in a similar fashion in SCN2.2 cells and the rat SCN. Many of the genes common to both models shared analogous patterns of stable or variable expression. *Cyclin D3*, brain-specific protein gene *Rb109*, and thioredoxin (*Txn2*) represent functionally diverse genes with stable expression in both models (**Fig. 5A and 5B**). Prominent examples of genes with variable expression in SCN2.2 cells and the rat SCN include nerve growth induced factor-A (*Ngfi-A*), metallothionein (*Mt1a*) and ubiquitin carboxyl-terminal hydrolase I (*Uchl1*). For many of these genes, relative levels of mRNA abundance were also comparable between these models.

Global circadian regulation. Recent studies profiling the transcriptome in the murine SCN have identified ≈100-365 circadian-regulated genes that mediate a wide

range of cellular functions (**114, 149**). In the present study, a comparable number of genes in SCN2.2 cells were distinguished by circadian profiles. Specifically, 162 genes in SCN2.2 cells showed circadian rhythms of mRNA abundance that surpassed stringent expression criteria (**Table 1**). The amplitude of these SCN2.2 rhythms in gene expression ranged from 1.5 to 12-fold differences between peak and minimum levels of mRNA abundance. By comparison, 301 genes in the rat SCN displayed circadian oscillations that were identified using the same expression and rhythm criteria. Because 35% of the unique genes with rhythmic patterns in SCN2.2 cells surpassing stringent expression criteria exhibited similar oscillations in the rat SCN, some of these genes may be critical for the circadian clock and pacemaker properties of SCN cells. To screen additional genes in SCN2.2 cells with rhythmic profiles that passed secondary expression criteria (**Table A.1, APPENDIX**), we used three different approaches: 1) validation of rhythmicity for a limited set of these genes using qt-PCR, 2) comparative analysis to determine whether these genes were both expressed based on stringent criteria and rhythmically-controlled in the rat SCN, and 3) establishment of a limited homology table between the rat U34A and mouse U74A (version 2) GeneChips using GeneSpring 6.1 (**Table 2**). Some of the rhythmic genes validated by qt-PCR in this supplementary screening analysis include inducible nitric oxide synthase *(iNos* or *Nos2*), calcium channel *Rob2*, and *Per2* (**Fig. 6 and 8**). Our homology screen identified 50 homologs or functionally-related genes that were rhythmically expressed in murine tissues and SCN2.2 cells. Circadian-regulated genes that were identified in SCN2.2 cells and in the murine SCN include pericentriolar material 1 (*Pcm1*), *DNA directed RNA polymerase II*,

the putative chloride channel *Clcn4-2*, *Id3a*, *Hsp 70 protein 5* (*Hspa5*) and *Snap25* (**Table 2; Fig. 7**). An interesting facet of our homology screen is that some genes with

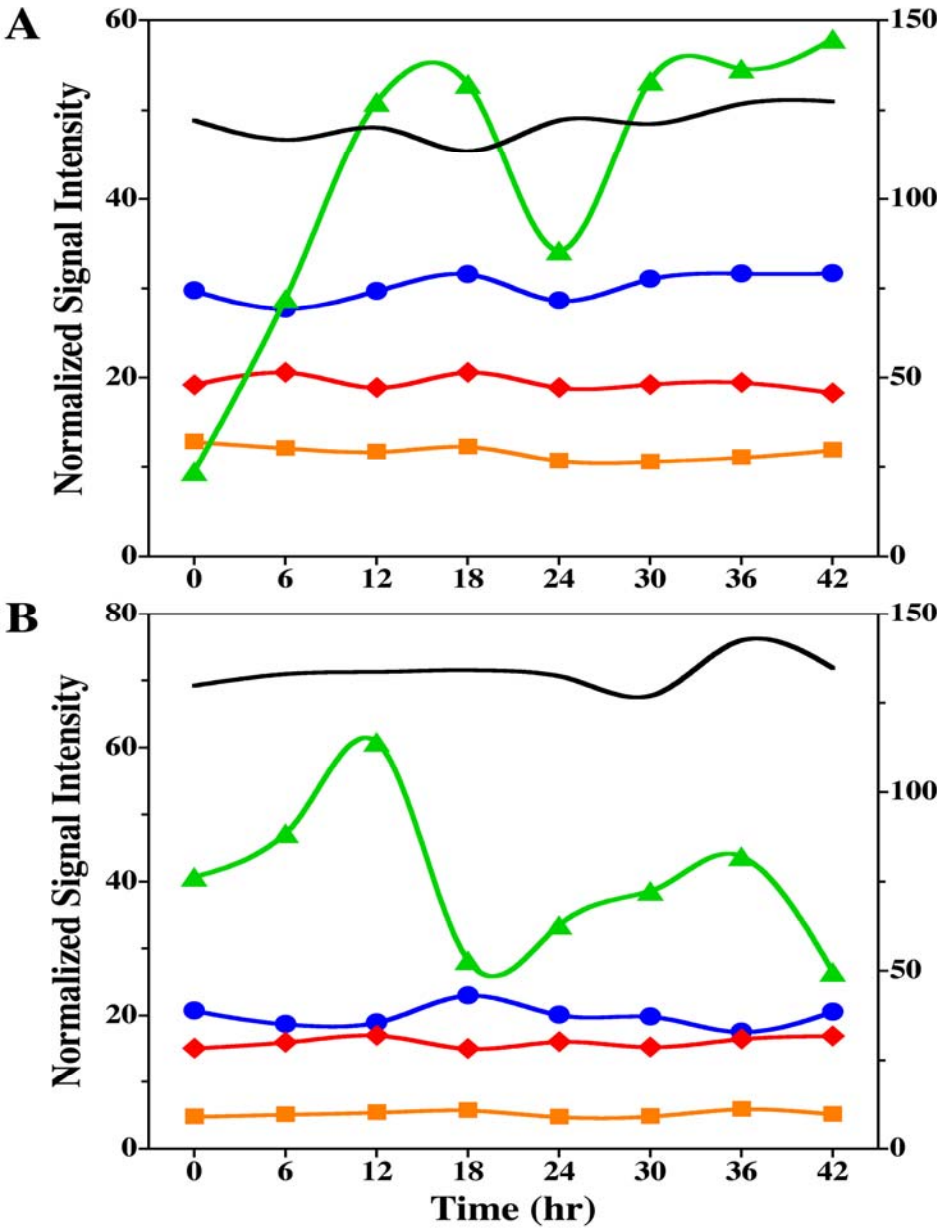

Fig. 5. Temporal profiles of representative genes that are stably or variably expressed in both SCN2.2 cells (**A**) and the rat SCN (**B**). Symbols denote determinations of mRNA abundance (n= 3) at 6-hour intervals for *Cyclin D3* (■), *Rb 109* (●), *Txn2* (♦) and *Ngfi-A* (▲). In this and subsequent figures, these values were derived by normalizing GeneChip Log base 2 signal intensity to the 50th percentile of all measurements per sample. The raw values for the 50th percentile of all measurements per sample are plotted as a black line in relation to the secondary ordinant in each panel. Thus, the normalized values between 3 and 60 for these genes indicate that their raw values were approximately 3- to 60-fold greater than those for the 50th percentile.

Table 1. *Comparison of gene expression and function in SCN2.2 cells and the rat SCN.*

A. ***Global facets of gene expression/regulation***

	SCN2.2 cells	Rat SCN	Common to both models
Expressed according to stringent criteria	**3993**	**2929**	**2430**
Stable genes fulfilling stringent expression criteria	**1035**	**584**	**185**
Rhythmic genes fulfilling stringent expression criteria	**162**	**301**	**57**
Percentage of examined genes with rhythmic profiles	**1.82%**	**3.38%**	**0.64%**

B. ***Functional Categorization of Rhythmic Genes***

	SCN2.2 cells	Rat SCN	Common to both models
Category 1 - Energetics	**24 (15%)**	**34 (11%)**	**13 (54%)**
Category 2 - Cellular and Systems-level Communications	**49 (30%)**	**64 (21%)**	**16 (33%)**
Category 3 - Protein Dynamics	**20 (12%)**	**28 (9%)**	**5 (25%)**
Category 4 - Cellular Development	**13 (8%)**	**17 (6%)**	**5 (38%)**
Category 5 - Defense and Detoxification	**5 (3%)**	**10 (3%)**	**0**
Category 6 - Cytoskeletal and Adhesion	**5 (3%)**	**10 (3%)**	**0**
Category 7 - Unknown or ESTs	**46 (28%)**	**138 (46%)**	**18 (39%)**

Comparison of gene expression and function in SCN2.2 cells and the rat SCN. (**A**) Global facets of gene expression/regulation are compared with regard to the number of transcripts that surpassed stringent expression criteria and whether these genes exhibited stable or rhythmic expression in SCN2.2 cells, the rat SCN, or both experimental models. For each comparison, the proportion of rhythmic genes relative to the total number of genes/probe sets on the GeneChip (8900) is also listed. (**B**) Rhythmic genes were subdivided into seven basic functional categories: 1) **Energetics**, 2) **Cellular and Systems-level Communication**, 3) **Protein Dynamics**, 4) **Cellular Development**, 5) **Defense and Detoxification**, 6) **Cytoskeleton and Adhesion** and 7) **Unknown or ESTs**. In each category, the number of cycling transcripts (and proportion relative to the total number of rhythmic genes) is compared between SCN2.2 cells, the rat SCN and both experimental models.

Table 2. *Functionally-related genes with rhythmic profiles in SCN2.2 cells and murine SCN and/or liver*

A. *Rhythmic genes that surpass stringent expression criteria in SCN2.2 cells*

GenBank ID	Locus Link ID	Description / Symbol
AA799672	117042	Ribosomal protein L6 (*Rpl6*)
J01435	26196	ATP synthase 8, mitochondrial (*mt-Atp8*)
AI171506	24552	Malic enzyme 1 (*Me1*)
L20821	81803	Syntaxin 4 (*Stx4a*)
AF035822	116500	Synaptosomal-associated protein, 29kD (*Snap29*)
U35245	64060	Vacuolar protein sorting homolog (*Vps33b*)
D43623	25756	Carnitine palmitoyltransferase 1b (*Cpt1b*)
AA892799	LOC298085	Similar to glyoxylate reductase/hydroxypyruvate reductase
AI177004	29637	Hmgc synthase 1 (*Hmgcs1*)
J02585	246074	Stearoyl-Coenzyme A desaturase 1 (*Scd1*)
L10152	25648	Solute carrier family 7, member 1 (*Slc7a1*)
D89983 and AI043631	58961	Ornithine decarboxylase antizyme inhibitor (*Oazi*)
X03347	LOC314174	P75 gag-fos fusion protein / similar to ubiquitin-like protein
L16764	294254	Heat shock protein 70 1b (*Hsp701b*/*Hspa1b*)
M30581	25391	ATPase, Ca++ transporting, ubiquitous (*Atp2a3*)
U38376	24653	Cytosolic phospholipase A2 (*Pla2g4a*)
S55427	24660	Peripheral myelin protein 22 (*Pmp22*) / growth-arrest-specific Gas-3 homolog
S63521	25617	Heat shock 70kD protein 5 (*Hspa5*)
AI236601	LOC288444	Similar to Heat shock protein (*Hsp105*)
AA891669	79434	Ras oncogene family (*Rab11b*)
U20796	259241	Nuclear receptor subfamily 1, group D, member 2 (*Nr1d2*)
L27843	29463	Nuclear protein tyrosine phosphatase (*Ptp4a1*)
U95920	81740	Pericentriolar material (*Pcm1*)
AF000942 and AI171268	25585	Inhibitor of DNA-binding 3 (*Id3*)

Table 2 continued

B. *Rhythmic genes that surpass secondary expression criteria in SCN2.2 cells*

GenBank ID	Locus Link ID	Gene descriptor
AA684929	NF	Similar to NADH-ubiquinone oxidoreductase
AB003991	25012	Synaptosomal-associated protein (*Snap25*)
AA818499	298423	Cytochrome P-450, 4a3 (*Cyp4a3*) / lauric acid omega-hydroxylase
AA818403	LOC299564	Similar to cytochrome P450 4F5 (*Cyp4f5*)
AF035156	117182	Hydroxysteroid 17-beta dehydrogenase 3 (*Dhb3*)
AA892512	LOC306750	Similar to LECT2
S79214	25681	Procollagen type X (*Col10a1*)
X74835	54240	Cholinergic receptor, nicotinic, delta polypeptide (*Chrnd*)
E12742	LOC305384 / 12425	Similar to cholecystokinin-A receptor OR cholecystokinin A receptor (Cckar)
L00111	24241	Calcitonin / calcitonin-related polypeptide, alpha (*Calca*)
X59608	Close to LOC287438	Similar to DNA directed RNA polymerase II subunit
Z36944	60586	Putative chloride channel (similar to Mm *Clcn4-2*)
NM_011504	114095	Stxbp3 syntaxin binding protein 3 Mm.12155 0.040 9.28 10
NM_025898	LOC366216	1500039N14Rik RIKEN cDNA/similar to *SNAP*-beta
2610317A05	unknown	2610317A05Rik RIKEN cDNA
2810009D21	unknown	2810009D21Rik RIKEN cDNA
1190017B18	unknown	1190017B18Rik RIKEN cDNA
C77032	unknown	C77032 EST none Mm.28726 0.069 11.79 10
NM_008838	unknown	Phosphatidylinositol glycan, class F (*Pigf*)
NM_025933	LOC290999	Similar to 2010110M21Rik RIKEN cDNA
XM_138272 / XP_138272	LOC366733	Similar to *RAP2A*

Circadian-regulated genes in SCN2.2 cells that show homology to rhythmic genes reported in the murine SCN and/or liver. Listed are the GenBank and Locus Link ID for rhythmic genes in SCN2.2 cells that surpassed stringent (top) or secondary (bottom) expression criteria and were circadian-regulated in the murine SCN and/or liver. Some murine homologs have not been identified in the rat GenBank or Locus Link databases and thus are specified as unknown.

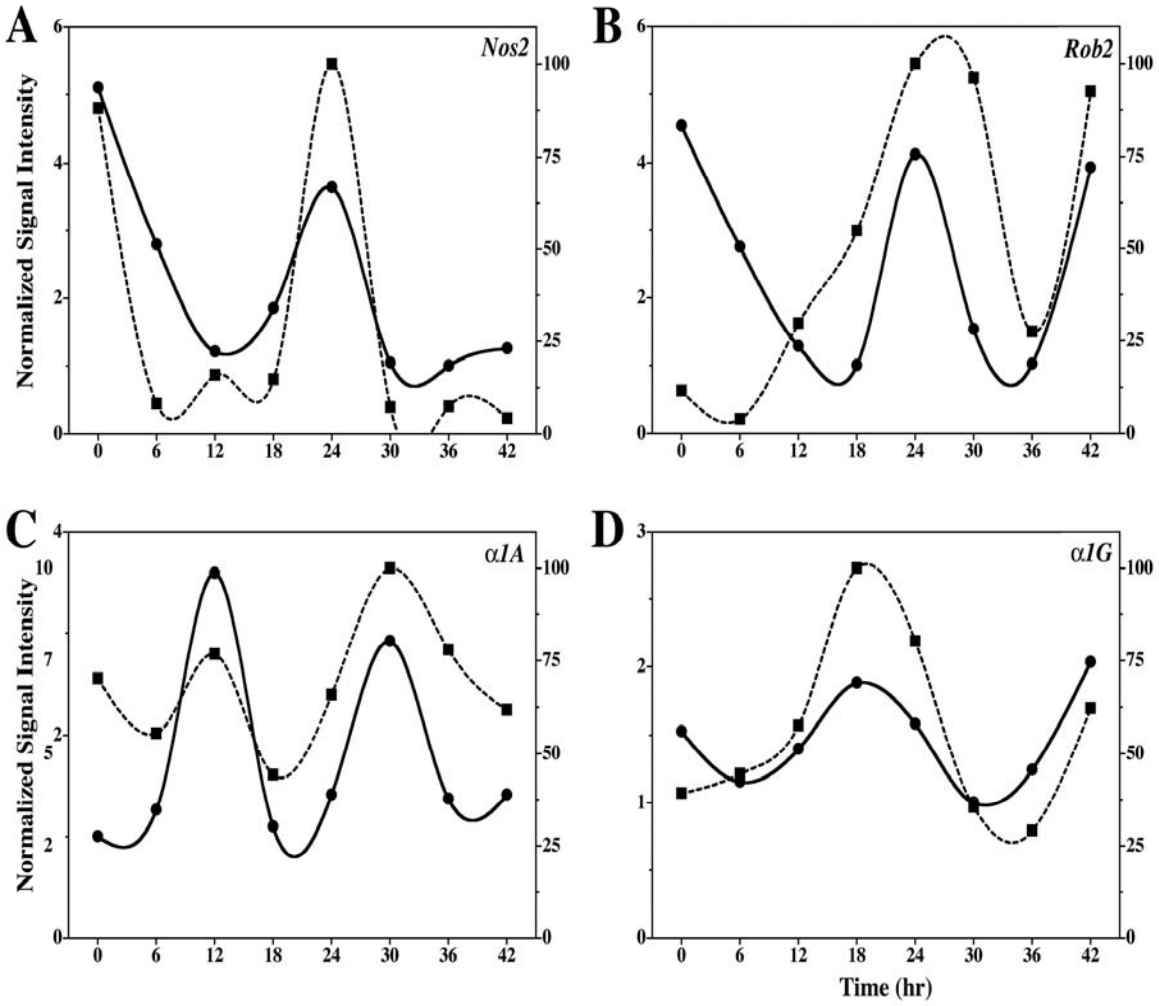

Fig. 6. Validation of GeneChip analysis examining circadian gene expression in SCN2.2 cells. GeneChip (●, solid line) and qt-PCR (■**,** dashed line) determinations of relative mRNA abundance at 6-hour intervals are compared for (**A**) inducible nitric oxide synthase (*iNos* or *Nos2*), (**B**) *Rob2* calcium channel *α1C* subunit, (**C**) calcium channel *α1A*, and (**D**) calcium channel *α1G*. For GeneChip analysis, determinations of relative mRNA were derived by normalizing values for Log base 2 signal intensity to the 50th percentile of all measurements per sample. For qt-PCR analysis, the plotted values correspond to the ratios of *iNos* or *Nos2*, *Rob2*, calcium channel *α1A* or calcium channel *α1G*/rRNA mRNA signal in which the maximal value for each experiment was set at 100%. GeneChip and qt-PCR values are respectively represented on the primary and secondary ordinant in each panel.

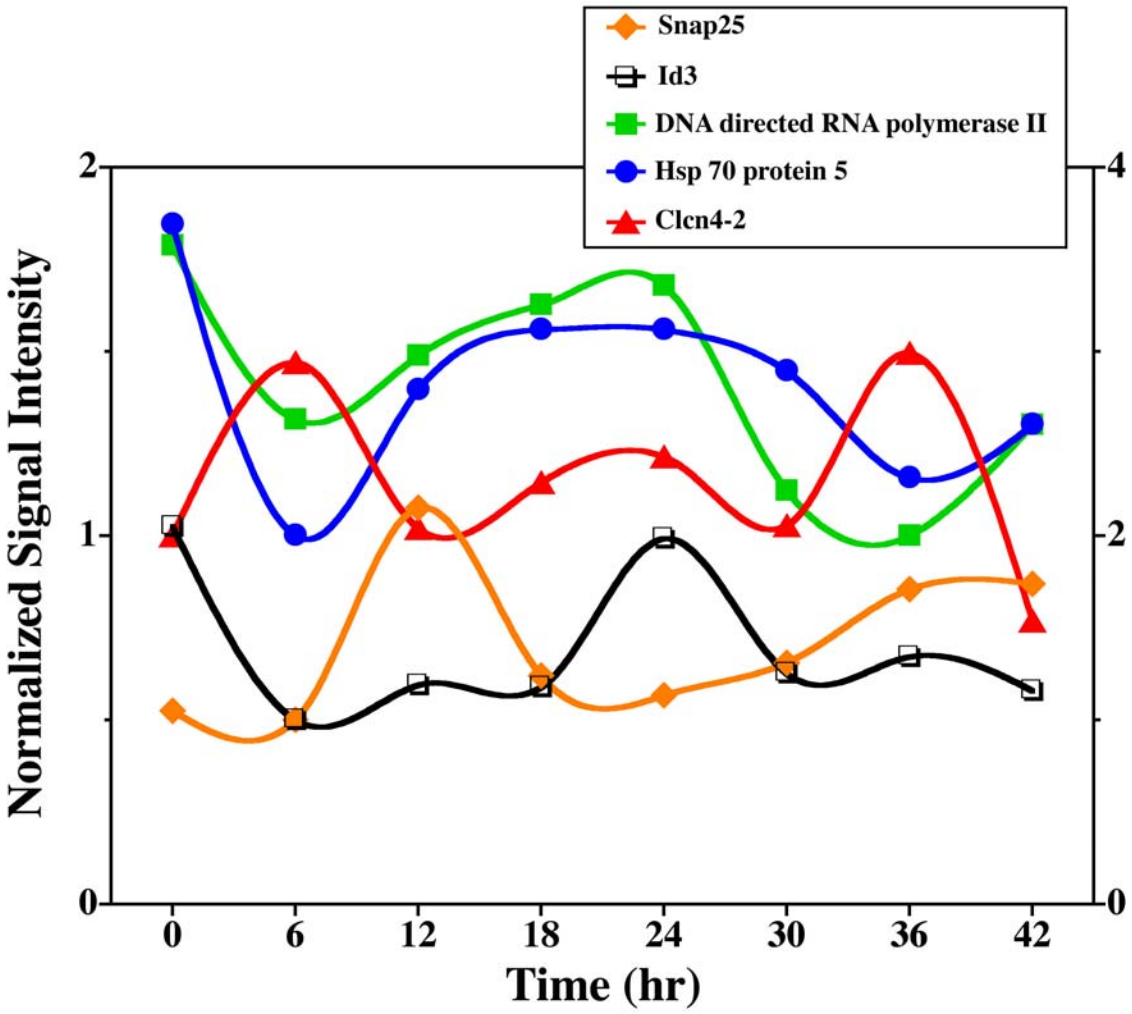

Fig. 7. Rhythmic regulation of *Id3* (□), *DNA-directed RNA polymerase II* (■), the putative chloride channel *Clcn4-2* (▲), *Hsp 70 protein 5* (●), and *Snap-25* (♦) expression in SCN2.2 cells. Symbols denote GeneChip determinations of mRNA abundance ($n = 3$) at 6-hour intervals. The circadian profiles for these genes in SCN2.2 cells were similar to those observed in the rat SCN (data not shown).

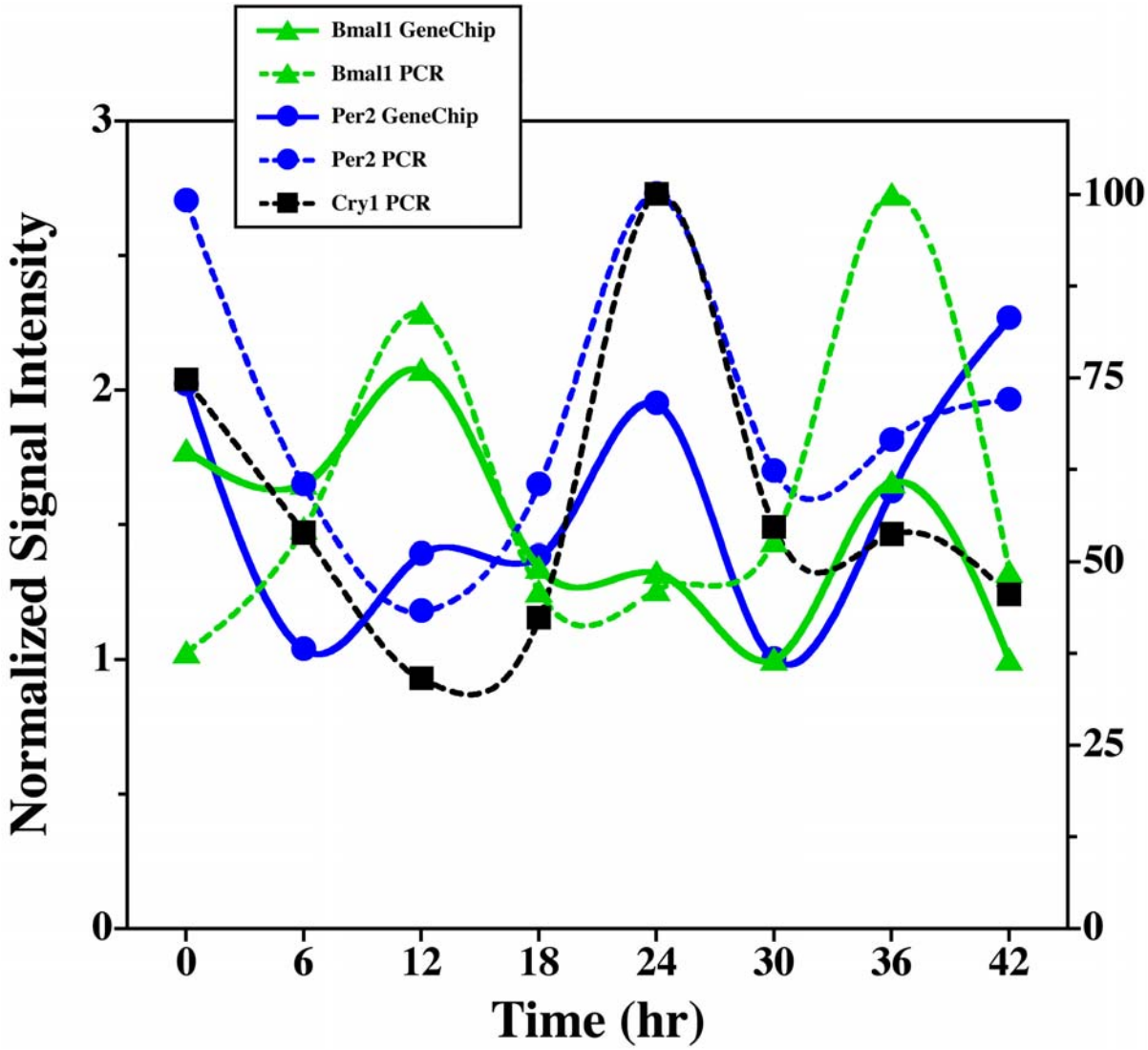

Fig. 8. Rhythmic patterns of *Per2* (●) and *Bmal1* (▲) expression in SCN2.2 cells. Symbols denote average values (*n*=3) for mRNA abundance at 6-hour intervals based on normalized **GeneChip** determinations (solid line) or on qt-**PCR** validation analysis (dashed line). The profile of *Cry1* (■) mRNA expression is depicted for comparison. The qt-**PCR** profiles are derived from triplicate analyses of RNA samples at each timepoint (n = 3) and the plotted values correspond to the ratios of species-specific *Per2*, *Bmal1* or *Cry1*/rRNA or *CypA* mRNA signal in which the maximal value for each experiment was set at 100%. GeneChip and qt-PCR values are respectively represented on the primary and secondary ordinant.

circadian patterns in both SCN2.2 cells and the rat SCN such as nerve growth induced factor-A (*Ngfi-A*) and ornithine decarboxylase antizyme inhibitor (*Oazi*) were rhythmically regulated in the murine liver, but not in the SCN (**33, 114, 149**).

To examine the phase of rhythmic genes expressed in SCN2.2 cells, we compared their first peak of cyclic mRNA abundance (maxima of normalized signal intensity) in relation to the first sampling interval and to the circadian expression profiles of core clock genes. For example, circadian-regulated genes exhibiting maximal mRNA abundance during the first sampling interval (hour 0) and recurrent 24-hour peaks thereafter were assigned to Phase Group (PG) I. In a similar fashion, rhythmic genes with peak mRNA expression during the second (hour 6), third (hour 12) or fourth (hour 18) sampling interval were assigned to PG II, III and IV, respectively. Based on both gene array and qt-PCR analyses, peak mRNA expression in SCN2.2 cells was observed at hour 0 and 24 for *Per2* and at hour 12 and 36 for *Bmal1* (*Mop3*) (**Fig. 8**) so the rhythms for these clock genes were respectively assigned to PG I and to PG III. Using these comparisons, phase was unambiguously assigned to 149 out of 162 genes with rhythmic profiles in SCN2.2 cells. Circadian phase could not be clearly assigned to the rhythmic patterns of 13 genes due to inconsistencies between experimental replicates and probe sets. In SCN2.2 cells, 56 genes displayed PG I rhythms in which peak mRNA abundance coincided with the zenith of *Per2* expression whereas 37 genes exhibited PG III oscillations in which peak levels were concurrent with the crest of *Bmal1* expression. Thirty-eight and 18 circadian-regulated genes were identified in PG II and PG IV, respectively. The predominant distribution of circadian-regulated genes in SCN2.2 cells within phase groups coinciding with peak *Per2* or *Bmal1* expression is compatible with

phase cluster analyses of rhythmic genes in the murine SCN (70). Similarly, 53 and 141 genes with cycling profiles in the rat SCN showed phase distributions that were respectively coincident with the maxima of *Per2* or *Bmal1* expression.

Functional analyses of clock-controlled genes in SCN2.2 cells. Consistent with recent studies demonstrating that eukaryotic circadian clocks rhythmically regulate the expression of genes mediating diverse aspects of cell physiology (**14, 23, 26, 32, 114, 69, 149, 150**), SCN2.2 cells exhibited circadian fluctuations in genes with a wide range of functions, such as metabolism, immunity, neurotransmission, and development. To examine the breadth of cellular processes regulated by the circadian clock, rhythmic genes in SCN2.2 cells that surpassed stringent expression criteria were organized according to one of seven broad physiological categories: 1) **Energetics**, 2) **Cellular and Systems-Level Communication**, 3) **Protein Dynamics**, 4) **Cellular Development**, 5) **Defense and Detoxification**, 6) **Cytoskeleton and Adhesion** and 7) **Unknown or ESTs** (**Table 1B**; **Table 2**). Based on their application to the 162 rhythmic genes surpassing stringent expression criteria in SCN2.2 cells, 15% regulate energetic processes such as cellular respiration, fatty acid recycling and steroid synthesis, 30% are involved in cellular or systems-level communication, 12% mediate the dynamics of gene expression by controlling protein translation, degradation or trafficking, 8% regulate aspects of cellular development, 3% are associated with defense and detoxification, 3% affect cytoskeletal elements, cellular adhesion or components of the extracellular matrix, and 28% are ESTs or genes with uncharacterized functions (**Table 1B**). The prevalence of rhythmic genes in the cellular and systems-level communication category may reflect their degree of representation on the rat U34A GeneChip (i.e., ≈45% of annotated genes

with known functions). However, the distribution of circadian-regulated genes across other functional categories was not related to a preferential or exclusive bias on the array. Based on analysis using Simplified Gene Ontology lists in GeneSpring 6.1, genes involved in energetics, protein dynamics, cellular development, defense and detoxification and cytoskeleton and adhesion were respectively represented by ≈7%, 7%, 20%, 15% and 6% of the probe sets on the array. Within the first four categories, rhythmic genes in SCN2.2 cells were further segregated into three or more functional clusters.

***Energetics*.** The rhythmic regulation of metabolic activity is a hallmark circadian property of the SCN. For example, the circadian utilization of 2-deoxyglucose (2DG) is a well-documented marker of endogenous rhythmicity in both the rat SCN and SCN2.2 cells (**8, 10, 137**). In addition, the SCN exhibits circadian regulation of genes encoding transporters for energy metabolites and metabolic enzymes (**53, 135**). Consistent with this evidence for the circadian control of SCN metabolism, 24 genes involved in energetic processes showed rhythmic expression profiles in SCN2.2 cells. These genes with energetic functions were subdivided into 4 functional clusters: 1) glucose metabolism and mitochondrial energy transduction (N=7); 2) lipid and fatty acid metabolism (N=7); 3) transporters of energy metabolites (transporters) (N=6); and 4) miscellaneous metabolism (N=4) (**The table on page 62**). Circadian-regulated genes involved in glucose metabolism include malic enzyme 1 (*Me1*), hexokinase 2 (*Hk2*), and glyoxylate reductase/hydroxypyruvate reductase (GenBank #AA892799), an enzyme that mediates the conversion of serine to glucose (**60**). The circadian clock in SCN2.2 cells also impacts upon mitochondrial energy transduction through the rhythmic expression of

mitochondrial ATP synthase 8 (*mt-Atp8*). Importantly, circadian regulation of *Glut 1* (*Slc2a1*), the primary facilitative transporter of D-glucose across the blood-brain barrier (**94, 156**), and *Mct1* (*Slc16a1*), a major transporter of ketone bodies and lactate in glial cells (**153**), was observed in both SCN2.2 cells and the rat SCN. Rhythmically-expressed constituents of the miscellaneous metabolism cluster include two genes involved in steroidogenesis, 3-hydroxy-3-methylglutaryl-Coenzyme A reductase (*Hmgcr*) and Hmgc synthase 1 (*Hmgcs1*).

To address the question of how clock-regulated genes impose circadian rhythms of metabolism on SCN cells, we constructed a GenMAPP of circadian-regulated genes identified using stringent expression criteria (**29, 31**). In SCN2.2 cells, many of the rhythmic genes in the **Energetics** category are critically positioned so as to provide for the coupling of metabolic pathways associated with fatty acid recycling and the synthesis of cholesterol and poly-unsaturated fats (**Fig. 9A**) (**42**). For instance, fatty acid reservoirs fueling beta-oxidation in the mitochondria are functionally linked to the citric acid cycle by means of acetyl-CoA. In turn, citrate generated in the citric acid cycle can be used to form fatty acid acyl-CoAs that can replenish fatty acid reservoirs or contribute to the formation of polyunsaturated fats, cholesterol, and, ultimately hormone production. Within these pathways, circadian regulation of gene expression was observed in SCN2.2 cells and validated in the rat SCN at four key points: Carnitine palmitoyltransferase 1b, Hmgc synthase 1 and Fatty acid synthase. Because these genes widely impact upon the regulation of synthetic, anabolic and catabolic processing of energy substrates, this finding suggests that circadian clock regulation of a small number of genes in crucial positions may provide effective strategy for transmitting temporal information throughout

different networks of cellular metabolism. It is interesting that circadian profiles of these strategically positioned genes share a common Phase Group assignment with that for *Per2*.

Despite ample evidence in both the present study and previous reports for the circadian regulation of genes involved energetic processes and redox status (**53, 135**), the functional significance of these and other metabolic oscillations in the SCN clock is unknown. According to a model developed by Pellerin and Magistretti (**116**), circadian clock regulation of transporters for energy metabolites may provide a basis for metabolic coupling between glial and neuronal cells within the SCN. During the subjective day, increased electrical activity in SCN neurons is associated with the release of the excitatory neurotransmitter such as glutamate, which subsequently induces glucose uptake and glycolysis in astrocytes. Thus, clock-regulated expression of *Glut 1* (*Slc2a1*) and *Mct1* (*Slc16a1*) may play a critical role in the rhythmic transportation of glucose across the blood-brain barrier and of lactate produced by astrocytes so as to fulfill the circadian metabolic requirements of SCN neurons.

***Cellular and systems-level communications*.** Communication of temporal information to the rest of the brain and to peripheral tissues is critical function for the pacemaker function of the SCN. Rhythms of mRNA expression were identified in SCN2.2 cells for 49 genes mediating cellular or systems-level communication. Circadian-regulated genes in the communication category were subdivided into 5 functional clusters: 1) neurotransmission (N=11); 2) extracellular factors (N=3); 3) G-protein coupled receptors and associated proteins (N=9); 4) cytosolic signal transduction (N=8); and 5) nuclear factors (N=18) (**The table on page 62**).

A

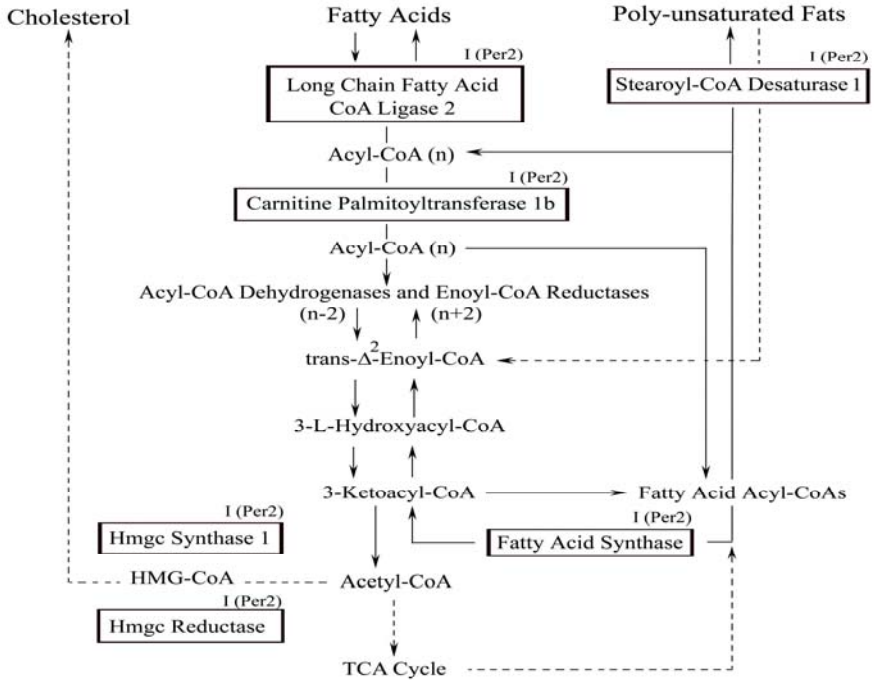

Fig. 9(a-c). GenMAPP analysis of circadian-regulated information flow in SCN2.2 cells in fatty acid and steroid metabolism, cell signaling cascades, and protein dynamics. GenMAPP analysis of circadian-regulated genes in SCN2.2 cells depicting their distribution in relation to information flow within pathways mediating (**A**) fatty acid and steroid metabolism, (**B**) G-protein coupled receptor, second messenger, and mitogenic signaling cascades, and (**C**) protein dynamics. Boxes indicate the relative positions of circadian-regulated genes surpassing stringent expression criteria. Phase group assignments of rhythmic genes and their coincidence with clock gene oscillations are denoted as I (*Per2*), II, III (*Bmal1b*) and IV. In some instances, no phase group was assigned due to inconsistencies between experimental replicates and probe sets. Solid lines denote probable interactions among rhythmically-expressed genes or other pathway components and/or products arising from these interactions. Dashed lines signify indirect or predicted functional interactions between circadian-regulated genes and critical elements of these pathways.

B

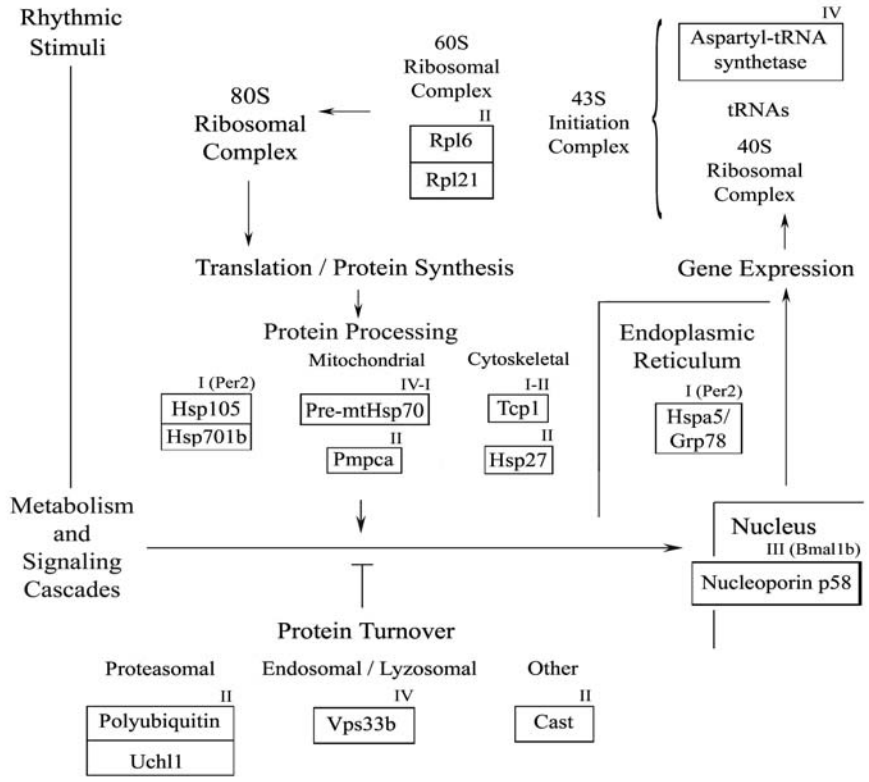

C

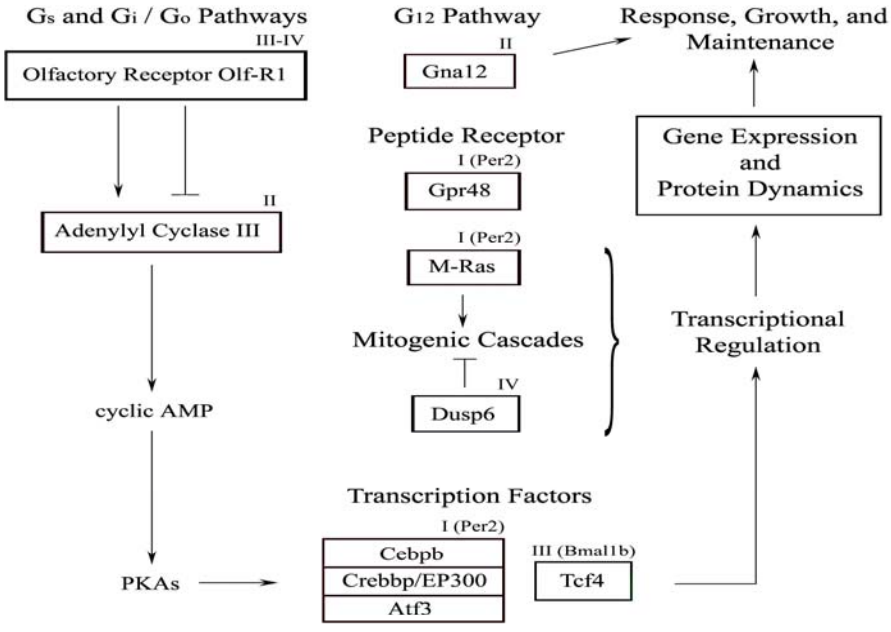

Fig. 9 continued.

To understand how specific aspects of neurotransmission in SCN cells are modulated by the circadian clock, we further classified the rhythmic 11 genes within this cluster according to the following subgroups: 1) glutamatergic metabolism and signaling (N=4); 2) synaptic function and maintenance (N=4); and 3) miscellaneous neurotransmission (N=3) (**The table on page 62**). The IP3 receptor coupling element and immediate early gene *Homer1* is an example of a clock-regulated gene associated with glutamatergic signaling in SCN2.2 cells and the rat SCN. Two ionotropic AMPA receptors genes *Gria1* and *Gria4* that passed secondary expression criteria (**Table A.1**) displayed circadian fluctuations of mRNA abundance in SCN2.2 cells. Circadian regulation of these glutamatergic signaling genes may contribute to the function of this neurotransmitter in circadian photoentrainment. Glutamate involvement in the transmission of entraining light signals by the retinohypothalamic tract to the SCN is supported by immunohistochemical localization of glutamate (**21**) and different subtypes of glutamate receptors within the retinorecipient subfield of the SCN (**41**, **151**) and by physiological studies demonstrating that similar to light, glutamate elicits time-dependent phase shifts in circadian rhythms *in vivo* and *in vitro* (**97**, **141**). In a similar fashion, glutamate has been shown to phase shift the SCN2.2 rhythmicity in luciferase-reported Ca^{2+}/cAMP response element (CRE) activity (**62**). In addition to the oscillations in these glutamatergic signaling elements, the rhythmic expression of *Glut-1* (glutamate transporter), *Gclc* and *Got2* may be important in processes by which this neurotransmitter mediates the circadian regulation of the SCN clock by light because these genes serve to replenish pre-synaptic reservoirs of L-glutamate or to regulate glutamate-based carbon fixation and amino acid metabolism.

Rhythmic genes in the synaptic function and maintenance cluster are associated with pre- and post-synaptic membranes and include *Ykt6*, *Stx4a*, *Snap29*, and the PSD-95/SAP90-associated gene *Dlgap1*. Interestingly, *Dlgap1*, which possesses guanylate kinase activity when functionally expressed, has been implicated in the post-synaptic organization of voltage-gated potassium channels and NMDA receptors (**111**). Consequently, the rhythmic expression of *Dlgap1* mRNA may reflect a divergent point of circadian gene regulation affecting multiple facets of post-synaptic function. Such divergent regulation may provide a platform for the intrinsic rhythm of SCN electrical activity *in vivo* and *in vitro* (**44**). Circadian rhythms of mRNA expression in SCN2.2 cells were also observed for genes that directly affect neuronal electrical properties and neurotransmitter production such as the voltage-gated potassium channel *Kcng1*, the inwardly-rectifying potassium channel *Kcnj14* and A-2 arylamine N-acetyltransferase (*Nat1*) (**The table on page 62**). Because rectifying potassium channels are thought to contribute to the modulation of cardiac pacemaking (**58**), circadian regulation of a voltage sensitive channel like *Kcnj14* may have some significance in the endogenous capacity of SCN cells to generate rhythmic patterns of electrical activity.

Of the remaining clock-controlled genes in the **Cellular and Systems-level Communication** category, most are G-protein coupled receptors (N=9), cytosolic signaling factors and transducers (N=8), or nuclear factors (N=18). To examine how temporal information may be transmitted from the cell membrane to the nucleus via these clock-regulated genes, we analyzed their functional positions within a GenMAPP encompassing G-protein coupled receptor, second messenger, or mitogenic signaling cascades (**Fig. 9B**) (**29, 31**). G-protein coupled receptors or associated proteins with

rhythmic patterns of mRNA expression in SCN2.2 cells included G-protein coupled receptor 48 (*Gpr48*), guanine nucleotide binding protein α12 (*Gna12*), muscle and microspikes RAS (*M-ras*), and the olfactory-like receptor (*Ol1*/*Olf-r1)*. Using secondary expression criteria, circadian profiles were also observed in SCN2.2 expression of somatostatin receptor subtype (*Sstr4*), cholecystokinin A receptor (*Cckar*), angiotensin II receptor (*Agtr2*), orexin receptor-1 (*Hcrtr1)*, 5-hydroxytryptamine 5A receptor (*Htr5a*), and the olfactory-like receptors *Hfl-vn1*, and *Tpcr13* (**Table A.1**). The rhythmic regulation of monoamine receptors in SCN2.2 cells is consistent with observations on the function of this neurotransmitter system in the SCN *in vivo* and *in vitro*. The monoamine, serotonin, is thought to play a role in photic regulation of the SCN clock because 5-HT agonists directly induce phase shifts or modulate the resetting action of light (**89, 126**, **130**).

Downstream of these G-protein signaling elements, circadian regulation of moieties involved in cyclic AMP and MAP kinase signaling pathways in SCN2.2 cells may have important functional implications because these pathways are thought to modulate the transmission of photic input to the SCN (**for review see 95**). Circadian-regulated genes in these signaling pathways such as adenylyl cyclase 3 (*Adcy3*) and MAP Kinase phosphatase 3 (*Dusp6 or Mpkp3*) may impact upon the regulation of cyclic AMP and phosphorelay transduction in SCN2.2 cells (**Fig. 9B**). By affecting cyclic AMP and MAP kinase signaling, the specific distribution of rhythmically-regulated genes within these pathways may differentially influence their interactions with other processes and thus provide an effective strategy for the circadian gating of SCN responses to input signals. CCAAT/enhancer binding protein beta (*Cebpb*), CREBBP/ EP300 inhibitory

protein 1, and activating transcription factor 3 (*Atf3*), provide representative examples of genes that may be circadian regulated as a function of their responsiveness to cyclic AMP.

Protein dynamics. The regulation of gene expression at the protein level is critical for the circadian clock function of the SCN. For instance, cyclical expression of translated gene products and post-translational modification are required for the appropriately timed progression and function of the self-sustained feedback loops that comprise the core clock mechanism (**9, 163**). Thus, cellular processes influencing protein dynamics such as protein synthesis, folding, modification, sorting, trafficking, and degradation are likely to have critical roles in the oscillatory properties of the SCN clock. Circadian regulation of mRNA levels in SCN2.2 cells was observed for 20 genes mediating protein dynamics. Clock-controlled genes in the **Protein Dynamics** category were further subdivided into 3 functional clusters: 1) degradation and synthesis (N=6), 2) protein sorting and trafficking (N=4), and 3) protein modification and folding (N=10) (**The table on page 62**). Ubiquitin carboxyl-terminal hydrolase L1 (*Uchl1*), ribosomal protein L6 and L21 (*Rpl6* and *Rpl21*), vacuolar protein sorting homolog (*Vps33b*), the nucleoporin *p58/p45*, and heat shock 27 protein 1 (*Hsp27/Hspb1*) are representative examples of circadian-regulated genes within these functional clusters.

Circadian regulation of genes involved in protein dynamics may ultimately serve to resonate temporal information across cellular pathways that are not subject to clock control at the mRNA level. To examine this possibility, we used GenMAPP 2.0 to determine whether a few circadian-regulated genes involved in protein synthesis, degradation, and processing could effectively modulate the flow of temporal information

in SCN2.2 cells (**Fig. 9C**) (**29, 31**). Circadian oscillations of mRNA expression in SCN2.2 cells were observed in processes associated with the 60S ribosomal subunit (*Rpl6* and *Rpl21*) and tRNA synthesis (*aspartyl-tRNA synthetase* [*Dars*]). Due to their location at the apex of pathways in the protein dynamics GenMAPP, rhythmic expression of these translation regulatory genes may have significant implications in clock control of gene function. Both of the 60S ribosomal genes *Rpl6* and *Rpl21* interact with the initiation complex to form the eukaryotic 80S ribosomal complex (**42, 156**) and aspartyl-tRNA synthetase functions as a dimeric enzyme or part of a multi-enzyme complex comprising aminoacyl-tRNA synthetases for several amino acids including methionine (**101**). Because more than 4% of the amino acids in *rPer2* are aspartyl residues, the rhythmic RNA expression of *Dars*, *Rpl6,* and *Rpl21* could modulate the availability of cognate tRNAs as well as the actual ribosomal reading of the mRNA sequences for clock and even non-clock genes, thereby imposing oscillations on the activity or function of their protein products.

In the **Protein Dynamics** GenMAPP (**Fig. 9C**), 7 genes associated with chaperone-like activities or post-translational processing and 4 genes involved in protein turnover and/or metabolism showed circadian expression profiles in SCN2.2 cells. *Hsp701b/Hspa1b*, *Hsp105*, *Hsp27/Hspb1*, *Hspa5/Grp78*, and pre-*mtHsp70* (mitochondrial type) are rhythmically regulated genes that encode heat shock proteins involved in the folding and targeted-destruction of proteins damaged by stress. Circadian regulation of *Pmpca* and *Tcp1* may also contribute to clock control of protein dynamics because these genes are involved in post-translational processing of nacent polypeptides (**68**, **92**).

SCN2.2 cells also exhibited circadian oscillations in the expression of two genes involved in the proteasome targeting pathway, *polyubiquitin* and an ubiquitin recycling enzyme *Uchl1*. Circadian regulation of *Uchl1* could modulate reservoirs of ubiquitin and thus influence the proteasome targeting of proteins. Because heat-shock 70 proteins are involved in targeting damaged proteins for proteasome-mediated degradation (**18**), the rhythmic regulation of *Hsp701b/Hspa1b* may contribute in parallel to the regulation of protein degradation. The possible role of these and other proteasome targeting genes in circadian clock function is supported by the recent finding that mutations of the *Slimb* gene, which functions in the ubiquitin–proteasome pathway, disrupts the circadian rhythm of activity in *Drosophila* (**46, 70**). It is also interesting that *Vsp33b* is rhythmically expressed in SCN2.2 cells because this gene is thought to facilitate vesicle-mediated protein trafficking to lysosomes and participate in membrane docking and fusion between late endosomal and lysosomal compartments (**42**). The specific functions of *Vsp33b* and genes involved in proteasome targeting in SCN cells are not known but the circadian regulation of these genes may enable the clock to both impose its influence across diverse cellular pathways and sustain the feedback loops comprising its core.

Circadian regulation of translational, post-translational, and protein degradation elements suggests that the modulation of functional gene expression beyond the transcriptional level may contribute to dissemination of temporal information across cellular networks. For example, by regulating the expression of nuclear pore genes such as the nucleoporin *p58*/*p45* and ribosomal genes such as *Rpl6* and *Rpl21*, the circadian clock could directly modulate the efficiency of information flow from the nucleus and of ensuing polypeptide synthesis. This strategy could establish rhythms of bandwidth

necessary to transmit large amounts of information across physiological nodes during certain times of the day. Furthermore, circadian regulation of post-translational and proteasomal elements could provide node-specific control over the packaging and duration of such information volleys. In particular, the rhythmic expression of genes encoding heat-shock proteins, components within the ubiquitin-proteasome pathway or endosomal/lysosomal elements could impose the influence of time respectively on the folding dynamics of newly synthesized (or damaged) polypeptides, half-life of proteins targeted for ubiquitin-mediated degradation, and the degradation or recycling of extracellular and intracellular constituents. In this regard, it is noteworthy that peak expression of several heat shock related genes including *Hsp 105*, *Hspa5*, and *Hsp701b/Hspa1b* occurred at times that would be optimal for influencing PG I rhythms which represent the majority of the circadian-regulated genes in SCN2.2 cells. Another interesting aspect of this GenMAPP analysis is that protein-processing elements responsive to internal stimuli such as glucose could play a role in adjusting how information is packaged and presented to specific physiological nodes. To exemplify this possibility, rhythms of glucose metabolism could harmonize information flow by modulating the induction of glucose-responsive heat shock proteins such as *pre-mtHsp70*/*Grp75* and *Hspa5*/*Grp78* (**Fig. 9C**) (**103, 133**). Collectively, the rhythmic regulation of translational, post-translational, and protein degradation elements are likely to have a broad impact upon the functional expression of rhythmic and stable gene transcripts.

Cellular development. In SCN2.2 cells, rhythmic mRNA expression was observed for 13 genes that mediate cellular development. Circadian-regulated genes in this

category were subdivided into 3 functional clusters: cell cycle (N=3); 2) DNA/chromatin-related (N=3); and 3) growth and differentiation (N=7).

Organisms ranging from cyanobacteria to mammals display rhythms of cell division that are ”gated” by a circadian oscillator (**20, 91**, **107**). The possible impact of the circadian clock in the indogenous control of the cell cycle in SCN cells is supported by the observation that SCN2.2 cells show rhythmic fluctuations of mRNA abundance in 3 genes involved in regulating the cell cycle. In SCN2.2 cells, the oscillations of mRNA expression observed in rat *cyclin E* Serine/threonine protein kinase (*Pctaire-2*) and the cell cycle protein p55CDC (*Cdc20*) (**The table on page 62**) may serve to couple the clock mechanism to the cell cycle. In addition, another element of cell cycle regulation, cyclin L1 (*Ccnl1*), displayed rhythmic RNA expression in the rat SCN.

Rhythmic genes within the differentiation and growth cluster in SCN2.2 cells included the developmental genes, ornithine decarboxylase antizyme inhibitor (*Oazi*), and interferon related developmental regulator 1 (*Ifrd)*. These genes were also rhythmically expressed in the rat SCN. Another developmental gene, *Bmp4*, was rhythmically regulated in SCN2.2 cells. Although the specific functions of this gene within the SCN are unknown, *Bmp4* has been shown to regulate transcriptional factors, some of which are also rhythmically expressed in both SCN2.2 cells and the rat SCN. In a variety of cell lines including embryonic stem cells, *Bmp4* has been shown to induce mRNA expression for immediate early genes such as *Ngfi-A (Egr1)* and members of the *Id*-gene family that inhibit the binding of basic helix-loop-helix (bHLH) transcription factors to DNA (**59**). The oscillations of these genes in SCN2.2 cells were validated either by parallel microarray analysis of the rat SCN or by qt-PCR.

Defense and detoxification. SCN2.2 cells exhibited rhythmic patterns of mRNA expression for 5 genes involved in **Defense and Detoxification** (**Tables 1 and 3**). Circadian-regulated genes in this category include the cell surface antigen (*RT1-Aw2*), p105 coactivator (*U83883*), an EST displaying similarity to mucin, prostaglandin-endoperoxidase synthase 2 (*Ptgs2*) and interleukin 6 receptor (*Il6r*). Inducible nitric oxide synthase (*iNos* or *Nos2*) was also categorized in the **Defense and Detoxification** category and represented a prominent example of a rhythmic gene that only surpassed secondary expression criteria (**Table A.1**). Nonetheless, circadian expression of *iNos* mRNA was verified in SCN2.2 cells by qt-PCR (**Fig. 6A**) and was observed in parallel analysis of the rat SCN. Based on evidence indicating that a competitive inhibitor of all 3 isoforms of NOS, L-NAME, blocks glutamate- and N-methyl-D-aspartate (NMDA)-induced phase shifts of the SCN rhythm in neuronal firing rate *in vitro* (**30, 157**), the gaseous neurotransmitter nitric oxide (NO) is thought to be involved in the pathway by which glutamate mediates the phase-resetting action of light signals on the SCN clock. However, *in vivo* analyses using mutant mice do not appear to support this function for NO in the SCN because animals lacking neuronal or endothelial isoforms of *Nos* (*nNos* and *eNos*, respectively) show normal circadian entrainment to light-dark cycles and phase-shifting responses to light (**74, 75**). The present evidence for the circadian regulation of *iNos* in both SCN2.2 cells and the rat SCN suggests that this isoform merits further analysis to address conflicting observations on NO function in the circadian resetting of the SCN clock mechanism by light.

Cytoskeleton and adhesion. Five genes with cytoskeletal or cellular adhesion functions, integrin α E1 (*Itgae*), CD44 antigen (*Cd44*), tissue inhibitor of

metalloproteinase 1 (*Timp 1*), tropomyosin (*Tmp1*), and Dynamin-like protein (*Dnml1*) exhibited circadian expression profiles in SCN2.2 cells. Circadian regulation in both SCN2.2 cells was observed in the expression of 10 additional genes in this physiological category that surpassed secondary expression criteria (**Table A.1**), including Troponin I type 3 (*Tnni3*), vascular cell adhesion molecule 1 (*Vcam1*), and neural cell adhesion molecule 1 (*Ncam1*). Rhythmic expression of cytoskeletal and cellular adhesion constituents within SCN cells is consistent with anatomical and functional evidence for SCN oscillations in cellular and synaptic plasticity and their role in regulation of circadian rhythms. In the hamster SCN, the distribution of astrocytes expressing glial fibrillary acidic protein (GFAP) fluctuates over the circadian cycle and this structural rhythmicity may participate in the regulation of extracellular glutamate levels (**81**). *Ncam* has been specifically implicated in the regulation of SCN circadian function by studies demonstrating that transgenic mutant mice lacking different isoforms of this gene and an associated glycoprotein that regulates plastic interactions between nerve cells, polysialic acid (PSA), are distinguished by activity rhythms with decreased free-running periods and altered patterns of light-dark entrainment (**140**).

Summary. The gene profiling analyses in the present study indicate that SCN-like global and temporal patterns of gene expression are conserved in the SCN 2.2 transcriptome. SCN2.2 cells and the rat SCN show similar properties with regard to relative levels of mRNA expression for many different genes, oscillations in the expression of the core clock genes, *Per2*, *Bmal1* (*Mop3*), and *Cry1*, and circadian regulation of many clock-controlled genes. Many of these circadian-regulated genes in SCN2.2 cells and the rat SCN were homologs or functionally-related genes that exhibit

rhythmic expression profiles in the murine SCN and/or liver (**114, 149**). Despite the similarities in circadian regulation of the transcriptome in SCN2.2 cells and the rat SCN, there was not complete overlap in the rhythmically-regulated genes between these experimental models (**Table A.2**). Furthermore, the number of genes with circadian profiles in SCN2.2 cells was lower than that observed in the rat SCN and described previously for the murine SCN (**114**). It is possible that this inequality in the extent of circadian gene expression may be related to comparative differences in the cellular heterogeneity of SCN2.2 cells and the SCN *in vivo*. Although SCN2.2 cells were developed as a heterogeneous, rather than clonal, cell line to provide adequate representation of most SCN phenotypes especially those with pacemaker properties, the immortalization strategy used to establish this line may have inherently selected for or against certain cell types. Consequently, circadian, and even global, gene expression may be more restricted in SCN2.2 cells because this line does not express the full complement of cellular phenotypes found in the SCN due to selection bias in immortalization procedures. This possibility is supported by molecular and antigenic analyses indicating that the many SCN2.2 cells exhibit SCN-like peptidergic phenotypes but the overall proportion of peptidergic neurons in the line is less than that normally found in the SCN *in situ* (**36**). Alternatively, the diminished extent of circadian-regulated gene expression in SCN2.2 cells may reflect the absence of other neural and endocrine inputs that normally influence SCN rhythmicity *in vivo*. Nonetheless, comparison of circadian gene expression in SCN2.2 cells and the rat SCN provides a robust filter for identifying genes that are rhythmically regulated by the circadian clock mechanism indigenous to SCN cells.

In SCN2.2 cells, genes with circadian profiles were functionally diverse, but were most frequently associated with metabolic, cellular and systems-level communication, and protein dynamics. The prevalence of rhythmic genes in these categories is consistent with studies documenting their importance in the circadian photoentrainment and pacemaker functions of the SCN. Furthermore, GenMAPP analysis of rhythmically-regulated genes involved in fatty acid and steroid metabolism, G-protein coupled receptors, second messengers and mitogenic cascades, and protein dynamics has yielded insight into how SCN2.2 cells manage information flow so as to modulate input to or output from the clock mechanism. In particular, circadian regulation of genes involved in protein synthesis and degradation, sorting and trafficking, and modification or folding may extend clock control to processes that are not rhythmically orchestrated at the transcriptional level.

In addition to profiling the extent of circadian expression in SCN cells (**Table 3**), the present analysis may have implications for understanding what molecular elements are necessary for the endogenous rhythm-generating and pacemaker properties of the SCN. Similar to the SCN *in vivo*, SCN2.2 cells are distinguished by the capacity to generate self-sustained rhythmicity in their own molecular or physiological processes and to restore behavioral rhythmicity to the entire animal when transplanted into SCN-lesioned hosts (**37**). Furthermore, these cells are capable of driving rhythms of clock gene expression and glucose metabolism in NIH/3T3 cells via the secretion of an unknown diffusible signal (**8, 10**). Although circadian expression of various clock and clock-controlled genes can be induced in cultures of the rat-1 and NIH/3T3 fibroblasts by serum-shock treatment or activation of various signal transduction pathways (**4, 15, 16**),

these cell lines are non-rhythmic in the absence of this stimulatory input or SCN2.2-derived signals and incapable of conferring this induced oscillatory behavior to other cells (**8, 10**). A possible explanation for the distinctions between the circadian properties of SCN2.2 cells and the rhythmic behavior of stimulated fibroblast lines is that fibroblasts may not express critical circadian output signals found in SCN cells. Consequently, comparison of circadian gene expression in SCN2.2 cells (or the rat SCN) with that in cells like NIH/3T3 fibroblasts or with other peripheral tissues, which contain all of the known components of the canonical clockworks, may provide an opportunity to identify candidate signals that mediate the pacemaking function of the SCN.

Table 3. ***Functional categorization of circadian-regulated genes in SCN2.2 cells (stringent expression criteria).***

GenBank ID	Locus Link ID	Gene descriptor	Phase group
Category 1 - Energetics (24)			
Cluster 1 - Glucose metabolism and mitochondrial energy transduction (7)			
S56464	**25059**	Hexokinase 2 (*Hk2*)	**I**
AI171506 *	**24552**	Malic enzyme 1 (*Me1*)	**I**
K00750 *	**25309**	Cytochrome c, somatic (*Cycs*)	**I**
J01435 *	**26196**	ATP synthase 8, mitochondrial (*mt-Atp8*)	**I**
AA892799	**298085**	Similar to glyoxylate reductase/hydroxypyruvate reductase	**II**
M59460	**64035**	Liver glycogen phosphorylase (*Pygl*)	**III**
U21662	**94273**	Mannosyl (α-1,6-)-glycoprotein β-1,2-N-acetylglucosaminyltransferase (*Mgat2*)	**III**
Cluster 2 - Lipid and fatty acid metabolism (7)			
J02585 *	**246074**	Stearoyl-Coenzyme A (CoA) desaturase 1 (*Scd1*)	**I**
M76767	**50671**	Fatty acid synthase (*Fasn*)	**I**
D43623	**25756**	Carnitine palmitoyltransferase 1b (*Cpt1b*)	**I**
D90109 *	**25288**	Long chain fatty acid coenzyme A (CoA) ligase 2 (*Facl2*)	**I**
AI030175	**LOC301592**	Similar to L-iditol 2-dehydrogenase / sorbitol dehydrogenase	**II**
X57988 *	**29534**	Peroxisomal membrane protein 3 (*Pxmp3*)	**IV**
AJ224120	**85249**	Peroxisomal membrane protein (*Pmp26p* or *Peroxin-11*)	**IV**

Table 3 continued

Cluster 3 - Transporters (6)

D63834 *	**25027**	Monocarboxylate transporter (*Mct1*/*Slc16a1*)	**I**
AA799645 *	**58971**	FXYD domain-containing ion transport regulator 1 (*Fxyd1*)	**I-II**
M30581	**25391**	ATPase, Ca++ transporting, ubiquitous (*Atp2a3*)	**III**
L10152	**25648**	Solute carrier family 7, member 1 (*Slc7a1*)	**III**
S68135 *	**24778**	Glucose transporter / solute carrier family 2,member 1 / (*Glut 1*/*Slc2a1*)	**III**
AA800202 *	**311423**	Similar to bicarbonate transporter related protein 1 (*Slc4 11*)	**IV**

Cluster 4 - Miscellaneous metabolism (4)

M29249 and X55286	**25675**	3-hydroxy-3-methylglutaryl-Coenzyme A (CoA) reductase (*Hmgcr*)	**I**
AI177004 *	**29637**	Hmgc synthase 1 (*Hmgcs1*)	**I**
X08056 *	**25257**	Guanidinoacetate methyltransferase (*Gamt*)	**II**
L19998 *	**83783**	Sulfotransferase family 1A, phenol-preferring, member 1 (*Sult1a1*)	**III**

Category 2 - Cellular and Systems-level Communication (49)

Cluster 1 - Neurotransmission (11)

Glutamatergic metabolism and signaling (4)

J05181 and S65555	**25283**	Glutamate-cysteine ligase catalytic subunit (*Gclc*)	**I-III**
AF093267 * and AF093268 *	**29546**	Homer1 and splice variant 1b, neuronal immediate early gene, 1 (*Homer1*)	**IV-I**
AA892012	**25721**	Glutamate oxaloacetate transaminase 2 (*Got2*)	**IV**
S59158 * (X63744 in rat SCN)	**29483**	Glutamate transporter (*Glut-1*) / solute carrier family 1, member 3 (*Slc1a3*)	**IV**

Table 3 continued

Synaptic function and maintenance (4)			
AF033027	**64351**	Prenylated SNARE protein (*Ykt6*)	**II**
L20821 *	**81803**	Syntaxin 4 (*Stx4a*)	**II**
U67137	**65040**	PSD-95/SAP90-associated / guanylate kinase associated protein (*Dlgap1*)	**III**
AF035822	**116500**	Synaptosomal-associated protein, 29kD (*Snap29*)	**IV**
Miscellaneous neurotransmission (3)			
AJ003065	**276720**	Inwardly-rectifying channel, subfamily J, member 14 (*Kcnj14*)	**I**
M81784	**296395**	Voltage-gated channel subfamily G member 1 (*Kcng1*)	**III**
U01344 *	**116631**	A-2 arylamine N-acetyltransferase 1 (*Nat1*)	**IV**
<u>Cluster 2 - Extracellular factors (3)</u>			
AA850734 and M32167	**83785**	Glioma-derived vascular endothelial cell growth factor (*Vegf*)	**I-IV**
M91595	**25662**	Insulin-like growth factor binding protein-2 (*Igfbp2*)	**III**
X14232	**25317**	Fibroblast growth factor 1 (*Fgf1*)	**III**
<u>Cluster 3 - G-protein coupled receptors and associated proteins (9)</u>			
AF061443	**286994**	G protein-coupled receptor 48 (*Gpr48*)	**I**
D89863	**25482**	Muscle and microspikes RAS (*M-ras*)	**I**
D85760	**81663**	Guanine nucleotide binding protein, alpha 12 (*Gna12*)	**II**
AA892635	**85428**	TC ras-like protein (*Tc10*)	**II**
AA891669	**79434**	Ras oncogene family (*Rab11b*)	**II-III**
U53475	**266688**	GTPase Rab8b (*Rab8b*)	**III**
AA893717	**315298**	Similar to Rac GTPase-activating protein	**III**
L34074	**60451**	Olfactory receptor (*Ol1/Olf-r1*)	**III-IV**
AF080435 *	**64013**	Phosducin-like protein (*Pdcl/Phlp*)	**IV**

Table 3 continued

Cluster 4 - Cytosolic signaling factors and transducers (8)

L27843	**29463**	Nuclear protein tyrosine phosphatase (*Ptp4a1*)	**I**
AB002086	**83809**	Phox47 protein (*p47*)	**II**
M55075	**64508**	Adenylyl cyclase, type III (*Adcy3*)	**II**
U10188	**25515**	Polo-like kinase homolog (Drosophila) (*Plk*)	**III**
AJ000347 *	**64473**	3(2),5-bisphosphate nucleotidase (*Bpnt1*)	**III**
D88672	**25097**	Phospholipase D (*Pld2*)	**III**
U42627	**116663**	Dual specificity phosphatase 6 (*Dusp6*)	**IV**
U38376 *	**24653**	Cytosolic phospholipase A2 (*Pla2g4a*)	**IV**

Cluster 5 - Nuclear factors (18)

E-box and immediate early factors (10)

Y00396	**24577**	V-myc avian myelocytomatosis viral oncogene homolog (*Myc*)	**I**
AA892137	**LOC311392**	Similar to CREBBP/ EP300 inhibitory protein 1	**I**
S77528 and X60769	**24253**	CCAAT/enhancer binding protein, beta (*Cebpb*)	**I**
X06769	**314322**	C-fos oncogene (*c-fos*)	**I**
AA875032 *	**NF**	Fos-related antigen, exon 4	**I**
M63282 *	**25389**	Leucine zipper protein / Activating transcription factor 3 (*Atf3*)	**I**
U09228 *	**84382**	New England Deaconess E-box binding factor / transcription factor 4 (*Tcf4*)	**III**
AF023087 *, U75397 *, and and M18416	**24330**	Nerve growth factor induced factor A (*Ngfi-A/Egr1*)	**III-IV**
AA799560	**171114**	N-myc downstream regulated gene (*Ndrg2*)	**III-IV**
U78102 *	**114090**	Krox-20 / early growth response 2 (*Egr2*)	**IV**

Table 3 continued

Other nuclear factors (8)			
X54250	**117140**	HIV type I enhancer-binding protein 1 (*Hivep1*)	**I**
M65251 *	**29721**	HIV type 1 enhancer-binding protein 2 (*Hivep2*)	**I**
L26292 *	**114505**	Kruppel-like factor 4 (*Klf4*)	**I**
U20796	**259241**	Nuclear receptor subfamily 1, group D, member 2 (*Nr1d2*)	**I**
AF000942 and AI171268 *	**25585**	Inhibitor of DNA-binding 3 (*Id3*)	**I**
L23148 *	**24370**	Inhibitor of DNA-binding 1, splice variant 1d1	**II-III**
X84210	**25492**	Nuclear factor I/A (*Nfia*)	**III**
M87634	**24370**	Forkhead box O1 (*Foxo1*)	**IV-I**

Category 3 - Protein Dynamics (20)

Cluster 1 - Degradation and synthesis (6)

X03347	**LOC366649**	P75 gag-fos fusion protein / Similar to ubiquitin-like protein	**I**
AA859882 *	**29545**	Ubiquitin carboxyl-terminal hydrolase 1 (*Uchl1*)	**II**
D16554	**192255**	Polyubiquitin	**II**
AA799672	**117042**	Similar to ribosomal protein L6 (*Rpl6*)	**II**
AA849648 *	**79449**	Ribosomal gene L21 (*Rpl21*)	**II**
AI009682 *	**116483**	Aspartyl-tRNA synthetase (*Dars*)	**IV**

Cluster 2 - Protein sorting and trafficking (4)

M15883	**116561**	Clathrin, light polypeptide (*Cltb*)	**II**
AF035951	**294286**	Kinesin family member, C1 (*Kifc1*)	**III**
U44979	**171529**	Kinesin-related protein 2 (*KRP2*)	**III**
U35245	**64060**	Vacuolar protein sorting homolog (*Vps33b*)	**IV**

Table 3 continued

Cluster 3 -Protein modification and folding (10)

AI236601 *	**Close to LOC288444**	Similar to Heat shock protein (*Hsp105*)	**I**
S63521	**25617**	Heat shock 70kD protein 5 (Hspa5/Grp78)	**I**
L16764	**294254**	Heat shock protein 70 1b (*Hsp701b/Hspa1b*)	**I**
AA875089	**25403**	Calpastatin (*Cast*)	**I-II**
AA900850	**24818**	T-complex 1 (*Tcp1*)	**I-II**
M57728	**296588**	Mitochondrial matrix processing protease, alpha subunit (*Pmpca*)	**II**
AF056208	**65053**	PAM COOH-terminal interactor protein 1 (*Pamci*)	**IV**
AI176658 and M86389	**24471**	Heat shock protein 27 protein 1 (*Hsp27/Hspb1*)	**II**
AF000899 *	**245922**	Nucleoporin p58 (*p58/p45*)	**III**
S75280	**LOC295778**	Similar similar to Grp75 (*Pre-mtHsp70/Grp75*)	**IV-I**

Category 4 - Cellular Development (13)

Cluster 1 - Cell cycle (3)

D14015	**25729**	Rat cyclin E (*Ccne*)	**I**
AF052695	**64515**	Cell cycle protein p55CDC (*Cdc20*)	**III**
AB005540	**314743**	Similar to serine/threonine protein kinase-2 (*Pctaire-2*)	**III**

Cluster 2 - DNA/chromatin related (3)

H33461 *	**117520**	Oxidation resistance 1 (*Oxr1*)	**III**
U95920 *	**81740**	Pericentriolar material (*Pcm1*)	**III**
AA964849 *	**25591**	ADP-ribosyltransferase 1 (*Adprt*)	**III**

Table 3 continued

Cluster 3 - Growth and differentiation (7)

AI014163 *	**29596**	Interferon related developmental regulator 1 (*Ifrd*)	**I**
D89983 * and AI043631	**58961**	Ornithine decarboxylase antizyme inhibitor (*Oazi*)	**I**
S55427	**24660**	Peripheral myelin protein 22 (*Pmp22*) / growth-arrest-specific Gas-3 homolog	**I**
AF020618	**171071**	Myeloid differentiation primary response gene 116 (*Myd116*)	**I**
U66471	**116679**	Cell growth regulator (*Cgr19*)	**II**
Z22607	**25296**	Bone morphogenic protein 4 (*Bmp4*)	**II**
AF087037	**54230**	B-cell translocation 3 (*Btg3*)	**IV**

Category 5 - Defense and Detoxification (5)

M58587	**24499**	Interleukin 6 receptor (*Il6r*)	**I**
M10094	**24737**	MHC class I cell surface antigen / RT1 class Ib gene (*RT1-Aw2*)	**II**
U83883	**64635**	p105 coactivator (*U83883*)	**II**
AA891054	**NF**	Similar to human mucin	**II**
S67722	**29527**	Prostaglandin-endoperoxide synthase 2 (*Ptgs2*)	**III**

Category 6 - Cytoskeletal and Adhesion (5)

AF020046	**83577**	Integrin alpha E1 (*Itgae*)	**I**
M61875	**25406**	CD44 antigen (*Cd44*)	**I**
AI169327	**116510**	Tissue inhibitor of metalloproteinase 1 (*Timp1*)	**I**
AA875132	**24851**	Tropomyosin 1 (*Tpm1*)	**III**
AF020212	**114114**	Dynamin-like protein (*Dnml1*)	**IV**

Table 3 continued

ESTs and Genes with Unknown Function (46)

AA892598 *	**LOC294523**	Similar to hypothetical protein MGC46970	**I**
AI008131	**LOC296217**	S-adenosylmethionine decarboxylase (*SamDC*)	**I**
AA799637	**EST**		**I**
AA799721	**LOC315096**		**I**
AA799971 *	**LOC313369**		**I**
AA800156 *	**LOC310071**		**I**
AA800708 *	**LOC295310**		**I**
AA800853 *	**LOC305302**		**I**
AA859996 *	**LOC305436**		**I**
AA892638 *	**EST**		**I**
AA892863 *	**close to LOC295922**		**I**
AA963449 *	**Close to Cyp51**		**I**
AI011706	**EST**		**I**
AI639039 *	**EST**		**I**

Table 3 continued

AA874889	**Close to Unc5h2**		**I**
AA800693 *	**Close to 83578**		**I**
AA892137	**EST**		**I**
AA893230	**EST**		**II**
AA891054	**EST**		**II**
AB000929	**81828**	Zona pellucida 2 glycoprotein (*Zp2*)	**II**
AA891499	**LOC317360**		**II**
AA799497	**EST**		**II**
AA799571	**LOC291710**		**II**
AA799711	**LOC288264**		**II**
AA799732	**LOC303794**		**II**
AA800200 *	**LOC298426**		**II**
AA800735	**EST**		**II**
AA800782 *	**LOC294082**		**II**
AA859626	**LOC306352**		**II**
AA893260	**close to LOC293779**		**II**

Table 3 continued

AA894259 *	**LOC304206**	**II**
AI639148 *	**LOC292262**	**II**
AI639425	**LOC287133**	**II**
AA874876	**Very close to LOC306194**	**II**
AA859926	**EST**	**III**
AA874827	**EST**	**III**
AA875037	**EST**	**III**
AA875348	**LOC287598**	**III**
AA891774	**LOC300983**	**III**
AA892339	**LOC299262**	**III**
AI639097 *	**EST**	**III**
AI639413 *	**LOC307334**	**III**
H33614	**EST**	**III**
H31604	**EST**	**III**
AA800882	**EST**	**IV**
AA874943 *	**EST**	**IV**

Functional categorization of circadian-regulated genes in SCN2.2 cells. Listed are the GenBank, Locus Link ID, functional category/cluster and Phase Group assignment for unique genes and ESTs that surpassed stringent expression criteria and displayed circadian oscillations of mRNA expression in SCN2.2 cells. Rhythmic genes are segregated into seven broad functional categories: 1) **Energetics**, 2) **Cellular and Systems-level Communication**, 3) **Protein Dynamics**, 4) **Cellular Development**, 5) **Defense and Detoxification**, 6) **Cytoskeleton and Adhesion** and 7) **Unknown or ESTs**. Several of these categories are subdivided into clusters to further delineate gene function. The asterisk denotes genes that were rhythmic in SCN2.2 cells and the rat SCN.

CHAPTER III

CIRCADIAN PROFILING OF THE TRANSCRIPTOME IN NIH/3T3 FIBROBLASTS: COMPARISON WITH RHYTHMIC GENE EXPRESSION IN SCN2.2 CELLS AND THE RAT SCN*

INTRODUCTION

Circadian clocks have evolved as endogenous biological timekeeping mechanisms that coordinate a wide range of biological processes with the 24-hour period of the daily solar cycle. In mammals, the suprachiasmatic nuclei (SCN) of the anterior hypothalamus function as a master clock that regulates overt circadian rhythms throughout the organism (**69**). The SCN clock is also capable of producing self-sustained circadian oscillations in many of its intrinsic molecular and cellular activities. SCN cells are marked by circadian regulation of neuropeptide secretion, cellular metabolism, and electrical activity *in vivo* and *in vitro* (**44, 137**). Moreover, recent gene profiling studies indicate that up to 10% of the transcriptome is rhythmically expressed in the SCN *in vivo* and in immortalized rat SCN cells (**114, 98**). These endogenous molecular oscillations in the SCN are a critical property of the clock mechanism and presumably its output signals that regulate circadian rhythmicity in other cells or tissues. Specifically, the SCN timekeeping mechanism consists of interlocking feedback loops in which the core components, *Bmal1* (*Mop3*),

---

*Used with permission. **Menger GJ, Allen GC, Neuendorff N, Nahm SS,Thomas TL, Cassone VM, and Earnest DJ.** Circadian profiling of the transcriptome in NIH/3T3 fibroblasts: comparison with rhythmic gene expression in SCN2.2 cells and the rat SCN. *Physiol Genomics.* Epub. 2007.

Period1 (*Per1*), *Per*2, *Cryptochrome1* (*Cry1*), *Cry*2 and *Rev-erbα*, are rhythmically regulated through mutual interactions with their protein products. In turn, the molecular feedback loops involving these genes coordinate downstream rhythmicity in SCN-specific output genes that mediate clock-controlled oscillations in other neural or endocrine tissues.

Although the SCN is vital to the function of the mammalian circadian system, the expression and rhythmic regulation of these core clock genes are not spatially confined to this neural locus. Instead, oscillations in the same genes forming the molecular core of the SCN clockworks occur widely in many peripheral cells and tissues (**139, 164, 160**). Studies using *in vitro* models have yielded compatible evidence indicating that peripheral or non-SCN cells are also capable of expressing clock gene oscillations. Rat-1 and NIH/3T3 fibroblasts exposed to serum shock or forskolin treatment are similar to immortalized cells derived from the rat SCN (SCN2.2) with regard to rhythmic fluctuations in clock gene mRNA abundance (**15, 4, 8, 9, 10**). However, this similarity in the oscillatory nature of core clock elements does not provide for equivalent functional properties because SCN cells have the capacity to act as pacemakers whereas peripheral tissues and cultured fibroblasts do not. For example, SCN2.2 cells, but not fibroblasts, restore circadian behavior when transplanted into arrhythmic, SCN-lesioned hosts *in vivo* (**37**) and also confer metabolic and molecular oscillations to cocultured cells via the secretion of an unknown diffusible signal (**8, 10**). Collectively, these findings raise the important question of why the molecular machinery found in the SCN and SCN2.2 cells does not propagate similar pacemaker function in fibroblasts.

A potential explanation is that SCN output signals necessary for its function in coordinating rhythmicity among individual clock cells and in downstream oscillators may not be expressed or circadian-regulated in stimulated fibroblasts. In the present study, we

explored this possibility by analyzing global and circadian facets of gene expression in NIH/3T3 fibroblasts. Using Affymetrix GeneChips, the transcriptome in forskolin-stimulated fibroblasts was profiled at 6-hour intervals over two circadian cycles and then compared to the patterns of gene expression observed in SCN2.2 cells and the rat SCN (**98**). This comparison of the NIH/3T3 and SCN transcriptomes was used to identify the extent of overlap and fundamental differences in their basic expression and circadian regulation of specific genes. Using bioinformatic tools, we next examined the functional distribution of both non-rhythmic and circadian-regulated genes that were found only in forskolin-stimulated NIH/3T3 fibroblasts or in SCN2.2 cells and the rat SCN. Because SCN-specific rhythms of gene expression were especially evident within pathways associated with intercellular communication and glucose metabolism, we probed implications of this information in differentiating candidate signals for the synchronization of SCN clock cells or pacemaker regulation of circadian rhythmicity in other cells. Based on evidence for the role of nitric oxide (NO) in resetting the SCN clock (**30, 157**) and the present observation that the inducible isoform of nitric oxide synthase (*iNos* or *Nos2*), an isozyme involved in NO production, is rhythmically expressed in the rat SCN and SCN2.2 cells but not in NIH/3T3 fibroblasts, this diffusible messenger was targeted for supplementary analysis examining the effects of pharmacological inhibition on the endogenous oscillatory and circadian pacemaker functions of SCN2.2 cells. Specifically, we used our coculture model to determine whether treatment of SCN2.2 cells with the NOS inhibitor, N^G-nitro-L-arginine methyl ester (L-NAME) alters their capacity to rhythmically regulate 2-deoxyglucose uptake and confer this rhythmicity to untreated NIH/3T3 fibroblasts.

MATERIALS AND METHODS

NIH/3T3 cultures and RNA extraction. For each of three biological replicates, NIH/3T3 cells (passages 4 and 5) were seeded on culture dishes (60mm; Corning, Corning, NY) and maintained at 37°C and 5% CO_2 in Dulbecco's Minimum Essential Medium (DMEM; Invitrogen, Carlsbad, CA) supplemented with 20% fetal bovine serum (FBS; HyClone, Logan, UT), 3000 µg/ml glucose and 292 µg/ml L-glutamine. At 48-hour intervals, the medium was changed and cultures were expanded 1:3 or 1:4. Prior to experimental analysis, cultures were plated in multiple T-75 flasks. At approximately 24 and 44 hours after plating, the culture medium was changed so as to respectively lower the FBS concentration to 10% and then to 5%. To facilitate cell cycle and circadian oscillation synchronization across cultures, cells were subjected to medium replacement and exposed to serum-free medium (DMEM) containing 15uM forskolin (Calbiochem, La Jolla, CA) for 2 hours. Cultures were rinsed and thereafter maintained in serum-free DMEM. Immediately after forskolin treatment, cells were harvested from individual flasks (approximate density: 1.3 x 10^6 cells/cm^2) at 6-hour intervals for 48 hours and total cellular RNA was extracted using RNeasy Midi-Kit protocols (Qiagen, Valencia, CA). RNA extracts from individual samples were treated with on-column Dnase-I digestion and concentrated with ethanol precipitations.

Affymetrix U74v2 GeneChip analysis. Prior to analysis, the quality of all NIH/3T3 RNA samples was assessed by electrophoresis on 1% agarose gels containing 0.1ug/ml ethidium bromide. Labeled cRNAs were produced from purified RNA collected at each time-point and hybridized on mouse U74v2 GeneChips. Experimental procedures including double-stranded cDNA synthesis and biotinylated cRNA preparation were

conducted according to recommended protocols described in Affymetrix GeneChip Expression Analysis Technical Manual (**82**) and processed as previously described for microarray analysis of SCN2.2 cells and the rat SCN (**98**). To assure the quality of labeling and fragmentation efficiency, unfragmented and fragmented cRNA products were analyzed on an Agilent 2100 bioanalyzer prior to hybridization on arrays. Fragmented biotinylated cRNA (15μg) was hybridized on Affymetrix GeneChip mouse U74 version 2 arrays at 45°C and 60rpm in a GeneChip Hybridization Oven 640 (Affymetrix, Inc., Santa Clara, CA) for 16 hours.

Following hybridization, arrays were washed and stained using Affymetrix protocols for antibody amplification staining on a GeneChip Fluidics Station 400 in conjunction with Affymetrix Microarray Suit 5.0 software. After a brief wash with a non-stringent buffer, the stained signals on the array were then amplified with a solution containing 3μg/ml anti-streptavidin biotinylated antibody (Vector Laboratories, Burlingame, CA), 1X morpholine ethane sulfonic (MES) buffer, 2mg/ml acetylated BSA, and 0.1mg/ml normal goat IgG for 10 min followed by a second staining with streptavidin phycoerythrin (SAPE) for 10 min at 25°C. After a final wash with a stringent buffer, the probe array was scanned at the excitation wavelength of 570 nm using an Agilent GeneArray Scanner (Palo Alto, CA).

After scanning, each image was first checked for major chip defects or abnormalities during hybridization as a quality control. Arrays were scanned using a global scaling strategy in which the average absolute signal intensity of all arrays was set to an arbitrary target signal intensity of 500 prior to uploading into GeneSpring 7.3 software (Agilent Technologies, Palo Alto, CA).

Data processing and global analyses. GeneChip signal intensity data from three biological replicates of NIH/3T3 cells were uploaded into GeneSpring 7.2 and filtered in a

similar fashion to that used for SCN2.2 cells (**98**). For each GeneChip probe set, signal intensities were converted to Log base 2 values and then normalized to the 50^{th} percentile of all measurements. Experimental averages of normalized data were calculated for each of 9 time points in NIH/3T3 cells. The data were then sequentially filtered at three levels. To verify gene expression, we filtered the probe sets according to two criteria: 1) detection of a "Present" flag in 55% or more of the time points and 2) a raw signal intensity value of ≥50 which was above the average experimental background signal in 55% or more of the time points. The temporal profiles of genes surpassing these expression criteria were filtered to isolate those showing stable expression. Stable genes were distinguished by temporal expression profiles that did not differ statistically (Standard correlation value: $p>0.995$) from a flat line created with the GeneSpring 7.3 "Draw Gene" tool. Finally, cycling genes with a peak-to-trough difference of 1.5-fold or greater and periodicities of 18-30 hours were identified among the remaining transcripts using methods similar to those described previously (**26, 98, 93**). The normalized data were cross-correlated ($p>0.90$) with cosine waves of specific phase and period using the PRISM software package (GraphPad, San Diego, CA). In addition, we imposed the requirement that rhythmic transcripts show at least one pair of non-overlapping standard error bars between time points with the highest and lowest values. The analytical and amplitude criteria used to identify cycling transcripts in NIH/3T3 cells are consistent with those applied in experimental analyses using cDNA or oligonucleotide arrays to profile circadian gene expression (**5, 26, 98, 93, 136**). Microarray data have been deposited in the National Center for Biotechnology Information's (NCBI) Gene Expression Omnibus (GEO) database (Accession Number GSE 5810).

To assess the false positive rate for profiling rhythmically expressed genes in our analysis, data files were randomized by converting each file to a two-dimensional data matrix and then assigning each element of the array a mapped integer key stored in a one-dimensional array. The one dimensional array of keys was randomized by a perl module (List::Utils) utilizing a Fisher-Yates algorithm. The shuffled keys were read from the array and converted to their corresponding location in the data matrix. Data values were then read from the data matrix and written to the output file sequentially, producing a randomized version of the original data file while maintaining the numerical composition of the file. This randomized data was then subjected to the same analytical and amplitude criteria used to identify cycling transcripts in the original data sets for NIH/3T3 cells. Based on this randomization analysis, we estimate false positive rates of approximately 21% for NIH/3T3 cells.

Bioinformatics and validation. Because some genes surpassing circadian expression filters were represented on the mouse U74v2 GeneChip multiple times, we used GeneSpring 7.3 and bioinformatic tools available as links from the National Center for Biotechnology Information (NCBI) (**109, 127**), including Basic Alignment Search Tool (BLAST) (**11**), to identify unique genes with circadian profiles in NIH/3T3 fibroblasts. To compare the expression profiles of specific genes in these fibroblasts with those found in SCN2.2 cells or the rat SCN, we identified genes that were commonly represented on the mouse (U74v2) and rat (U34a) GeneChips using the "Genome Homology" tool in GeneSpring 7.3. For a small subset of clock and clock-controlled genes, quantitative PCR (qt-PCR) was used to validate rhythmic expression in NIH/3T3 fibroblasts. Circadian expression of genes cAMP responsive element modulator (*Crem*), fatty acid synthase (*Fasn*), aryl hydrocarbon receptor nuclear translocator (*Arnt*), fibroblastic growth factor 7

(*Fgf7*), stearoyl CoA desaturase (*Scd1*), and the transcription factor *Sef/If2(Tcf4)* and the core clock genes *Per2*, *Bmal1 (Mop3)*, *Cry1*, was validated by qt-PCR. Quantification of relative mRNA abundance was performed using SYBR-Green real-time PCR technology (Applied Biosystems, Inc. [ABI], Foster City, CA). To generate single-strand cDNAs, total cellular RNA (1-2μg) was reverse transcribed using Superscript II (Invitrogen) and a primer mixture of oligo-dTs and random hexamers. Using the cDNA equivalent of 30ng of total RNA, duplicate aliquots of each sample were then PCR amplified in an ABI PRISM 7700 sequence detection system (56). The following probes and primers were designed using PrimerExpress software (ABI):

mPeriod 2 forward: 5'-ATGCTCGCCATCCACAAGA-3'

mPeriod 2 reverse: 5' -GCGGAATCGAATGGGAGAAT- 3'

mCry1 forward: 5'-CTGGCGTGGAAGTCATCGT-3'

mCry1 reverse: 5'-CTGTCCGCCATTGAGTTCTATG-3'

mBmal1 (Mop3) forward: 5'-CCAAGAAAGTATGGACACAGACAAA-3'

mBmal1 (Mop3) reverse: 5' - GCATTCTTGATCCTTCCTTGGT-3'

Aryl hydrocarbon forward: 5'-GCATGGGCTCACGAAGGT-3'

Aryl hydrocarbon reverse: 5'-AACAGGGTCCACGGAGCTAGT-3'

cAMP responsive element modulator forward: 5'-GGCTGCTGCCACAGGTG-3'

cAMP responsive element modulator reverse: 5'-CACCTTGTGGCAAAGCAGTAGT-3'

Fgf7 forward: 5'-AAGGGACCCAGGAGATGAAGA-3'

Fgf7 reverse: 5'-TGCCACAATTCCAACTGCC-3'

Scd1 forward: 5'-AACACCATGGCGTTCCAAA-3'

Scd1 reverse: 5'-GGTGGGCGCGGTGAT-3'

CypA forward: 5'-TGTGCCAGGGTGGTGACTT-3'

CypA reverse: 5'-TCAAATTTCTCTCCGTAGATGGACTT-3'

To control for differences in sample RNA content, either cyclophilin A (*CypA*) mRNA or ribosomal RNA (rRNA) was amplified with the cDNA equivalent of 1ng total RNA from the same samples. For all reactions, the comparative C_T method described in the ABI Prism 7700 Sequence Detection System User Bulletin #2 was utilized to calculate the relative mRNA abundance for a given target gene. Using this method, the amount of target gene mRNA in each sample was normalized first to corresponding *CypA* mRNA or rRNA levels, and then relative to a calibrator consisting of pooled cDNA from multiple samples that was analyzed on each reaction plate. Relative abundance of target mRNA was represented as a percentage of the maximal value obtained within an individual experiment.

Analysis of circadian phase and gene tree clustering. Consistent with our transcriptional profiling analysis of SCN2.2 cells (**98**), the phase of rhythmic genes in NIH/3T3 cells was determined by comparing the first peak of cyclic mRNA abundance (maxima of normalized signal intensity) in relation to the first four sampling intervals and to the circadian expression profiles of core clock genes. Based on this comparative relationship, rhythmically-expressed genes showing peak mRNA abundance during the first (hour 0), second (hour 6), third (hour 12) or fourth (hour 18) sampling interval with recurrent 24-hour peaks thereafter were respectively assigned to Phase Group (PG) I, II, III, and IV. For genes within each phase group, gene tree clustering was used to identify clusters of transcripts with similar expression patterns. Genes displaying common expression patterns were positioned on nearby branches separated by a distance of 0.02 or less using the Gene Tree clustering tool in GeneSpring 7.3. Clustered branches fulfilling

this separation threshold were comparatively labeled in relation to the circadian expression profiles of clock or other clock-controlled genes within the cluster.

RESULTS AND DISCUSSION

Global and circadian properties of gene expression in NIH/3T3 cells. Global expression and circadian regulation of the NIH/3T3 transcriptome was examined over two cycles. In forskolin-stimulated NIH/3T3 cells, 5,830 (47%) of the 12,500 probe sets on the mouse U74v2 GeneChip fulfilled expression criteria. Of these detected probe sets, most (94%) displayed either stable (N=2391) or non-circadian (N=3111) patterns of expression (**Table 4A**). Relative to the total number of probe sets, a small proportion (2.6%) consisting of 157 unique genes and 166 ESTs or genes of unknown function was distinguished by circadian profiles in fibroblasts (**Fig. 10**). Oscillations in NIH/3T3 expression profiles for some of these transcripts and the core clock genes *Per2*, *Cry1*, and *Bmal1* (*Mop3*) were validated by qt-PCR (**Fig. 11**). For NIH/3T3 rhythms in mRNA abundance, the amplitude of differences between peak and minimum levels ranged from 1.5 to 3.6-fold. The clock genes *Per2* and *Cry1* were among those oscillations with the highest rhythm amplitude in NIH/3T3 cells. The extent of circadian expression in the NIH/3T3 transcriptome is consistent with recent studies of serum-treated rat-1 fibroblasts (**32**) and in rat 3Y1 embryonic fibroblasts (**47**) in which the relative percentage (1-2%) and number of rhythmic genes (≈41-85) were similarly low. Based on direct comparisons of homologous transcripts, NIH/3T3 cells showed only a limited set of rhythmically-expressed genes in common with serum-treated rat-1 fibroblasts (10%) and embryonic fibroblasts (15%) (**32, 47**). *Annexin*, *Rora*, *Cdk4*, Ubiqutin-like protein 4 (*Ubl4*), histone *H2a*, and RAN GTPase activating protein 1 represent genes with circadian profiles that were common among NIH/3T3 cells and these fibroblast lines (**Table A.3**).

Table 4. ***Comparison of gene expression and function in NIH/3T3 fibroblasts, SCN2.2 cells and the rat SCN.***

A. Global facets of gene expression/regulation

	NIH/3T3	SCN2.2	SCN	Common
Array Type	**mouse U74v2**	**rat U34A**	**rat U34A**	
Total Probe sets	**12500**	**8800**	**8800**	**2255**
Probe sets passing expression criteria	**5830**	**3993**	**2929**	**413**
Stable genes fulfilling stringent expression criteria	**2391**	**520**	**584**	**60**
Rhythmic genes fulfilling stringent expression criteria	**323**	**162**	**301**	**4**
Percentage of examined genes with rhythmic profiles	**2.6%**	**1.8%**	**3.4%**	**0.2%**

B. Functional categorization of non-rhythmic genes

	NIH/3T3	SCN2.2	SCN	Common
Category 1 - Energetics	**55 (2.6%)**	**37 (3.9%)**	**32 (5.3%)**	**10 (6.2%)**
Category 2 - Cell Communication (including Neurotransmission)	**455 (21.7%)**	**232 (24.2%)**	**178 (29.3%)**	**30 (18.5%)**
Category 3 - Protein Dynamics	**241 (11.5%)**	**45 (4.7%)**	**16 (2.6%)**	**5 (3.1%)**
Category 4 - Cellular Development	**1082 (51.6%)**	**547 (57.2%)**	**331 (54.5%)**	**108 (66.7%)**

Comparative analysis of gene expression and function in NIH/3T3 cells, SCN2.2 cells, and the rat SCN. (**A**) Array type, total number of probe sets, global characterization of transcripts fulfilling expression criteria and whether these genes were stably or rhythmically expressed in NIH/3T3 cells, SCN2.2 cells, the rat SCN, or in common among all oscillator models. For individual and common determinations, the proportion of rhythmic genes relative to the total number of genes/probe sets on the mouse and rat GeneChips is also listed. (**B**) Functional characterization of genes with non-rhythmic expression profiles based on their segregation into seven basic categories: 1) **Energetics**, 2) **Cell Communication** (including neurotransmission genes), 3) **Protein Dynamics**, 4) **Cellular Development**, 5) **Defense and Detoxification**, 6) **Cytoskeleton and Adhesion**, and 7) **Unknown or ESTs**. In each category, the number of non-rhythmic transcripts (and percentage relative to the total number of functionally annotated genes with acyclic profiles) is compared between NIH/3T3 cells, SCN2.2 cells, the rat SCN and all experimental models.

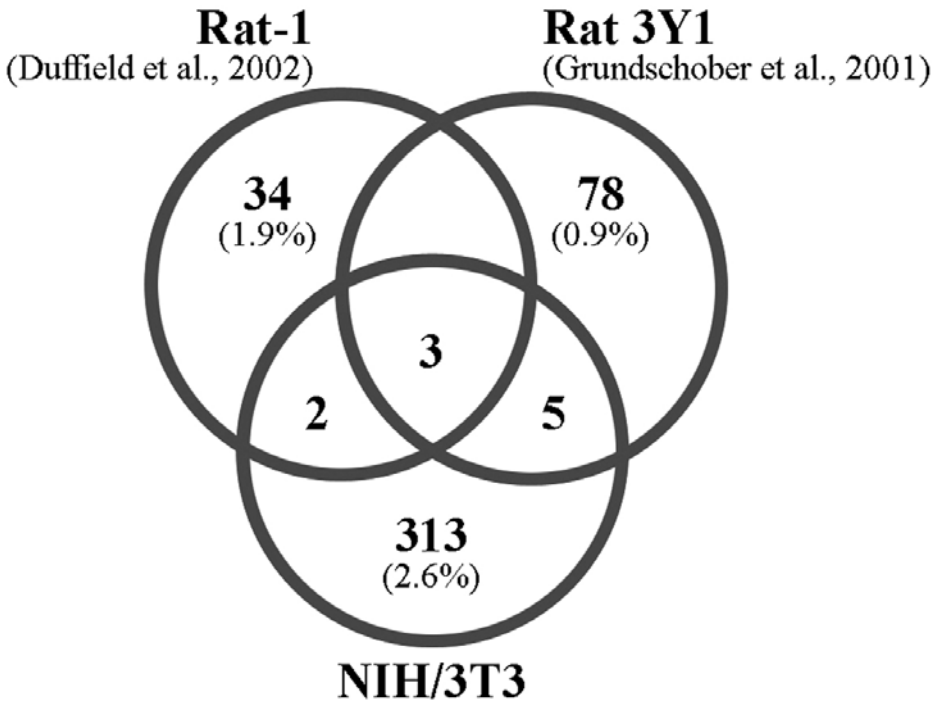

Fig. 10. Venn diagram comparing circadian expression of homologous or functionally related genes in NIH/3T3 cells with that reported for rat-1 (**32**) and rat 3Y1 fibroblasts (**47**). Specific genes with rhythmic profiles in NIH/3T3 cells and rat 3Y1 or rat-1 fibroblasts are listed in **Table A.3**. For each fibroblast line the percentage of rhythmic gene expression in proportion to the total number of genes or probe sets examined is denoted in parentheses.

The overlap in circadian gene expression between NIH/3T3 and rat-1 fibroblasts was especially evident within cell signaling genes associated with the Ras/MAPKinase pathway (**32**). The limited degree to which the circadian regulation of specific genes was common among NIH/3T3, rat-1, and rat 3Y1 embryonic fibroblasts may reflect differences in experimental analysis across these studies, including the developmental and/or species-specific origin (mouse verses rat) of these lines, the type of stimulus used to induce rhythmicity (forskolin versus serum shock), specific criteria for identifying rhythmicity, sampling interval and duration of analysis and the array type (Affymetrix or cDNA). The narrow scope and overlap of fibroblast oscillations in gene expression reported in this and previous studies are similar to that found among peripheral tissues *in vivo* (**33**). Collectively, these observations support the view that circadian regulation of the transcriptome is largely cell- or tissue-specific so as to provide for the local coordination of important processes associated with their distinct functions.

Circadian phase and gene tree analyses. Based on comparisons of first peak of cyclic mRNA abundance in relation to the sampling intervals during the initial cycle (**see Methods**), rhythmic genes in NIH/3T3 cells were distributed across all phases of the circadian cycle. The circadian patterns and phase distributions of the clock genes *Per2* and *Bmal1* (*Mop3*) and several other rhythmic transcripts were corroborated by qt-PCR (**Fig. 11**). In NIH/3T3 fibroblasts, peak mRNA levels were observed at hour 0 and 24 for *Per2* and at hour 12 and 36 for *Bmal1* (*Mop3*) so the profiles for these clock genes were respectively categorized as PG I and PG III oscillations. Of the 323 rhythmically-expressed unique genes or ESTs in NIH/3T3 fibroblasts, 238 exhibited PG I oscillations in which peak mRNA abundance coincided with the zenith of *Per2* expression whereas

23 exhibited PG III oscillations in which peak levels were contemporaneous with the crest of *Bmal1* expression. The remaining groups of 25 and 37 transcripts with circadian profiles were distributed in PG II and IV, respectively.

Rhythmically-expressed transcripts were analyzed further using gene tree clustering to determine whether the full temporal profiles were similar among a number of genes within each phase group. Within each phase group, clusters of rhythmic genes with similar expression profiles were assigned to a common branch. Gene lists of transcripts contained in these clusters are available at http://genenet.tamu.edu/servlet/GSWG. An interesting ramification of this analysis is that the specific temporal patterns of expression differ even among core clock components and other rhythmic genes with coincident peaks of mRNA abundance and thus common phase designation.

Functional analyses of non-rhythmic and circadian gene expression in NIH/3T3 cells. To assess how fundamental cellular processes are differentially expressed in forskolin-stimulated NIH/3T3 fibroblasts, the Gene Ontology lists in GeneSpring 7.3 were used to separately organize non-circadian and clock-controlled genes according to seven broad functional categories: 1) **Energetics**, 2) **Cell Communication**, 3) **Protein Dynamics**, 4) **Cell Development**, 5) **Defense and Detoxification** 6) **Cytoskeleton and Adhesion** and 7) **Unknown or ESTs**. Of the 5,502 detected probe sets with non-rhythmic expression profiles in forskolin-stimulated fibroblasts, 2,100 functionally-annotated genes were analyzed in this fashion. Functional categorization of these non-rhythmic genes revealed that 2.6% control energetic processes (N=55), 1.3% regulate aspects of neurotransmission (N=27), 20.4% are involved in cellular communication

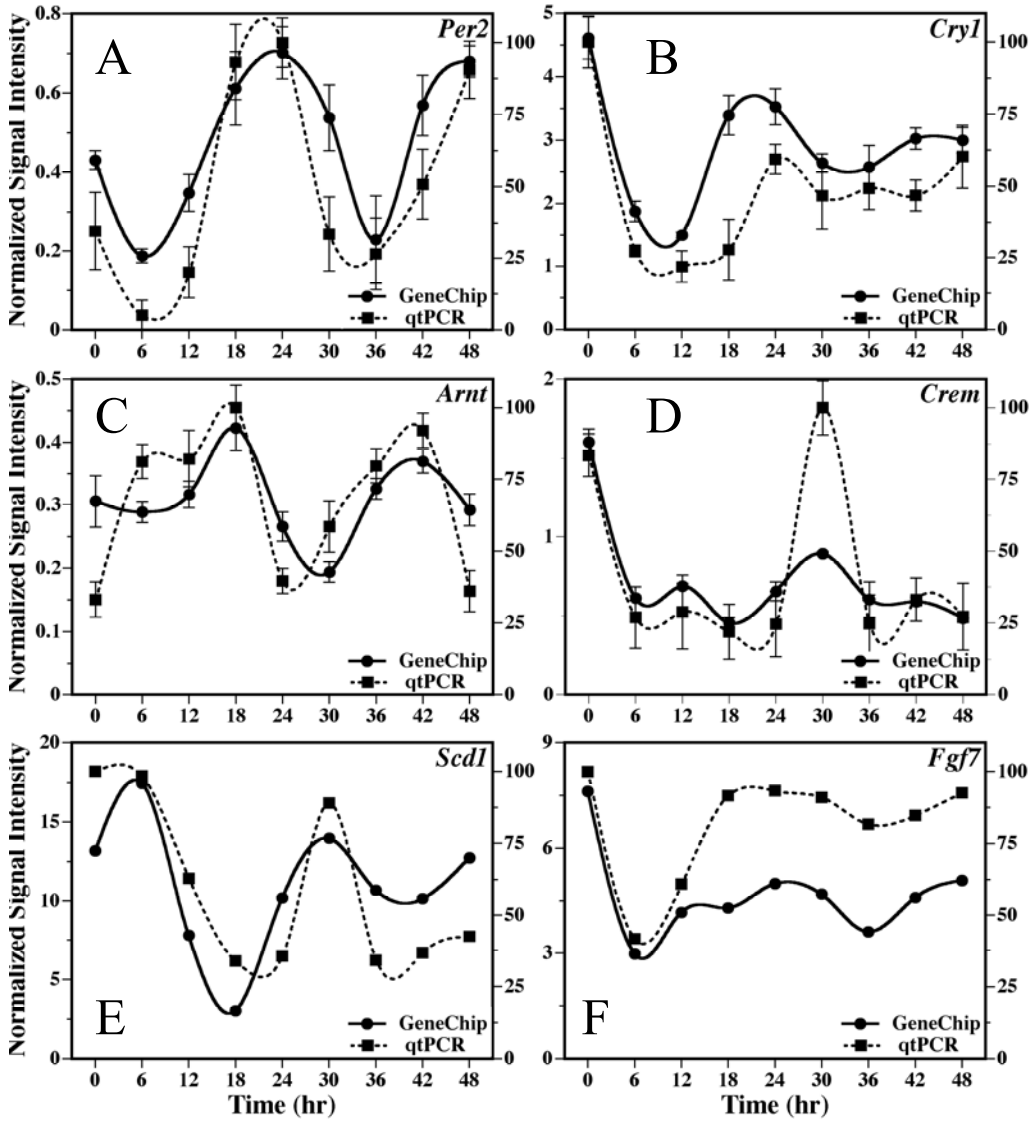

Fig. 11. Validation of GeneChip analysis examining Clock gene and circadian-regulated gene expression in NIH/3T3 fibroblasts. The profiles for GeneChip (λ, solid line) and qt-PCR (ν**,** dashed line) determinations of relative mRNA abundance are compared for (**A**) Period 2 (*Per2*), (**B**) Cryptochrome 1 (*Cry1*) (**C**) aryl hydrocarbon receptor nuclear translocator (*Arnt*), (**D**) cyclic AMP response element modulator (*Crem*), (**E**) stearoyl Co-enzyme A desaturase 1 (*Scd1*), and (**F**) fibroblastic growth factor 7 (*Fgf7*). For *Per2*, *Cry1*, *Arnt*, and *Crem* (**A**-**D**), the plotted values represent the averages (± SEM) of experimental replicates (n = 3) whereas individual determinations are shown for *Scd1* and *Fgf7* (**E**-**F**) to provide comparison within a given experiment. GeneChip determinations were established by normalizing values for Log base 2 signal intensity to the 50th percentile of all measurements per sample. For qt-PCR analysis, the plotted values correspond to the ratios of *Per2*, *Cry1, Arnt*, *Crem*, *Scd1*, *and Fgf7*/*CypA* mRNA signal in which the maximal value for each experiment was set at 100%. GeneChip and qt-PCR values are respectively plotted in relation to the primary and secondary ordinant in each panel.

N=428), 11.5% mediate the dynamics of gene expression by controlling protein translation, degradation, or trafficking (N=241), 51.6% regulate aspects of cell development including growth and maintenance (N=1082), 2.6%, are associated with defense and detoxification (N=55), and 9.9% affect cytoskeletal elements, cellular adhesion, or components of the extracellular matrix (N=208). Approximately 3,400 genes could not be assigned to a specific category due to a lack of sufficient functional annotation (**Table 4B**).

The 157 unique genes with circadian expression profiles in NIH/3T3 cells were similarly segregated into these broad categories and then subdivided further into specific functional clusters. In NIH/3T3 fibroblasts, 11% of the annotated genes with rhythmic expression profiles (N=17) were involved in the regulation of energetic processes. These genes with energetic functions were subdivided into 4 functional clusters: 1) glucose metabolism and mitochondrial energy transduction (N=2), 2) lipid and fatty acid metabolism (N=3), 3) transporters of energy metabolites (transporters) (N=4), and 4) miscellaneous metabolism (N=8) (**Table A.4**). In comparison with the SCN where there is ample evidence for the circadian regulation of genes associated with glucose metabolism and mitochondrial energy transduction (**98**), it is noteworthy that only two genes, 2,3-bisphosphoglycerate mutase (*Bpgm*) and ATP-specific succinyl-CoA synthetase beta subunit (*Scs/Sucla2*), in this functional cluster were rhythmically expressed in NIH/3T3 fibroblasts. The greatest proportion/number of genes with circadian profiles (35%, N=55) were involved in other forms of cellular communication.

Rhythmic genes in this category were further subdivided into functional clusters: 1) neurotransmission (N=2); 2) cytosolic signaling factors and transducers (N=25), 3) nuclear factors (N=22), 4) G-protein coupled receptors and associated proteins (N=5), and 5) extracellular factors (N=1). In the neurotransmission cluster, rhythmic mRNA expression in NIH/3T3 cells was similarly limited to two genes, glutamate cysteine ligase (*Gclm*) and the voltage-dependent calcium channel L type, α1C (*Cacna1c*). Of the rhythmically regulated genes with cytosolic signaling and transduction functions, two were involved in the regulation of the cAMP pathway: the cAMP-specific phosphodiesterases 4B (*Pde4b*) and 7A (*Pde7a*). In the nuclear factors cluster the rhythmically-expressed genes, CCAAT/enhancer binding protein (*C/EBP*), cAMP-response element modulator (*Crem*), cAMP inducible gene 3 / immediate early response 3 (*Ier3*), transcription factor 4 (*Tcf4*) and activating transcription factor 4 (*Atf4*), were also associated with the cAMP pathway. The sole extracellular factor with a circadian profile in NIH/3T3 fibroblasts was fibroblast growth factor 7 (*Fgf7).* Twenty-six genes (17%) with rhythmic patterns of expression in NIH/3T3 cells were involved in different aspects of protein dynamics including protein degradation and synthesis (N=15), protein sorting and trafficking (N=7), and protein modification and folding (N=4). Twenty-four rhythmic genes (15%) exhibited common functions in the regulation of cellular development. Rhythmic genes within the cell development category were involved in the regulation of cell cycle (N=5), maintenance of DNA and chromatin (N=10), and growth and differentiation (N=9). The defense and detoxification category encompassed 13% of the rhythmic genes in NIH/3T3 fibroblasts (N=21). Rhythmically regulated genes with defense and detoxification functions included small inducible cytokine subfamily D1,

cytokine inducible SH2-containing protein (*Cish*), and myeloid cell leukemia sequence 1 (*Mcl1*). Circadian regulation was observed in 14 annotated genes with cytoskeletal or cellular adhesion functions (9%) and representative examples of rhythmic genes in this category included hyaluronic acid receptor (*Cd44*), h2-Calponin 2 (*Cnn2*), and Integrin alpha V (*Cd51/Itgav*) (**Table A.4**). Differential representation on the mouse U74v2 GeneChip may be an influential factor in the observed prevalence of non-rhythmic genes mediating cell development and of rhythmic genes involved in cell communication because analysis using the Simplified Gene Ontology lists in GeneSpring 7.3 indicates that the probe sets on the array were biased for genes in these functional categories (≈21.3% and 11.1%, respectively).

Cross-model comparison of global and circadian properties. Because our analyses of circadian gene expression in the rat SCN and SCN2.2 cells used the same array technology and applied the same expression and rhythm amplitude criteria as well as the cross- correlation with cosine waves (**98**), we next compared the NIH/3T3 and SCN transcriptomes with regard to global properties and temporal regulation of gene expression. The breadth of gene expression in NIH/3T3 and SCN2.2 cells was similar (47% and 45%, respectively) and greater than that observed in the rat SCN (33%). In NIH/3T3 fibroblasts, 5,830 out of the 12,500 probe sets (47%) on the mouse U74v2 GeneChip surpassed expression criteria. Relative to the 8,800 probe sets on the rat U34a GeneChip, 3993 in SCN2.2 cells and 2929 in the rat SCN fulfilled expression criteria (**Table 4A**). Further comparisons revealed that the proportion of genes with stable expression profiles was greater in NIH/3T3 cells (19%, N=2391) than in SCN2.2 cells (12%, N=1035) or the rat SCN (7%, N=584), whereas the extent of circadian gene

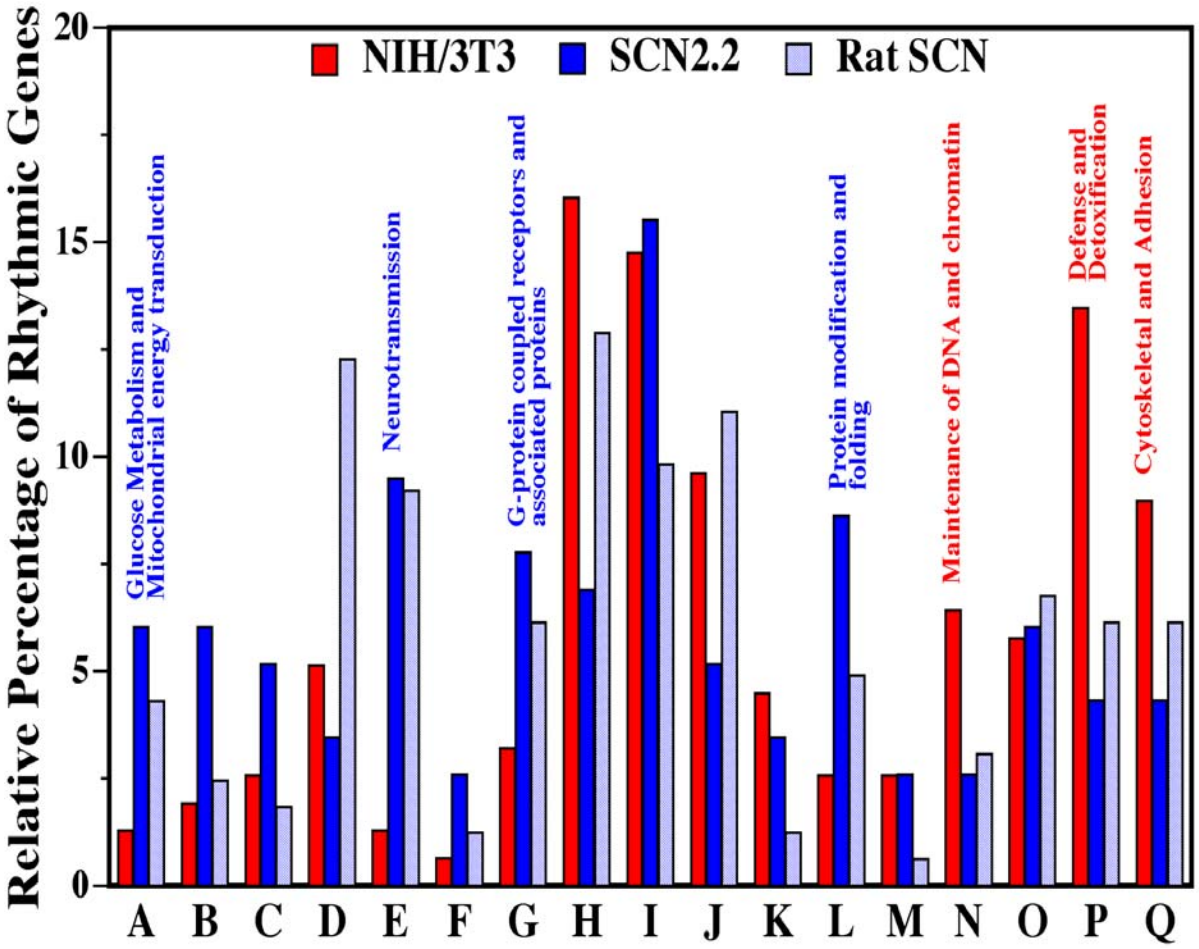

Fig. 12. Comparative functional classification of circadian gene expression in NIH/3T3 fibroblasts, SCN2.2 cells, and the rat SCN. In accord with our previous microarray analyses (**98**), rhythmically expressed transcripts in these oscillator models were comparatively subdivided into fifteen functional clusters, Glucose metabolism and mitochondrial energy transduction (A), Lipid and fatty acid metabolism (B), Transporters (C), Miscellaneous metabolism (D), Neurotransmission (E), Extracellular factors (F), G-protein coupled receptors and associated proteins (G), Cytosolic signaling factors and transducers (H), Nuclear factors (I), Protein degradation and synthesis (J), Protein sorting and trafficking (K), Protein modification and folding (L), Cell Cycle (M), Maintenance of DNA and chromatin (N), Growth and differentiation (O), and two functional categories, Defense and Detoxification (P), and Cytoskeletal and Adhesion (Q). Bars depict the percentage of rhythmic transcripts in each functional cluster or category relative to the total number of annotated genes with circadian profiles in NIH/3T3 fibroblasts (N=157), SCN2.2 cells (N=116), and the rat SCN N=163). Specific functional clusters and categories in which the proportion of rhythmic gene expression was differentially greater in NIH/3T3 fibroblasts, or in SCN2.2 cells and the rat SCN are respectively labeled in red and blue.

expression was similar across these oscillator models (2.6, 1.8, and 3.4%, respectively; **Table 4A**).

We also compared NIH/3T3 fibroblasts, SCN2.2 cells, and the rat SCN with regard to the functional distribution of genes with circadian profiles (**Fig. 12**). In all of these oscillator models, circadian fluctuations were observed in genes with a wide range of functions although rhythmic gene expression was typically more prevalent within certain functional categories or clusters. NIH/3T3 fibroblasts, SCN2.2 cells and the rat SCN exhibited some similarities in the functional distribution of circadian-regulated genes with cytosolic signaling factors, transducers, and nuclear factors in the cellular communication category commonly representing a large proportion of the annotated genes with rhythmic profiles. Corresponding to this functional distribution, genes mediating cellular communication are also prevalent among the cadre of rhythmic transcripts observed in mammalian peripheral tissues such as the liver, heart, and kidney (**149, 147, 67, 114, 33**). However, there were notable differences in the functional configurations of circadian gene expression in NIH/3T3 fibroblasts relative to those found in SCN2.2 cells and the rat SCN. Compared to the functional distribution of SCN oscillations, circadian rhythmicity in NIH/3T3 cells was differentially evident among genes associated with maintenance of DNA and chromatin (N), defense and detoxification (P), and cytoskeletal elements and adhesion (Q). Relative to NIH/3T3 fibroblasts, circadian profiles in both SCN2.2 cells and the rat SCN were more prevalent among genes involved in glucose metabolism and mitochondrial energy transduction (A), neurotransmission (E), the regulation of G-protein coupled receptors and associated proteins (G), and protein modification and folding (L). The extent of circadian regulation

was similar among all three oscillator models only for genes affiliated with cell growth and differentiation (O) (**Fig. 12**).

We then collectively assessed NIH/3T3 fibroblasts, SCN2.2 cells, and the rat SCN for overlap as well as fundamental differences in the temporal regulation of 2,255 probe sets with common representation on both the mouse U74v2 and rat U34a GeneChips (**Fig. 13**). Of these 2,255 probe sets, 413 (18%) fulfilled expression criteria used in this study. Many of these genes (N=344) were distinguished by stable (N=60) or non-circadian (N=284) expression profiles in NIH/3T3 fibroblasts, SCN2.2 cells, and the rat SCN (**Table 4A**), and functional annotations were identified for 162 of these non-rhythmic probe sets using our filters. Functional analysis of the commonality in the non-circadian expression of these annotated genes (N=162) across all three oscillator models revealed that these genes control diverse biological processes but were most prevalent in the cell communication (17.5%; N=27) and cellular development categories (67%; N=108) (**Table 4B**). It is interesting that the NIH/3T3 fibroblasts, SCN2.2 cells, and the rat SCN showed similar proportions of non-circadian gene expression in the cellular development and defense and detoxification categories (**Table 4B**).

Overlap in circadian gene expression across NIH/3T3 fibroblasts, SCN2.2 cells, and the rat SCN was limited to 4 of the commonly represented genes on the mouse and rat arrays (0.2%; **Fig. 13**): stearoyl-coenzyme A desaturase 1 (*Scd1*), long chain fatty acyl CoA synthase (*Facl*), transcription factor 4 (*Tcf4*), and Ngfi-A/early growth response 1 (*Egr-1*) (**Table A.4**). These rhythmic genes are involved in fatty acid or lipid metabolism (*Scd1* and *Facl*), or function as nuclear factors in cell communication pathways (*Tcf4* and *Egr-1*). Circadian expression of the core clock genes *Per2*, *Cry1*, and *Bmal1* was also

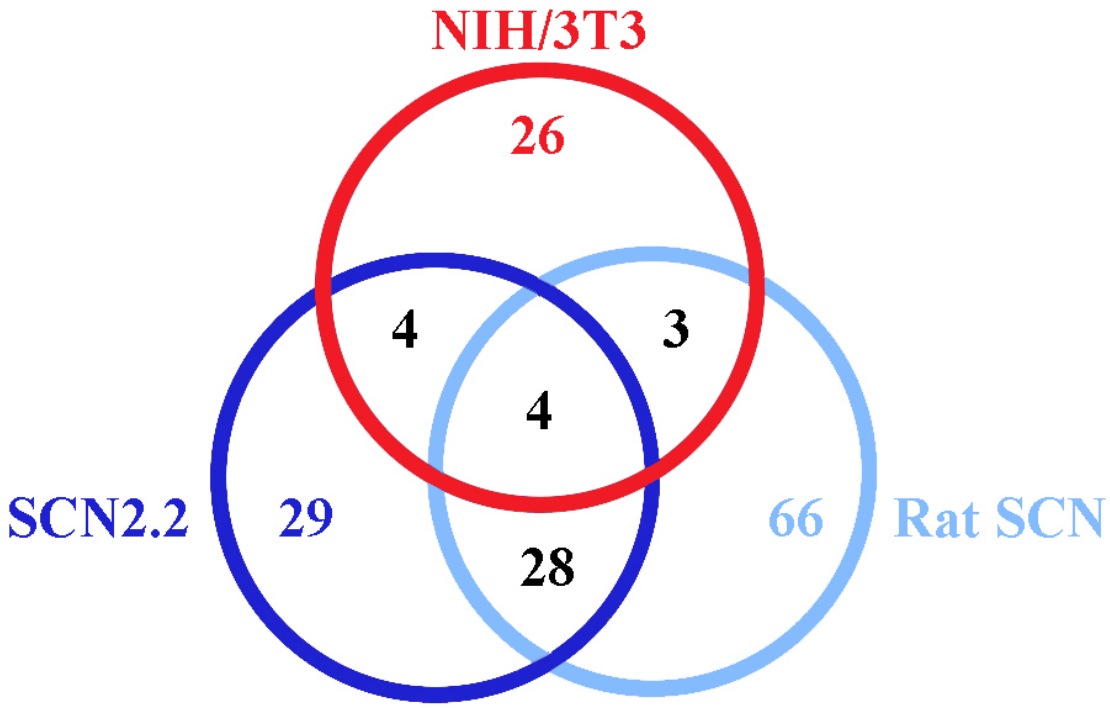

Fig. 13. Venn diagram illustrating overlap and differences in the circadian expression of commonly-represented genes among NIH/3T3 fibroblasts, SCN2.2 cells and the rat SCN. Probe sets for homologous or functionally related genes with mutual representation on both the mouse U74v2 and rat U34a GeneChips (N=2255) were analyzed and rhythmically-expressed genes in NIH/3T3 cells were compared with those identified previously in SCN2.2 cells and the rat SCN (**98**).

common among all three models, although this observation is based on qt-PCR analysis because the mouse and rat GeneChips are largely different with regard to the representation of specific clock genes. The limited degree of overlap in circadian gene expression between NIH/3T3 fibroblasts, SCN2.2 cells, and the rat SCN is consistent with reported comparisons of microarray data indicating that only 10% of the rhythmically-expressed transcripts were common to the SCN, peripheral tissues, and cultured fibroblasts (**33**), and that the canonical clock genes constituted the principal portion of this overlap in circadian gene expression. In both this review and the present comparative analyses, it is noteworthy that nuclear factors were identified as a prevalent functional categorization among the remaining common genes with circadian profiles. This observation suggests that the circadian regulation of nuclear factors may play a critical role in the common oscillatory function of different tissues throughout the body.

To complement this analysis of overlap between experimental models, the temporal expression profiles of the 2255 commonly represented probe sets were subsequently assessed for differences between NIH/3T3 fibroblasts and SCN cells. For genes and ESTs with non-circadian profiles, 194 (8.6%) were expressed in NIH/3T3 fibroblasts but not in SCN2.2 cells and the rat SCN. Of the annotated genes with non-circadian profiles that were exclusively expressed in NIH/3T3 cells, many were associated with cell communication (N=45; 23%) or cellular development (N=15; 8%) (**Table A.4**). It is interesting that the differential expression of non-circadian genes in NIH/3T3 cells includes three in the energetics category that function either in the transport of neurotransmitters [5-hydroxytryptamine (serotonin) transporter (*Slc6a4*) and glycine

transporter 1 (*Glyt1*)] or in the regulation of glucose metabolism [glycerol-3-phosphate dehydrogenase (*Gdm1*)]. Only 10 non-circadian genes (0.4%) were expressed in SCN2.2 cells and the rat SCN but not in NIH/3T3 fibroblasts. These genes with SCN-specific non-circadian profiles included defender against cell death (*Dad-1*), prostaglandin F2 receptor negative regulator (Ptgfrn), chemokine (C-X3-C motif) ligand 1 (*Cx3cl1*), ADP-ribosylation factor 4 (*Arf4),* farensyl diphosphate synthase (*Fdps*), isopentenyl-diphosphate delta isomerase (*Idi1*), par-3 (partitioning defective 3) homolog (*Pard3*), actin beta (*Actb*), serum and glucocorticoid-regulated kinase (*Sgk*), and gephyrin (*Gphn*).

For rhythmic genes and ESTs, 26 (1.2%) were marked by circadian expression in NIH/3T3 fibroblasts but not in SCN2.2 cells and the rat SCN (**Fig. 13**). Annotated genes with fibroblast-specific circadian profiles were primarily involved in the regulation of cellular communication (N=8; 0.4%), and defense and detoxification pathways (N=6; 0.3%). Based on our previous microarray study (**98**), 28 annotated genes, 8 of which were identified using supplementary screening analyses, exhibited circadian expression patterns in SCN2.2 cells and the rat SCN but not in NIH/3T3 fibroblasts (**Table 5**). It is noteworthy that functionally annotated genes with SCN-specific rhythms of expression were predominantly involved in the regulation of intercellular communication (N=16) and energetic processes related to glucose metabolism and transport (N=7). The distribution of circadian-regulated genes in the former functional category may have some significance with regard to SCN-specific signals necessary for the endogenous generation of self-sustained rhythmicity, temporal synchrony among individual clock cells or pacemaker coordination of circadian rhythmicity in downstream oscillators. Inducible nitric oxide synthase *(iNos* or *Nos2*), syntaxin 4 (*Stx4a*), A-2 arylamine N-

acetyltransferase 1 (*Nat1*), Glycine receptor, alpha 1 subunit (*Glra1*), cytosolic phospholipase A2 (*Pla2g4a*), SAP kinase/mitogen-activated protein kinase 12 (*Mapk12/Erk-6*), serine-threonine kinase receptor/activin a receptor type II-like 1 (*Acvrl1*), calcitonin/calcitonin-related polypeptide, alpha (*Calca*), and pregnancy upregulated non-ubiquitously expressed CaM kinase (*Pnck*) are notable examples of genes in intercellular communication pathways with circadian expression profiles that were unique to SCN2.2 cells and the rat SCN. The identification of *Nos2* as a distinctive SCN output signal using this comparative microarray and bioinformatics approach is particularly intriguing in relation to previous functional studies targeting the other isoforms of this enzyme, neuronal *Nos* (*nNos* or *Nos1*) and endothelial *Nos* (*eNos* or *Nos3*). These studies suggest that NO signaling is not essential for SCN circadian function because mutant mice lacking *nNos* or *eNos* show normal activity rhythms with regard to their free-running patterns, entrainment to light-dark cycles, and phase-shifting responses to light (**74**). However, the function of *Nos2* in the SCN and the regulation of circadian rhythms has not been examined, presumably based on the implications of these studies and the prevailing bias that this isozyme is expressed by macrophages (**88**), but not SCN cells.

Table 5. ***Functional categorization of annotated genes with circadian profiles in SCN cells but not NIH/3T3 fibroblasts***

GenBank ID	Gene descriptor (symbol)
Category 1 - Energetics (N=7)	
Glucose Metabolism and Electron Transport Chain	
AI171506	Malic enzyme 1 (*Me1*)
K00750	Cytochrome c, somatic (*Cycs*)
J01435	ATP synthase 8, mitochondrial (*mt-Atp8*)
Transporters	
D63834	Monocarboxylate transporter (*Mct1/Slc16a1*)
S68135	Glucose transporter/solute carrier family 2, member 1/(*Glut 1/Slc2a1*)
Miscellaneous metabolism	
AI177004	Hmgc synthase 1 (*Hmgcs1*)
L19998	Sulfotransferase family 1A, phenol-preferring, member 1 (*Sult1a1*)
Category 2 - Cell Communication (N=16)	
Neurotransmission	
L20821	Syntaxin 4 (*Stx4a*)
U01344	A-2 arylamine N-acetyltransferase 1 (*Nat1*)
U08259*	N-methyl-D-aspartate receptor NMDAR2C subunit *(Grin2c)*
D00833*	Glycine receptor, alpha 1 subunit *(Glra1)*
AF007758*	Synuclein 1, alpha *(Snca)*

Table 5 - continued	
GenBank ID	**Gene descriptor (symbol)**
Cytosolic signaling factors and transducers	
U38376	Cytosolic phospholipase A2 (*Pla2g4a*)
X96488*	SAP kinase/mitogen-activated protein kinase 12 *(Mapk12/Erk-6)*
L36088*	Serine-threonine kinase receptor/activin a receptor type II-like 1 *(Acvrl1)*
L00111*	Calcitonin/calcitonin-related polypeptide, alpha *(Calca)*
D86556*	Pregnancy upregulated non-ubiquitously expressed *CaM kinase (Pnck)*
U16359*	Inducible nitric oxide synthase *(iNos/Nos2)*
Nuclear factors	
M63282	Leucine zipper protein/activating transcription factor 3 (*Atf3*)
U78102	Krox-20/early growth response 2 (*Egr2*)
M65251	HIV type 1 enhancer-binding protein 2 (*Hivep2*)
AF000942	Inhibitor of DNA-binding 3 (*Id3*)
L23148	Inhibitor of DNA-binding 1, splice variant 1d1

Category 3 - Protein dynamics (N=2)	
Degradation and synthesis	
AA859882	Ubiquitin carboxyl-terminal hydrolase 1 (*Uchl1*)
AA849648	Ribosomal gene L21 (*Rpl21*)

Category 4 - Cellular Development (N=3)	
Maintenance of DNA and chromatin	
H33461	Oxidation resistance 1 (*Oxr1*)
AA964849	ADP-ribosyltransferase 1 (*Adprt*)

TABLE 5 - continued	
GenBank ID	**Gene descriptor (symbol)**
Growth and differentiation	
D89983	Ornithine decarboxylase antizyme inhibitor (*Oazi*)

Category 5 - Defense and Detoxification (N=0)

Category 6 - Cytoskeletal elements and Adhesion (N=0)

Functional categorization of annotated genes with circadian expression profiles in SCN2.2 cells and the rat SCN but not NIH/3T3 fibroblasts. Genbank ID, gene descriptor and symbol, and functional category/cluster are denoted for each gene that was rhythmically expressed in both SCN2.2 cells and the rat SCN. Genes with SCN-specific rhythmic profiles were identified using previous expression criteria (**98**) and classified in accord with the functional categories as listed in Table 1. In addition, the energetics and cell communication categories were subdivided into the following clusters to further delineate gene function: **Glucose metabolism and mitochondrial energy transduction, Transporters**, **Miscellaneous metabolism**, **Neurotransmission**, **G-protein coupled receptors and associated proteins**, **Nuclear factors**, **Protein degradation and synthesis**, **Protein modification and folding**, **Maintenance of DNA and chromatin**, and **Growth and differentiation**. Asterisks denote rhythmic genes that were identified using secondary expression criteria (**98**).

Summary. Previous studies have suggested comparisons of array data provide negligible information beyond the indication that circadian gene expression is highly disparate among different tissues or cell types. Our comparative analyses of gene expression profiles in NIH/3T3 fibroblasts, SCN2.2 cells and the rat SCN are certainly consistent with this general observation, but also underscore some implications of the limited overlap and substantial differences in rhythmic transcripts across these oscillator models. In conjunction with the canonical clock genes, *Per2*, *Cry1* and *Bmal1*, genes that mediate fatty acid or lipid metabolism (*Scd1* and *Facl*), or function as nuclear factors in cell communication pathways were the only rhythmically expressed transcripts in common among NIH/3T3 fibroblasts, SCN2.2 cells and the rat SCN. Further analysis is warranted to determine whether genes in these functional clusters are responsible for the common oscillatory properties of the SCN and other tissues or cells throughout the body. The present identification of SCN-specific differences provides further insight into why the SCN *in vivo* and SCN2.2 cells, but not fibroblasts, are capable of generating self-sustained rhythmicity and functioning as circadian pacemakers. *Nos2* and other circadian-regulated genes involved in the regulation of intercellular communication were differentially identified as critical circadian signals expressed only in SCN cells. Based on our analysis of NOS function in this study, these genes will provide a suitable focus for identifying signaling pathways responsible for the coupling of SCN oscillators or the coordination of rhythmicity in other cells and tissues.

CHAPTER IV

INVOLVEMENT OF THE NO/NOS2 SIGNALING PATHWAY IN THE CIRCADIAN PROPERTIES OF IMMORTALIZED SCN (SCN2.2) CELLS*

INTRODUCTION

An important functional property of the SCN is that its cells are capable of generating self-sustained molecular and physiological oscillations. Circadian rhythms in cellular metabolism, neuropeptide secretion, electrical activity, and gene expression are endogenous to the SCN *in vivo* and persist following isolation of SCN cells *in vitro* (**69**). Importantly, these molecular and physiological oscillations are not only an ensemble property of the entire nucleus but are also generated by individual SCN neurons, suggesting that the SCN contains a network of cell-autonomous oscillators. When maintained on microelectrode plates, individual neurons in dissociated culture of the rat SCN express independent oscillations in firing rate that differ widely with regard to circadian phase and period, despite the presence of synaptic connections (**158**). In similar fashion, SCN cells in brain slice preparations also exhibit multi-phasic waveforms in *Per-1*-driven GFP-fluorescence (**128**). Because this rhythmic behavior is derived from the autonomous oscillations of individual neurons (**128**), identification of the processes responsible for the relative coordination of rhythmicity across multiple cellular clocks is

---

*Used with permission. **Menger GJ, Allen GC, Neuendorff N, Nahm SS,Thomas TL, Cassone VM, and Earnest DJ.** Circadian profiling of the transcriptome in NIH/3T3 fibroblasts: comparison with rhythmic gene expression in SCN2.2 cells and the rat SCN. *Physiol Genomics.* Epub. 2007.

of critical importance for understanding the mechanisms by which individual SCN clock cells are coupled and function as a pacemaker that regulates circadian rhythms in other cells and tissues.

Based on comparative microarray analyses described in the previous chapter, the observed prevalence of circadian expression profiles in SCN2.2 cells and the rat SCN among genes mediating intercellular communication may have some significance with regard to SCN-specific signals necessary for the endogenous generation of self-sustained rhythmicity and the temporal coordination of oscillations among individual clock cells or in other tissues. Among these intercellular signaling genes with SCN-specific circadian expression profiles, the identification of inducible nitric oxide synthase *(iNos* or *Nos2*), an isozyme involved in nitric oxide (NO) production, is intriguing for several reasons. First a role for the diffusible messenger, NO, in SCN pacemaker function is compatible with previous findings indicating that diffusible signals mediate the pacemaker function of SCN2.2 cells in conferring rhythmicity to cocultured fibroblasts (**8, 10**) and the restoration of behavioral rhythmicity by SCN transplants *in vivo* (**143**). Furthermore, *Nos* function in SCN regulation of circadian rhythms is supported by the observation that treatment with L-NAME, a reversible inhibitor of all three isoforms of NOS in the CNS (**80**), alters the endogenous generation of metabolic rhythmicity in SCN2.2 cells and their capacity to pace oscillations in cocultures of untreated NIH/3T3 fibroblasts (**98a; Used with permission.**) (**Fig. 14**). In addition, other *Nos* isoforms, neuronal *Nos* (*nNos* or *Nos1*) and endothelial *Nos* (*eNos* or *Nos3*), but not *Nos2,* have been targeted for functional analysis of their involvement in SCN circadian function. These studies demonstrate that mutant mice lacking *nNos* or *eNos* show normal activity rhythms with

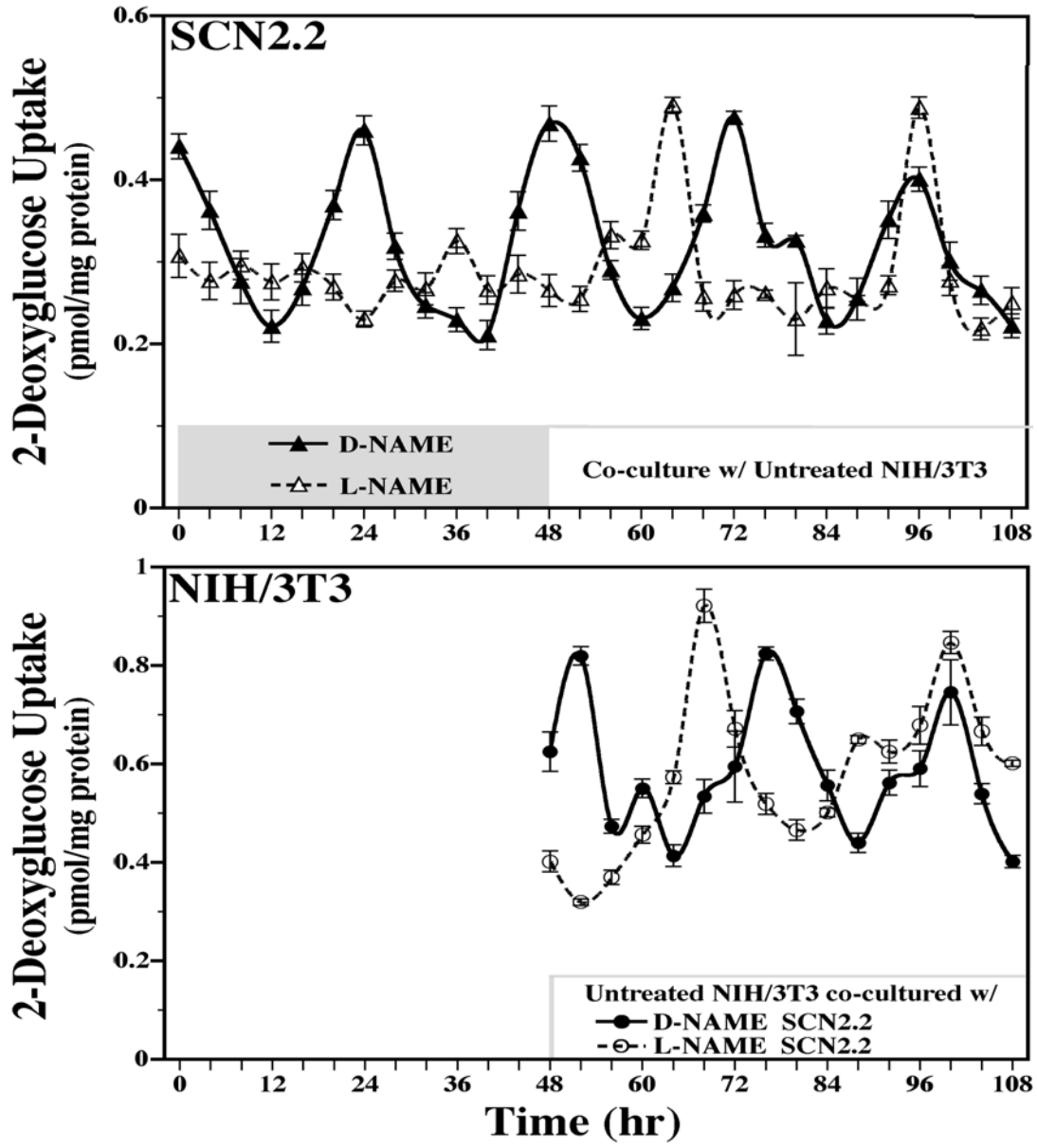

Fig. 14. Temporal profiles of 2-DG uptake in cocultures containing L-NAME- or D-NAME-treated SCN2.2 cells (top panel) and untreated NIH/3T3 fibroblasts (bottom panel). SCN2.2 cells were treated for 48 hours with the NOS inhibitor L-NAME (dashed line, Δ) and then cocultured for 60 hours with untreated NIH/3T3 cells (dashed line, ○). Control cultures of SCN2.2 cells were treated with its inactive enantiomer D-NAME (solid line, ▲) and then cocultured with untreated NIH/3T3 fibroblasts (solid line, ●). The shaded region in the top panel demarcates the interval of SCN2.2 treatment with L-NAME or D-NAME (hour 0-48). Symbols denote determinations of 2-DG uptake (n = 3; mean ± SEM) at 4-hour intervals. Values for 2-DG uptake are plotted as a function of time such that time 48 denotes when treated SCN2.2 cells were first cocultured with untreated NIH/3T3 fibroblasts. Asterisks indicate sampling intervals during which peak values for 2-DG uptake were significantly greater ($p < 0.05$) than those observed during preceding or succeeding minima. Used with permission (**98a**).

regard to their free-running patterns, entrainment to light-dark cycles, and phase-shifting responses to light (**74, 75**). Thus, *Nos2* function in the SCN clock and the regulation of circadian rhythms warrants further investigation.

The function of *Nos2* in SCN regulation of circadian rhythms has not been examined presumably based on the implications of these studies and the prevailing bias that this isozyme is expressed by macrophages (**88**), but not by SCN cells. Using our coculture model, the present experiments examined the effects of antisense inhibition of iNOS expression on the endogenous oscillatory and pacemaker properties of SCN2.2 cells. Morpholino antisense oligonucleotides were used to determine whether knock-down of *iNos* expression in SCN2.2 cells alters their rhythmic regulation of 2-deoxyglucose uptake and communication of this rhythmicity to cocultures of untreated NIH/3T3 fibroblasts. In comparison with approaches using transgenic mice in which a specific gene has been targeted for knock-out or disruption, application of this antisense method in our coculture model provides a unique advantage in examining *iNos/Nos2* function because NOS2 expression can be conditionally inhibited in SCN2.2 cells without affecting its expression in NIH/3T3 fibroblasts. This aspect presents an opportunity for dissociation of effects on the central pacemaker versus peripheral oscillators. Moreover, the utility of antisense morpholinos in knocking-down gene expression in SCN2.2 cells is supported by its successful application in previous studies (**8, 10**).

MATERIALS AND METHODS

Propagation of cell lines and general culture conditions. SCN2.2 and NIH/3T3 fibroblast lines of low passage number were propagated without antibiotics on culture dishes (60 mm; Corning, Corning, NY, USA) and maintained at 37 °C and 5% CO_2 in minimum essential medium containing 10% fetal bovine serum (FBS), 3000 μg/ml glucose, and 292 μg/ml L-glutamine. Culture dishes containing SCN2.2 cells were pre-coated with laminin. During cell propagation, the medium was changed at 48-h intervals, and cultures were split every 2–3 days when at confluence.

Experiment 1. Is nitric oxide (NO) produced by SCN2.2 cells? Confluent SCN2.2 cultures were subcultured onto laminin and poly-L-lysine coated glass culture dishes (35 mm, World Precision Instruments, Sarasota, FL, USA) in normal growth medium. Confluent cultures were rinsed two times with Dulbecco's phosphate-buffered saline (PBS; without calcium or magnesium, CMF), maintained in phenol red-free, HEPES buffered MEM with L-glutamine (imaging medium), and then treated with DAF-FM diacetate (final concentration 10 uM diluted in 0.2% DMSO) (Molecular Probes, Eugene, Oregon, USA) or vehicle for 1 hour at 37 °C and 5% CO_2. After treatment with DAF-FM, cultures were again rinsed with CMF and re-exposed to fresh imaging medium. Cultures were incubated at 37 °C and 5% CO_2 for an additional 30 minutes to allow for the de-esterification of internalized DAF-FM diacetate. This method for detecting low concentrations of nitric oxide (NO) is based on the principles that DAF-FM diacetate is a cell-permeable reagent that reacts with NO when deacetylated by cellular acetates. This intracellular reaction increases the fluorescence emission characteristics (515 nm) of the label by ~160-fold (quantum yield, ~ 0.81) (**Molecular Probes Product**

Information Sheet MP 23841, May, 2001). Imaging of intracellular NO was performed using 10-40X objectives an Olympus IX70 inverted microscope at the Real Time Imaging Lab Texas A&M Biology Shared Instrumentation Facility. Image acquisition of representative DAF-FM diacetate- and vehicle-treated cells was achieved using an Orca-ER CCD camera (Hamamatsu, Bridgewater, NJ, USA) and SimplePCI imaging software (Compix, Cranberry Township, PA, USA).

Experiment 2. Are the endogenous oscillatory and circadian pacemaker properties of SCN2.2 cells altered following antisense inhibition of iNos/Nos2? Using a coculture environment similar to that established in previous studies (**8, 10**), this experiment was conducted to examine the effects of antisense inhibition of *iNos/Nos2* in SCN2.2 cells on their capacity to generate endogenous metabolic rhythms, and to communicate this rhythmicity to untreated NIH/3T3 fibroblasts. SCN2.2 cells derived from a single passage were plated on multiple 6-well companion plates (Falcon, Oxnard, CA, USA) and treated at time of seeding with antisense (n=3) or invert of antisense (n=3) Morpholino oligonucleotides (Gene Tools, LCC, Philomath, OR, USA) directed against rat-specific *iNos /Nos2* mRNA. The published sequence of *iNos /Nos2* was used to design an antisense oligonucleotide to the region of the mRNA containing the initiation ATG codon (**109, 72**). The *iNos /Nos2* antisense and invert of antisense oligonucleotides were designed so as to have the same length (25-mers) and base composition (5′-GCAAGCCATGTCTGTGACTTTGTGC -3′ and 5′-CGTGTTTCAGTGTCTGTACCGAACG -3′, respectively). In parallel to these oligonucleotide-treated SCN2.2 cultures on companion wells, colonies of NIH/3T3 cells were established and maintained separately on cell-impermeable inserts (23 mm; pore

size=1 μm). Delivery of Morpholino oligonucleotides (final concentration=1.3 μM) into individual wells containing SCN2.2 cells was performed using the Endo-Porter delivery reagent, a system designed to promote endocytosis-mediated delivery of substances into the cytosol of adherent and non-adherent cells (Gene Tools, LCC, Philomath, OR, USA). The Endo-Porter delivery reagent was pre-mixed with prepared stock solution of Morpholino oligomers (invert and antisense). At the time of final passage SCN2.2 cells were treated medium containing the invert or antisense Morpholino oligonucleotide/Endo-Porter solution for 48 h. After removal of the delivery solution, the cells were rinsed two times with Dulbecco's phosphate-buffered saline (PBS; without calcium or magnesium) and then maintained in normal growth medium and cocultured with inserts containing untreated NIH/3T3 fibroblasts. After 20h in coculture, samples were collected at 4-h intervals for 52h to determine 2-deoxyglucose (2-DG) uptake in each coculture compartment. This analysis was performed on six companion wells and inserts at each time point across duplicate experiments. Cells were harvested with TRIzol reagent (Invitrogen, Carlsbad, CA, USA). Determinations of 2-DG uptake were then analyzed with a liquid scintillation counter.

Measurement of 2-DG uptake. SCN2.2 and NIH/3T3 cells were assayed for uptake of 2-DG using methods described previously (**37, 8, 10**). Peak values for rhythmic 2-DG uptake were identified when relative 2-DG levels were statistically higher than those observed during the preceding or succeeding minimum.

Western blot analyses. Morpholino antisense inhibition of iNOS/NOS2 peptide levels was verified by Western blot analysis using the Novex Western Transfer Apparatus (Invitrogen). Samples from each time point were homogenized individually with TRIzol

reagent and soluble protein was extracted according to the manufacturer's protocols. In experiment **2**, individual protein samples from antisense- or invert of antisense-treated SCN2.2 cells at each time point (n=3) were precipitated. The samples were boiled in sodium dodecyl sulfate sample buffer and loaded at 90 μg protein per lane onto 10% Tris–glycine gels. Following separation at 25 mA for approximately 2 h, proteins were transferred onto 0.45 μm nitrocellulose membranes and blocked overnight with 4% dried milk in Tris-buffered saline (TBS)–Tween (0.05%). With interceding rinses in TBS, membranes were probed for 48 h at 4 °C with rabbit anti- iNOS/NOS2 polyclonal antibody (pAb; 2 μg/ml; BD Biosciences) or rat anti-Tubulin monoclonal antibody (mAb) [YL1/2] (1:10,000; Abcam, Inc., Cambridge, MA, USA) followed by a 2-3-h incubation with horseradish peroxidase (HRP)-conjugated goat anti-rabbit IgG (at 1:20,000; Bio-Rad, Hercules, CA, USA) or rabbit anti-rat IgG (at 1:20000; Abcam, Inc.). Immunoreactive signal for iNOS/NOS2 or tubulin was generated by enzyme-catalyzed chemiluminescence (Perkin Elmer, Boston, MA, USA) and detected on film (Biomax; Kodak, Rochester, NY, USA). Optical density measurements for size-appropriate bands were obtained using Molecular Analyst software (Bio-Rad, Hercules, CA, USA).

Statistical analysis. Time-dependent fluctuations were identified by one-way analysis of variance (ANOVA). Paired comparisons between determinations of 2-DG uptake at specific time points were analyzed post hoc for statistical differences using the Newman-Keuls sequential range test. For Western blot analyses, standard t-tests were performed to determine if iNOS/NOS2 protein levels as measured relative to TUBULIN protein levels in the same samples were significantly different between invert of antisense- and antisense-treated SCN2.2 cell cultures.

RESULTS AND DISCUSSION

Experiment 1. SCN2.2 cells produce NO and express NOS2. Because recent microarray and qt-PCR results have demonstrated that SCN2.2 cells do indeed express *Nos2* mRNA (**98**), we sought to first determine if these pacemaker cells produce NO and then whether these cells express NOS2 protein. Imaging of intracellular NO using the cell permeable fluorescent indicator DAF-FM diacetate revealed that NO is present in both neuronal and glial cell types comprising SCN2.2 cultures (**Fig. 15**). Based upon the heterogeneity of cellular morphologies in SCN2.2 cell cultures, we found that glial cells charcterized by large flat cell bodies and stellate extensions typically exhibited diffuse NO-labeling whereas cells exhibiting neuronal features such as small, round soma and thin processes showed more intense labeling (**Fig. 15**). These findings suggest that glial and neuronal components of the SCN may produce different levels of NO and/or exhibit different patterns of subcellular compartmentalization. The possible distinctions in NO production between glia and neurons in SCN2.2 cultures is interesting and may reflect differences in how NO synthases (NOS) are regulated within and across these cell types. For instance, concentrated levels of NO indicated in neuronal type SCN2.2 cells may reflect higher NOS levels or activitiy whereas less intense NO-labeling observed in SCN glial cells may indicate lower NOS levels or activity. An intriguing question is whether NO production fluctuates in a circadian fashion across these different SCN2.2 cells.

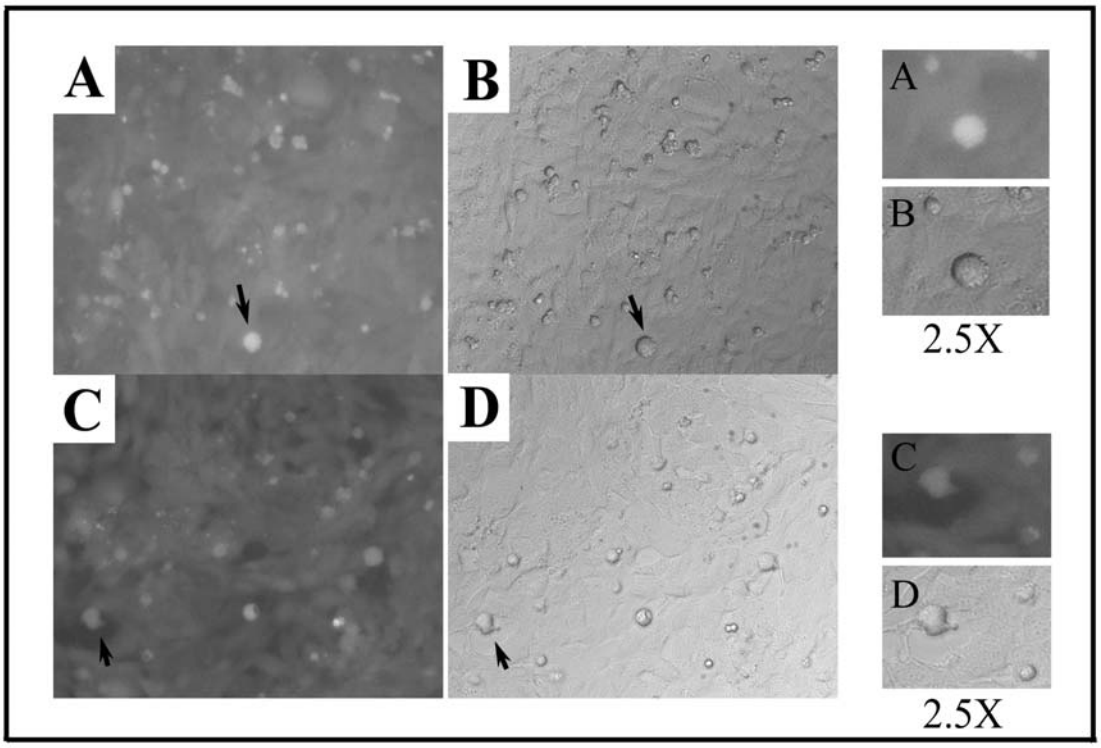

Fig. 15. Cellular distribution of nitric oxide in confluent cultures SCN2.2 cells as determined by DAF-FM diacetate labeling. Representative images of DAF-FM diacetate labeling (A and C) and their respective Nomarski images (D and F) in two different fields of view in SCN2.2 cell cultures. Images to the right reflect 2.5X magnification of neuronal type SCN2.2 cells indicated by arrows. These cells are charcterized by round cell bodies and neuronal type extensions. All images were captured using 20X objective magnification and enhanced in Adobe Photoshop 7.0.

It is also possible that post-translational processes and subcellular compartmentalization of NOS isoforms may contribute to patterns of NO distribution and activity observed in different SCN2.2 cell types (**7, 144, 112**). Through post-translational processes such as palmitoylation, NOS isoforms can be differentially modified and directed to the cell body or plasma membrane (**112**). Since both neuronal and inducible isoforms of NOS (*Nos1* and *Nos2*, respectively) are expressed in neurons and glia of the CNS (**100, 117**) and all three isoforms are expressed in the hypothalamus (**74, 75, 154**), the observed differences in NO localization in neuronal and glial components of SCN2.2 cultures may be related to differences in post-translational processing and subcellular compartmentalization among NOS isoforms.

Expression of NOS2 protein in SCN2.2 cells. Despite the prevailing bias that *Nos2* is only expressed by macrophages **(88),** our microarray data indicate that the mRNA encoding this isozyme is expressed in SCN2.2 cells and the rat SCN (**98**). Before examining the functional implications of *Nos2* expression, we next determined whether NOS2 protein was expressed in SCN2.2 cells. Western blot analysis revealed that NOS2 is expressed in SCN2.2 cells and its expression markedly increases after treatment with forskolin (30uM) (**Fig. 16**), which has been shown to augment the amplitude of molecular oscillations in SCN2.2 cells (**62**).

Experiment 2. Endogenous oscillatory and circadian pacemaker properties of SCN2.2 cells are altered following antisense inhibition of Inos/Nos2. To assess the functional involvement of *Nos2* in the circadian properties of SCN2.2 cells, we examined the effects of antisense inhibition of NOS2 expression on the capacity of SCN2.2 cells to endogenously generate metabolic rhythms and to convey these oscillations to cocultured

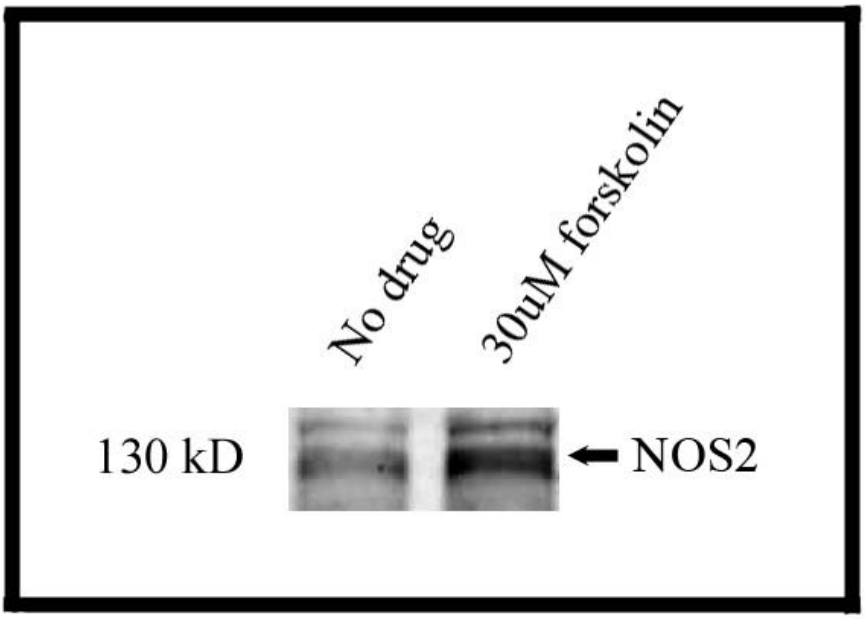

Fig. 16. Western blot analysis of forskolin-mediated increase in NOS2 abundance in SCN2.2 cells. Positive immunoreactivity for NOS2 protein is shown for SCN2.2 cells treated with vehicle (DMSO) (left lane) or 30 μM forskolin (right lane). 90 μg of total protein, as measured by the bicinchoninic acid method (Pierce, Rockford, IL, USA), were loaded in each well. Arrow indicates the predicted molecular weight of NOS2 (approximately 130 kD).

cells. Previous functional studies using L-NAME, to globally inhibit *Nos* and NO activity in the SCN (**80, 98a - used with permission.**) have provided little opportunity to distinguish between *Nos2* and other isoforms, neuronal Nos (*nNos/Nos1*) and endothelial Nos (*eNos/Nos3*), with regard to their relative importance in SCN circadian function. Consequently, analysis using Morpholino antisense approaches were necessary to directly assess *Nos2* function in the endogenous rhythm-generating and circadian pacemaker properties of SCN2.2 cells.

Sample collection for concurrent analysis of INOS/NOS2 protein levels and rhythmic 2-DG uptake was initiated 68 h after the onset of oligonucleotide treatment of SCN2.2 cells based on preliminary observations indicating that antisense oligonucleotides have no inhibitory effect on INOS/NOS2 expression in SCN2.2 cells prior to this interval. However, samples collected during the middle of the sampling period (96h) revealed that antisense treatment had a statistically significant effect in inhibiting NOS2 protein levels in SCN2.2 cells that were cocultured with NIH/3T3 cells (**Fig. 17**). NOS2 protein levels in antisense-treated SCN2.2 cells were 50% lower than those found in invert of antisense oligo-treated cells (**Fig. 17**).

Consistent with previous studies (**8, 9, 10**), the temporal profiles of 2-DG uptake in invert-treated SCN2.2 cells and cocultured NIH/3T3 fibroblasts were marked by circadian rhythmicity for two cycles *in vitro*, with a 4h phase delay in NIH/3T3 rhythmicity relative to that observed in SCN2.2 cells (**Fig. 18**). For both cell types in cocultures containing invert of antisense-treated SCN2.2 cells and NIH/3T3 cells, 2-DG uptake showed significant variation ($p<0.05$), with rhythmic peaks occurring at 24-h intervals. Maximal levels of 2-DG uptake significantly greater than the corresponding

A

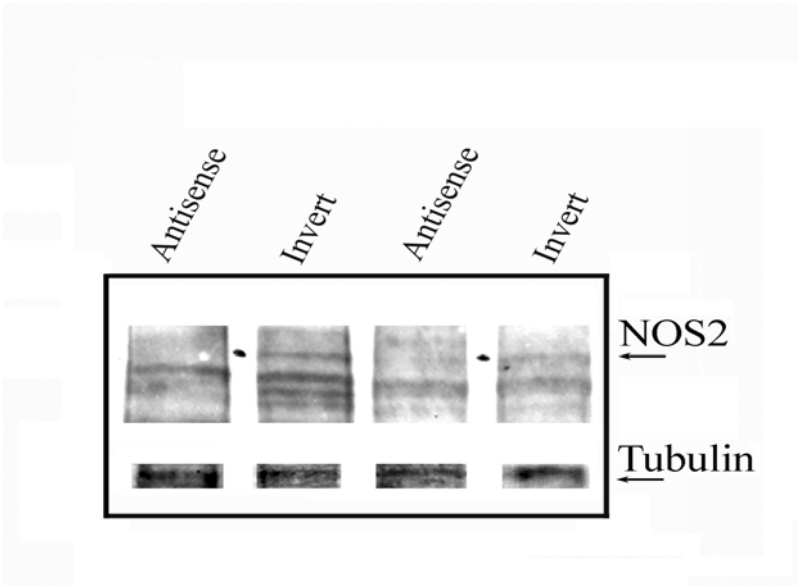

B

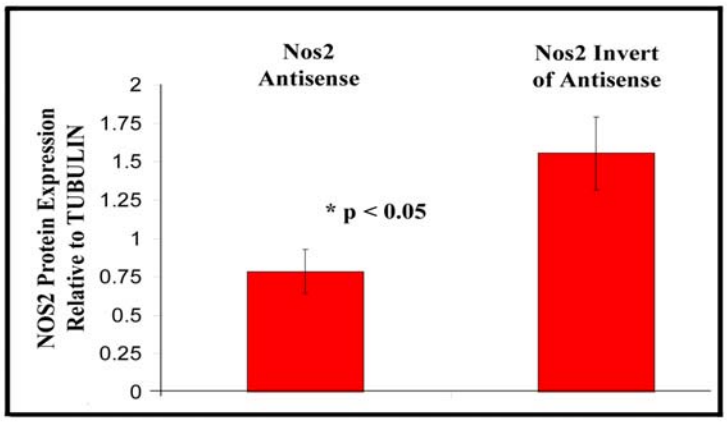

Fig. 17. Western blot analyses of NOS2 and TUBULIN protein levels in Morpholino-treated SCN2.2 cells cocultured with NIH/3T3 cells. Comparison of NOS2 (**A**) and TUBULIN (**B**) protein levels in SCN2.2 cells treated with either invert of antisense oligonucleotides (Invert) or *Nos2* antisense oligonucleotides (Antisense). Arrows indicate the NOS2 isoform (the predicted molecular weight approximately 130 kD) (above). Densitometric analysis of gels was utilized to quantify NOS2 protein levels in SCN2.2 cells and then normalized for TUBULIN in each treatment. Bars represent the mean (S.E.M.) determinations. NOS2-AS treatment significantly reduced NOS2 protein levels compared to with that observed for invert-treated cells. The asterisk (*) indicates statistical significance as determined by a standard T-test ($p<0.05$) (below).

minimum and occurred at 72 and 96 hours after transfection in invert-treated SCN2.2 cells and at 76 and 100 h post-treatment in cocultured NIH/3T3 cells. In contrast, SCN2.2 cells treated with *Nos2* antisense oligonucleotides abolished the rhythm of 2-DG uptake in SCN2.2 cells and in cocultured NIH/3T3 fibroblasts. 2-DG uptake in antisense-treated SCN2.2 cells did not show significant maxima (**Fig. 18**).

Summary. Based upon these observations, three independent but non-exclusive roles for the Nos2/NO pathway may be at work in SCN2.2 cells. First, the diminished abundance of NOS2 and presumably reduced function of the *Nos2*/NO pathway may upset the normal operation of SCN2.2 cell physiology. Alternatively, disruption of this pathway may directly impact the normal function of the canonical clockwork mechanism. However, because the self-sustained rhythmic properties of the SCN are thought to arise from the coupling of cell-autonomous SCN oscillators (**158, 61, 128**), reduced function of the Nos2/NO cell signaling pathway could disrupt the coupling and synchronization among populations of SCN2.2 oscillator cells. Consequently, desynchrony between individual SCN oscillator cells would seemingly compromise the ensemble function of the SCN in coordinating circadian rhythms in cells outside the SCN as well as its endogenous clock function. Enright (**1980**) suggests that changes of the coupling strength between oscillators will produce changes in the rhythm amplitude or period length and result in irregular ensemble rhythmicity (**39**). Indeed, SCN2.2 cells treated with Morpholino antisense oligonucleotides directed at the *Nos2* gene exhibited an abolished circadian rhythm of 2-deoxyglucose uptake relative to invert of antisense oligo-treated SCN2.2 cell cultures. These findings indicate the involvement of the NO/*Nos2* cell-signaling pathway in the coordination of circadian rhythms in SCN2.2 cells.

Since NO is known to function as a gaseous neurotransmitter, NO may also function as a diffusible messenger in the coordination or synchronization of metabolic oscillations among populations of NIH/3T3 cells. For NIH/3T3 cells, altered transmission of diffusible synchronizing signals from SCN2.2 cells would presumably diminish their ensemble rhythm amplitude of 2-deoxyglucose uptake in accord with the aforementioned properties descibed by Enright (**1980**) (**39**). Concomitantly, desynchrony among SCN2.2 oscillator cells may affect the circadian regulation of output signals responsible for driving rhythmicity in cocultured NIH/3T3 cells. Because the circadian rhythm of 2DG uptake was abolished in untreated NIH/3T3 cells cocultured with *Nos2* antisense-treated SCN2.2 cells, NO may function by either or both of these mechanisms. Thus, the metabolic rhythms of both SCN2.2 cells and NIH/3T3 fibroblasts may be sensitive to any loss of the temporal coordination between a large population of oscillating cells. Because the SCN clock is an autonomous property of individual SCN neurons (**158, 61**), the capacity of a population of SCN2.2 pacemaker cells to express endogenous rhythmicity and coordinate high-amplitude circadian signals controlling oscillations in NIH/3T3 fibroblasts is likely to depend upon their communication and coupling. The findings of this study suggest that *iNos/Nos2* contribute to this functional coupling and open the door for addressing two critical questions: 1) Is *Nos2* necessary to drive NIH/3T3 rhythms and 2) is it a necessary signal for SCN ensemble function or for the SCN to secrete a diffusible signal.

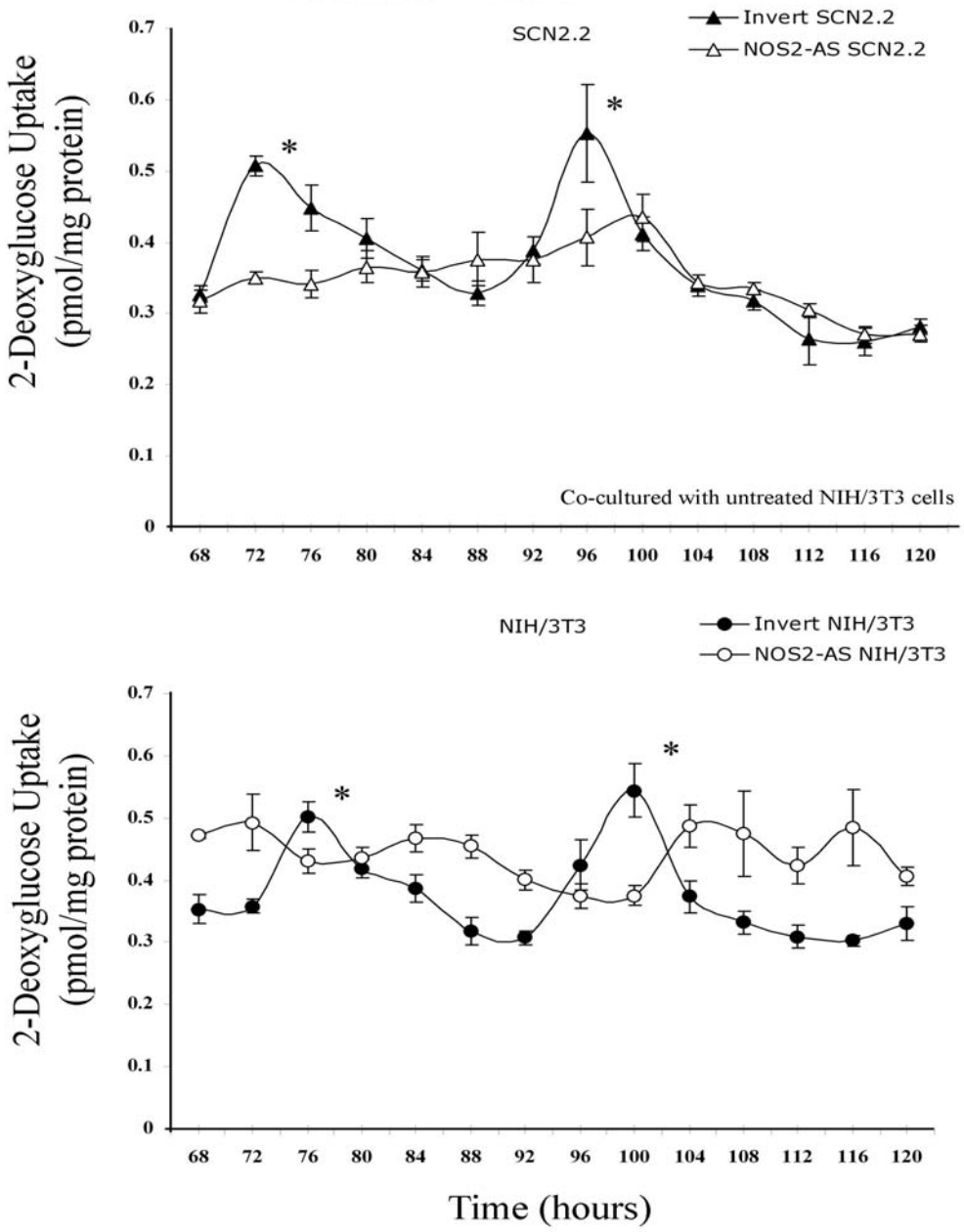

Fig. 18. Temporal profiles of 2-DG uptake in cocultures containing INVERT or ANTISENSE treated SCN2.2 cells (top panel) and untreated NIH/3T3 fibroblasts (bottom panel). SCN2.2 cells were treated for 48 hours with NOS2 ANTISENSE morpholino (-△-) and then cocultured with untreated NIH/3T3 cells (-○-) for 20 hours before sampling sampling began at 68 hours. Control cultures of SCN2.2 cells were treated with NOS2 INVERT morpholino (-▲-) and then cocultured with untreated NIH/3T3 fibroblasts (-●-). Symbols denote determinations of 2-DG uptake (n = 3-6; mean ± SEM) at 4-hour intervals. Asterisks indicate sampling intervals during which peak values for 2-DG uptake were significantly greater ($p < 0.05$) than those observed during preceding or succeeding minima.

CHAPTER V

GENERAL DISCUSSION AND CONCLUSIONS

Biological timekeeping systems have evolved in diverse taxa so that these organisms can adapt their internal biology and lifestyles in accord with the periodic environment. One of these timekeeping systems, the circadian timekeeping system, provides for the organization of physiological processes that are coupled to specific times of the light:dark cycle as well as the timing of other functionally-affiliated events inside the cell and throughout of the organism. Much of our understanding of circadian timekeeping systems is derived from founding studies of circadian rhythms in diverse organisms such as the fruit fly, bioluminescent bacteria, and nocturnal rodents. Victor Bruce, Karl Ashoff, Surge Daan, and Colin S. Pittendrigh, a prominent figure in the discipline of biological timing, established the foundation for the field by demonstrating that circadian rhythms of physiology and behavior are manifest in both single-celled and multi-cellular creatures. Further to their credit, these scientists established the formal properties used in the determination and analysis of bona fide circadian rhythmicity – properties that still serve as benchmarks in distinguishing circadian oscillations which damp from circadian rhythms that are self-sustaining. For both single- and multi-celled organisms, three formal properties are used to assess bona fide circadian rhythmicity, i.e. circadian rhythms necessarily exhibit 1) entrainment, 2) temperature compensation, and 3) persistency of a near 24-h rhythm in the absence of external input (**122**).

In creatures ranging from prokaryotes to humans, the circadian timekeeping system is configured such that three mechanistic components, designated in accord with their distinctive functional roles in 1) input pathways, 2) a core oscillator, or 3) output

pathways, interact to give rise to overt circadian rhythms of physiology and behavior. In mammals, this configuration is structured such that the suprachiasmatic nuclei (SCN) function as a master oscillatory locus that receives photic signals by means of the RHT and transmits output by means of neuronal and diffusible signals. Some of these outputs coordinate circadian rhythms throughout the body whereas others presumably feedback to the SCN via autocrine, paracrine, or neuroendocrine mechanisms.

It had been accepted for many years that the SCN function as a unique master oscillatory locus by driving circadian rhythms throughout the body via its output signals. This perception arose from several experimental observations. First, that ablation of the SCN abolished coordinated circadian rhythms in a wide range of molecular, physiological, and behavioral activities and that transplantation of only SCN tissue could restore rhythmicity in SCN-lesioned animals supported the notion that the SCN possessed intrinsic circadian properties which non-SCN tissues lacked (**104, 79, 147, 129, 69, 138**). Another avenue of experimentation demonstrated that the SCN actually constituted a network of cell-autonomous oscillators as individual SCN cells were shown to exhibit independently-phased circadian oscillations of neuronal electrical activity in one study and, in another, multi-phasic, cell-autonomous circadian rhythms of *Period1*-driven GFP-fluorescence (**158, 128**). Yet, more intriguing was the observation that even in the absence of exogenous synchronizing stimuli, including agents emulating RHT-derived signals, i.e. glutamate and PACAP, SCN tissue was still able to exhibit intrinsic 24h rhythms of metabolism, electrical activity, and gene and neuropeptide expression, *in vitro* (**131, 34, 44, 110, 131, 137**). Thus, the SCN was seen to exhibit not only unique cell-autonomous properties of circadian timekeeping but also indigenous pacemaker

properties, e.g. SCN cells could synchronize their circadian rhythms, even in the absence of external stimuli, and drive rhythms elsewhere in the body. The observation of these special properties of the SCN supported the notion that the SCN functioned as a collection of circadian pacemaker cells - pacemaker cells that were inherently different from cells residing in peripheral (non-SCN) tissues.

Circa 1997, Steve Reppert's and other laboratories began unveiling the molecular architecture of the core clockwork operating within the SCN (**131, 132**). It was shown at the message (mRNA) level and via protein profiling or direct gene knock-out studies that the core clock components oscillated in a circadian manner and functionally comprised molecular feedback loops that not only regulated the daily progression of their own rhythmic expression but, also, the normal 24-hour progression of overt circadian rhythms, in general. These findings fully supported a synthesis of ideas proposing that circadian rhythms of behavior and physiology extended from circadian rhythms of gene expression, a doctrine examined in this body of work. That the oscillations of the core clock genes were self-sustaining within the SCN, *in vivo and in vitro*, also gave rise to the designation of these genes as the 'molecular gears' of the 'SCN clockwork' (**131, 132**). Hence, since the SCN was believed to be inherently distinct from non-SCN tissues, the discovery that these molecular gears were expressed in the SCN began to fill in some of the gaps in explaining just how SCN cells were unique from non-SCN cells. However, very important experimental observations would soon emerge and actually uproot the notion that the SCN alone were distinguished by the expression of clockwork genes.

During the late 1990s, the use of serum-shock and cell synchronization paradigms in cell culture-based experiments was unequivocally demonstrating that non-SCN cells,

i.e. rat-1 and NIH/3T3 fibroblasts, could also display high-amplitude circadian oscillations of clock gene expression (**15, 16, 8, 9, 10**). And, by the turn of the century, real-time analysis of gene expression in non-SCN tissues had revealed that intrinsic circadian rhythms of clock gene expression were definitely not an exclusive feature of the SCN. The real-time recordings of circadian oscillations of PERIOD2::LUCIFERASE expression in non-SCN tissue explants and in individual cells derived from transgenic PERIOD2::LUCIFERASE-SV40 knock-in mice removed all doubt that even non-differentiated cells, i.e. fibroblasts pulled from the tip of the mouse tail, could exhibit persistent cell-autonomous rhythms of gene expression in the absence of SCN cell-derived signals (**162, 159**). Thus, the earlier perception that the SCN functioned to drive circadian rhythms throughout the body was not completely correct. What seemed to be a more precise interpretation of the sum of all experimental observations to this point was that the SCN functioned to synchronize or provide coordination among downstream oscillators residing in non-SCN tissues.

The finding that molecular rhythms were also presents in non-SCN cells and tissues prompted scientists in the field, even SCN-centrics, to redress the fundamental properties of the SCN that distinguished its cells from cells residing in peripheral tissues. To accomplish this task, two general experimental fronts were at work within the field: 1) comparative microarray-based analyses of the transcriptomes in SCN and peripheral tissues and 2) comparative physiological and functional analyses of cell-culture models that emulated the SCN and peripheral tissues.

First, microarray-based studies were undertaken to identify SCN cellular pathways regulated by the core clockwork in the mouse, a model system with a relatively well-

annotated genome at the time, to, not only, verify and characterize the gene-based doctrine of circadian regulation of cell function but, also, to shed light on molecular elements that might distinguish the SCN from non-SCN tissues such as liver, heart, and kidney (**114, 149, 147, 67**). These microarray-based studies clearly demonstrated that the molecular clockwork operating in the SCN coordinated rhythmicity in the expression of numerous genes that controlled diverse biochemical, cellular and physiological processes within the murine SCN, *in vivo* (**114, 149**). But, for comparative analyses, i.e. murine SCN vis-à-vis liver, heart, and kidney, the quintessential finding was that very few of the rhythmic genes expressed in the SCN were rhythmically expressed in any of a number of peripheral tissues (**33**). At the level of the transcriptome, distinctions between the SCN and peripheral tissues were easily seen.

This first experimental front also sought to identify genes and cell pathways that might function as SCN output signals, e.g. neuronal and diffusible signals that conveyed coordination of rhythmicity to non-SCN tissues, by means of their rhythmic expression in the SCN. Because some of these rhythmic genes, i.e. Prokineticin 2 and Tgf-α, were found to operate within neuronal or cell signaling pathways, these genes were fair game to screen as candidate output signals in the coordination of circadian rhythmicity in non-SCN tissues (**24, 73, 145**). However, a major hurdle in pursuing the goal of identifying output signals was gene selection: Which of the hundreds of genes expressed in the SCN were relevant to the indigenous functional properties of the SCN? While functional classification of the genes rhythmically expressed in SCN tissue could provide some insight regarding the potential role of a gene in a SCN output pathway, it did not completely compensate for the strategic confines of some of the earlier microarray-based

studies. In general, these studies did provided a characterization of the scope, function, and functional diversity and prevalence of rhythmic genes expressed in SCN and non-SCN tissues. However, what was needed to achieve the goal of directly identify candidate SCN output signals was the use of microarray-based analyses as an exclusionary screen.

The second experimental front at work in the field focused on comparative physiological and functional analyses of cell-culture models that emulated the SCN and peripheral tissues. To examine the physiological and functional properties of the SCN that distinguish its cells from those residing in peripheral tissues, David Earnest and co-workers developed an immortalized SCN (SCN2.2) cell line. SCN2.2 cells were shown to retain many of the properties of the SCN, *in vivo* and *in vitro*, and display functional properties that are unique vis-à-vis non-SCN cells, i.e. NIH/3T3 fibroblasts. For instance, a prominent feature of SCN2.2 cell cultures is their capacity to exhibit intrinsic circadian rhythms of endogenous molecular and metabolic functions, a characteristic not observed in cultures of non-SCN cells, presumably because these cells lack the capacity to self-synchronize. Another notable property is that SCN2.2 cells can communicate circadian rhythms of metabolism and gene expression to co-cultures of NIH/3T3 fibroblasts by means of a diffusible signal. Again, this property is not observed in non-SCN cells, as inferred from the observation that NIH/3T3 cells cannot coordinate or synchronize rhythms in co-cultured fibroblasts (**8, 10**). Thus, at physiological and functional levels, marked distinctions are also observed between SCN cells and non-SCN cells: 1) SCN2.2 cells show intrinsic synchrony whereas NIH/3T3 fibroblasts do not and 2) SCN2.2 cells can coordinate rhythms in non-SCN cells whereas NIH/3T3 fibroblasts cannot.

The tractability of SCN2.2 cells as an *in vitro* model and the clear functional distinctions observed between SCN2.2 cells and NIH/3T3 fibroblasts provided us with an opportunity to address goals that earlier microarray-based analyses of SCN and non-SCN tissues could not address. Namely, it was now possible to identify of a small set of rhythmic genes expressed within SCN cells, *in vivo* and *in vitro*, that were likely to underlie the unique functional properties of SCN cells. In fact, a direct microarray-based comparison of SCN2.2 cells and the rat SCN seemed to be a good first approach in pursuing the identification of rhythmic genes expressed in SCN cells that were functionally-relevant to their indigenous properties. We considered this approach to be the initial stages of a new, third, experimental front that incorporated a much needed and robust microarray-based screen to identify a small group of candidate genes and cell pathways by means of excluding genes not likely involved in the unique properties of SCN cells. We hypothesized that comparative circadian profiling of the transcriptome in SCN2.2 cells and the rat SCN, *in vivo*, would isolate a set of genes relevant to the functional properties observed in SCN2.2 cells (**CHAPTER II**). We predicted that these genes would work in cell pathways to 1) couple the cell-autonomous rhythm properties of individual SCN cells so as to permit ensemble 24-hour rhythms of cell function and / or 2) coordinate circadian rhythms in non-SCN cells.

Based on this initial comparative analysis (**CHAPTER II**), we found that many SCN-like global and circadian properties of gene expression were conserved in SCN2.2 cells. SCN2.2 cells and the rat SCN show 1) similar properties with regard to mRNA expression levels for many rhythmic and non-circadian genes, 2) oscillations in the expression of the core clock genes, and 3) many (35%) of the rhythmically-regulated

genes in SCN2.2 cells display rhythmic mRNA expression in the rat SCN, *in vivo*. A major finding derived from this study was that a predominance of genes rhythmically expressed in both SCN2.2 cells and the rat SCN were affiliated with cellular or systems-level communications and energetics pathways. Using functional and cartographic analyses, several of the rhythmic genes operating in these pathways were found to function at strategic points of pathway regulation. Thus, an important insight derived from the findings of this study was that the flow of temporal information to and from the clockwork mechanism in SCN cells might be achieved through the rhythmic regulation of key elements operating within cell signaling and energetics pathways.

Notably, at the heart of this comparative microarray-based analysis, was the identification of a special set of genes. This set of genes was special because it housed genes rhythmically expressed in both SCN models and many of these genes showed functional relevance to the indigenous properties of SCN cells by means of their affiliations with cellular or systems-level communications and energetic pathways. Nerve growth factor induced–A (*Ngfi-A*), Inducible nitric oxide 2 (*iNos/Nos2*), Monocarboxylate transporter (*Mct1/Slc16a1*), Glucose transporter/solute carrier family 2, member 1/ (*Glut1/Slc2a1*), Phosducin-like protein (*Pdcl/Phlp)*, and SAP kinase/mitogen-activated protein kinase 12 (*Mapk12*/*Erk-6*) are prominent examples of the 57 genes in this group. Knowledge that these genes were rhythmically regulated in the SCN and SCN2.2 cells and operating in cell pathways that potentially underpinned one or more of the unique properties of SCN cells was a major step towards advancing the field's understanding of the molecular basis of SCN cellular function.

Soon, however, pressure was mounting for us to start addressing the $64,000 question: Did one or more of these genes or their affiliated cellular pathways actually underpin the capacities of SCN2.2 cells to exhibit intrinsic rhythmicity and coordinate oscillatory properties in co-cultured NIH/3T3 cells? What was needed was an experimental determination of functional relevance. But which of the 57 genes in this special set was most likely to be functionally relevant to the hallmark indices of circadian function exhibited by SCN2.2 cells? And, should we focus on candidate genes that might function in cell pathways to coordinate rhythms in downstream oscillators or those that might underlying the capacity of SCN2.2 cells to self-synchronize? Indeed, one or more of the genes identified at the heart of this study could influence both types of indigenous properties.

One of the signaling pathways that rose to the top was the NO/*Nos2* signaling pathway. *Nos2* was the only one of three NOS isoforms that was found by means of our comparative circadian profiling study to be rhythmically expressed in SCN2.2 cells and the rat SCN. And, previous analysis of generalized inhibition of NOS isoforms was shown to disrupt the endogenous rhythmic properties of SCN2.2 cells whereas isoform-specific knockouts (*Nos1* and *Nos3*) in mice produced no significant perturbations of circadian behavioral properties, *in vivo*. Based on these observations, we hypothesized that the NO/*Nos2* pathway, functioned importantly in the coupling of individual SCN oscillator cells. The testing of this hypothesis using the SCN2.2 cell line seemed to be a logical path to pursue. Yet, critical insight that provided additional support for investigating this pathway was extended from a plausible alternate hypothesis: the NO/*Nos2* pathway might also function as a SCN output pathway that coordinates circadian rhythms in co-

cultured NIH/3T3 cells. This alternate hypothesis was given force and form by the second major aim of our experimental front - Circadian profiling of the transcriptome in NIH/3T3 cells: comparison to SCN2.2 cells and the rat SCN (**CHAPTER III**). Because SCN2.2 cells were shown by Allen and co-workers (**2001**) to retain the capacity to synchronize circadian oscillations in co-cultured NIH/3T3 fibroblasts by means of a diffusible factor, we hypothesized that rhythmic genes expressed in SCN2.2 cells and the rat SCN but not NIH/3T3 fibroblasts would function critically in the capacity of SCN cells to coordinate circadian oscillations in non-SCN cells (**8, 10**).

To test this hypothesis, it was necessary to conduct a thorough circadian profiling of the transcriptome in NIH/3T3 fibroblasts (**CHAPTER III**). Motivation for such an analysis arose from the fact that a comprehensive understanding of the genes and cell pathways regulated by the clockwork in NIH/3T3 cells was lacking. Indeed, knowledge of the scope, diversity, and functional facets of circadian regulation in NIH/3T3 cells was not only critical for the generation of hypotheses regarding the functional distinctions seen between SCN and non-SCN cells but, also, important in identifying common elements of circadian regulation among different types of oscillators. Secondly, the set of genes identified by our initial comparative analysis (SCN2.2 cells vis-à-vis rat SCN) was still rather large (N=57) (**CHAPTER II**). Because non-SCN cells had been shown to exhibit intrinsic rhythms of gene expression, it was necessary to address the issue of whether some of the genes housed within this initial set of rhythmic genes were also rhythmically expressed in NIH/3T3 fibroblasts, even though these cells did not exhibit similar functional features of SCN2.2 cells. Thus, by means of an exclusionary screen, a *modus operandi* exploited by Richter and co-workers in identifying the hypothalamus as

the region of the mammalian brain housing the circadian clock, we predicted that we would identify a small subset of rhythmic genes that were specific to SCN cells and highly likely to function critically in either synchronizing and / or coordinating circadian oscillations in non-SCN tissues.

Based on the circadian profiling of the transcriptome in NIH/3T3 cells, a small proportion (2.6%) consisting of 157 unique genes and 166 ESTs or genes of unknown function was distinguished by rhythmic profiles in these fibroblasts (**CHAPTER III**). A prevalence of these rhythmic transcripts was functionally-affiliated with cell communication, defense and detoxification, and cytoskeletal pathways. These findings are consistent with reports of rhythmic genes expression in other fibroblasts (rat-1 and 3Y1 fibroblasts) (**32, 47**). For instance, genes such as *Annexin*, *Rora*, *Cdk4*, Ubiqutin-like protein 4 (*Ubl4*), histone *H2a*, Ig kappa chain V-region, and RAN GTPase activating protein 1 represent rhythmically-expressed genes that were commonly regulated in NIH/3T3 cells and other fibroblast lines (**Table A.4**). The comparable extents and similar functional profiles of circadian regulated genes observed among NIH/3T3 cells and these other fibroblasts lines provided additional substantiation, beyond that already established by our co-culture model (**8, 10**), for the use of NIH/3T3 cells as a peripheral oscillator model in our comparative microarray-based screen.

Next, to screen for output signals that functionally distinguish SCN cells from peripheral-type oscillators in which the canonical clockworks are similarly regulated, the rhythmic behavior of the transcriptome in forskolin-stimulated NIH/3T3 fibroblasts was analyzed and compared to rhythmic genes identified in SCN2.2 cells *in vitro* and the rat SCN (**CHAPTER III**). This comparative examination revealed that similar to the

circadian profiling of the SCN2.2 and rat SCN transcriptomes, NIH/3T3 fibroblasts exhibited rhythmic fluctuations in the expression of the core clock genes and functionally diverse transcripts, many of which functioned cellular communication pathways. Overlap in circadian-regulated transcripts among NIH/3T3 fibroblasts, SCN2.2 cells and the rat SCN was limited to the core clock genes and four other genes that mediate fatty acid and lipid metabolism or function as nuclear factors. Because earlier microarray-based studies had not report these metabolic genes to be commonly expressed among SCN and non-SCN oscillators, our comparative microarray-based screen provided new insight and stimulated questions regarding the functional roles of metabolic pathways within the mammalian timekeeping system.

Yet, the highlight of this microarray-based screen was the identification of a select subset of candidate genes (N=28) that were shown to exhibit 1) SCN cell-specific circadian expression and 2) functional roles in cell pathways that potentially contribute to the indigenous properties of SCN cells function, i.e. self-synchrony and coordination of rhythmicity in non-SCN cells. Indeed, this comparative microarray-based analysis of SCN cells and NIH/3T3 cells effectively chiseled our initial set of 57 genes to 28 genes. Prominent examples of these 28 genes include Malic enzyme 1 (*Me1*), Monocarboxylate transporter (*Mct1/Slc16a1*), Glycine receptor, alpha 1 subunit *(Glra1),* N-methyl-D-aspartate receptor NMDAR2C subunit *(Grin2c),* Krox-20/early growth response 2 (*Egr2*), and, as previously mentioned, Inducible nitric oxide synthase *(iNos/Nos2).* Thus, the identification of genes rhythmically expressed in the SCN *in vivo* and SCN2.2 cells, but not NIH/3T3 cells provided the field with opportunities to investigate a very select subset of candidate genes that likely underlie SCN-specific properties.

While several cellular pathways/mechanisms are known to be functionally involved in the coupling or synchronization of individual SCN cells, including electrical and chemical-based coupling (**87, 25, 13, 6, 90**), our comparative microarray screen provided momentum for addressing whether the NO/*Nos2* signaling pathway (a novel candidate) contributes to either the functional coupling of individual SCN2.2 oscillator cells, the coordination of metabolic rhythmicity in cocultured NIH/3T3 cells, or both properties. We now had a good candidate gene pathway and we now could address that $64,000 question. Experiments described in CHAPTER IV show that SCN2.2 cells produce NO and express NOS2 protein independent of forskolin stimulation. We also show that antisense oligonucleotide-mediated reduction in the expression of the *Nos2* gene alters the capacity of SCN2.2 cells to exhibit 1) sustained endogenous circadian rhythms of metabolism and 2) coordination of oscillatory properties in non-treated cocultured NIH/3T3 cells. Because the SCN clock is an autonomous property of individual SCN cells (**158, 61**), the capacity of a population of SCN2.2 pacemaker cells to express endogenous rhythmicity and coordinate high-amplitude circadian signals controlling oscillations in NIH/3T3 fibroblasts is likely to depend upon their communication and coupling. The findings presented in Chapter IV suggest that NO/*Nos2* contributes to this functional coupling.

The examination of *Nos2* function in SCN2.2 cells have provided a foundation for future experiments aimed at investigating the function of other cellular elements that potentially underpin the unique pacemaker properties of SCN2.2 cells (**CHAPTER III**). Indeed, a primary goal of our microarray-based screen was the identification of a select subset of genes that likely permit SCN cells to function within this context. Thus, the

functional roles of the remaining 27 SCN cell-specific rhythmic genes should be explored with similar rigor as that applied in our study of *Nos2*. Along these lines, the importance of genes that did not display circadian regulation but did show SCN cell-specific expression should not be minimized. Antisense oligonucleotide-mediated knockdown of gene expression was a powerful tool in determining that *Nos2* was, indeed, functionally relevant to the unique properties of SCN2.2 cells and this approach is very applicable to future examinations of other candidate genes, rhythmic and non-rhythmic. Ultimately, animal gene knockout models will be necessary components in the study of these genes' functions, *in vivo*.

The subsequent challenges in understanding the specific contributions of these candidate genes to the properties of SCN cells and the function of the mammalian timekeeping system, in general, will depend upon maintaining distinctions between two properties: 1) the coordination of rhythmicity in downstream oscillators and 2) self-synchrony. For example, it is known that NO functions broadly in cell physiology; cellular biochemicals known to interact directly with nitric oxide synthases include calcium-dependent calmodulin CAM Kinase, soluble guanylyl cyclase, and flavanine adenine dinucleotide (FAD). NO can affect both ras- and calcium-based signaling pathways directly (**7, 112, 109**). So, examining how these diverse signaling components and pathways interact to affect the capacity of SCN cells to function as a network or their capacity to coordinate rhythmicity in downstream cells are important but distinct investigative pursuits? Because our investigation of *Nos2* function in relation to the pacemaker properties of SCN2.2 cells (**CHAPTER IV**) has not precisely addressed distinctions between the coordination of rhythmicity in downstream oscillators and self-synchrony, future experiments are necessary.

Experiments taking advantage of the cell-heterogeneous nature of the SCN2.2 culture model can facilitate valuable insight regarding these mechanistic distinctions. Because coupling between individual SCN neurons has been shown to be critical to the ensemble clock properties of the SCN (**13, 87**), we can address the importance of NO/*Nos2* in relation to the physical and biochemical network properties of SCN2.2 cells (neurons and glia). Additionaly, we will need to explore the functional importance of NO/*Nos2* in the coordination of intracellular pathways affecting the autonomous clock property of SCN cells. Critical questions include whether NO production and diffusion rates vary over time, whether the NO/*Nos2* pathway provides chemical coupling of SCN2.2 neurons directly or through downstream signaling components, i.e. soluble guanylyl cyclases, ras, and calcium, and whether SCN2.2 glial cells are necessary for this coupling (**Fig. 19**). The outcome of these experiments will be critical in shaping questions regarding NO/*Nos2* function *in vivo*. In a similar fashion, continued investigation of genes selectively identified as SCN outputs by means of our comparative examinations of the transcritpome in bona fide peripheral oscillator and circadian pacemaker models will be useful in advancing our understanding of circadian timing as it extends from cell to tissue to organism – then back to the cell.

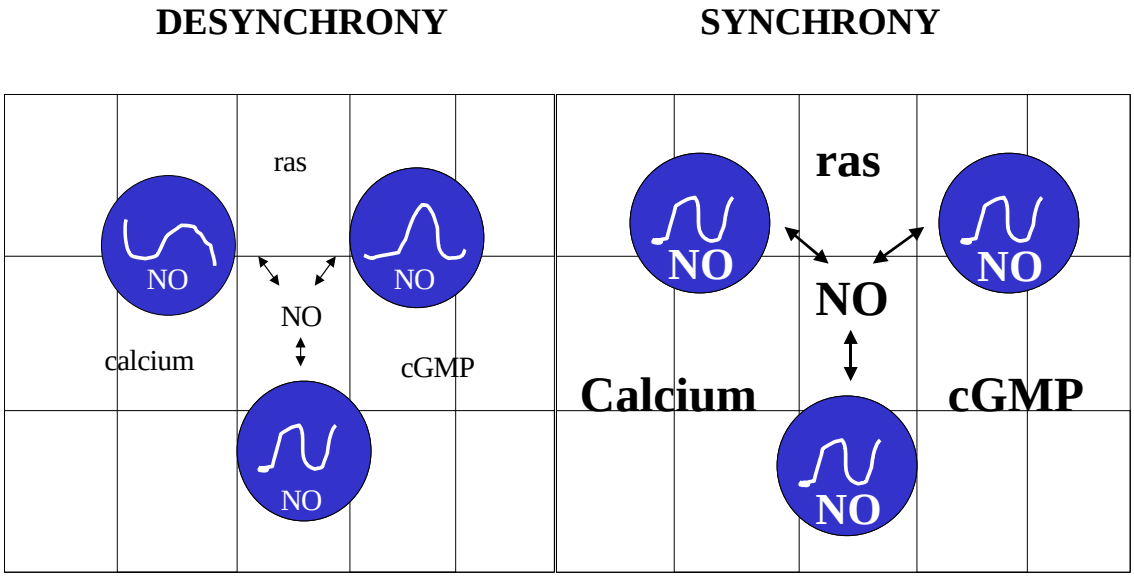

Fig. 19. Possible modes of NO/NOS2 operation in SCN2.2 cells. In a population a desynchronized SCN oscillators, NO may function critically in relation to the cell autonomous clock property of individual SCN neurons (blue ●) or in the coordination of interacellular pathways that function to synchronize the electrical activities of these neurons and, presumably, metabolic activities in glial cells (grid). Importantly, these two modes of NO function in SCN2.2 cells need not be mutually exclusive. While it is not known if NO levels vary over time in SCN2.2 cell cultures, evidence for circadian fluctuations of extracellular NO, as assessed by the presence of nitrite in the dorsal SCN (**102**), suggests NO has the potential to act as a rhythmic synchronizing signal for SCN2.2 cells and, perhaps, for cocultured NIH/3T3 cells as well. Circadian peaks in the expression of Nos2/NO could broadcast temporal cues through several cell-signaling pathways affected by NO.

In summary, a major distinction between SCN and non-SCN cells is not necessarily attributable to inherent differences in their capacities to exhibit clockwork oscillations but rather their different capacities to self-synchronize and extend oscillatory coordination to non-SCN cells. The subsequent challenges in understanding the specific roles of pacemaker genes such as *Nos2* in the function of the mammalian timekeeping system will depend on the parsing of important functional distinctions. Investigation of cell pathways facilitating the functional coupling of SCN cells (**158**, **128**) is immensely important in regards to enhancing our knowledge of how the SCN functions as a self-sustaining network of circadian oscillators. Equally important is the identification and investigation of potential SCN output pathways that coordinate oscillatory behavior in cells residing in non-SCN peripheral tissues. Our comparative analysis of circadian gene expression in SCN2.2 cells, the rat SCN, and NIH/3T3 fibroblasts offers important insights and implications in the selective analysis of circadian signals involved in the coupling of SCN oscillators and the regulation of rhythmicity in downstream oscillator cells. Specifically, our study has provided the field with a select subset of candidate genes to examine in these functional contexts. One of these genes is *Nos2*.

Yet, our analyses do possess some caveats that must be mentioned. First, despite the similarities in circadian regulation of the transcriptome in SCN2.2 cells and the rat SCN, there was not complete overlap in the rhythmically-regulated genes between these experimental models as SCN2.2 cells are not completely representative of the SCN. This difference may be related to comparative differences in the cellular heterogeneity of SCN2.2 cells and the SCN *in vivo* or may reflect the absence of extra-SCN factors that normally influence SCN rhythmicity *in vivo*. Secondly, for SCN2.2 cells, our functional

analysis revealed that a majority of annotated circadian-regulated genes were associated with cellular and systems-level communication functions. Although the prevalence of rhythmic genes in this category is consistent with studies documenting their importance in the circadian photoentrainment and pacemaker functions of the SCN, a marked bias for genes affiliated with cellular and systems-level communication was represent on the rat genome U34 GeneChips used in this examination. Finally, our comparative analysis of the transcriptome in NIH/3T3 cells, the rat SCN, and SCN2.2 cells did not cover all of the genes represented on each of the different GeneChips but, rather, the set of homologous genes commonly represented on both GeneChips. It is probable that new SCN-specific genes as well as new commonly-regulated genes will arise from future bioinformatic analyses of our GEO data sets as knowledge of gene homology and gene function advances. Thus, new insights and novel interpretations may evolve from the data and findings of this study as it is revisited from time to time.

REFERENCES

1. **Abrahamson EE and Moore RY.** Suprachiasmatic nucleus in the mouse: retinal innervation, intrinsic organization, and efferent projections. *Brain Res* 916: 172-191, 2001.

2. **Abrahamson EE and Moore RY.** Lesions of suprachiasmatic nucleus efferents selectively affect rest-activity rhythm. Mol Cell Endocrinol 252(1-2): 46-56, 2006.

3. **Aggelopoulos NC and Meissl H.** Responses of neurons of the rat suprachiasmatic nucleus to retinal illumination under photic and scotopic conditions. *Journal of Physiology* 523: 211-222, 2000.

4. **Akashi M and Nishida E.** Involvement of the MAP kinase cascade in resetting of the mammalian circadian clock. *Genes Dev* 14: 645-649, 2000.

5. **Akhtar RA, Reddy AB, Maywood ES, Clayton JD, King VM, Smith AG, Gant TW, Hastings MH and Kyriacou CP.** Circadian cycling of the mouse liver transcriptome, as revealed by cDNA microarray, is driven by the suprachiasmatic nucleus. *Cur Biol* 12: 540-550, 2002.

6. **Albus H, Vansteensel MJ, Michel S, Block GD, Meijer JH.** A GABAergic mechanism is necessary for coupling dissociable ventral and dorsal regional oscillators within the circadian clock. *Curr Biol* 15: 886-93, 2005.

7. **Alderton WK, Cooper CE, and Knowles RG.** .Nitric oxide synthases: structure, function and inhibition. *Biochem J* 357: 593-615, 2001.

8. **Allen GC.** Functional properties of the suprachiasmatic nucleus: comparative analysis of the central pacemaker verses peripheral oscillators. Thesis. TAMU, 2001.

9. **Allen GC, Farnell Y, Bell-Pedersen D, Cassone VM, and Earnest, DJ.** Effects of altered clock gene expression on the pacemaker properties of SCN2.2 cells and oscillatory properties of NIH/3T3 cells. *Neuroscience* 127: 989-999, 2004.

10. **Allen G, Rappe J, Earnest DJ, and Cassone VM.** Oscillating on borrowed time: diffusible signals from immortalized suprachiasmatic nucleus cells regulate circadian rhythmicity in cultured fibroblasts. *J Neurosci* 21: 7937-7943, 2001.

11. **Altschul SF, Gish W, Miller W, Myers EW and Lipman DJ.** Basic local alignment search tool. *J Mol Biol* 215: 403-410, 1990.

12. **Aschoff J.** Circadian rhythms: influences of internal and external factors on the period measured in constant conditions. *Z Tierpsychol* 3: 225-49, 1979.

13. **Aton SJ, Colwell CS, Harmar AJ, Waschek J, Herzog ED.** Vasoactive intestinal polypeptide mediates circadian rhythmicity and synchrony in mammalian clock neurons. *Nat Neurosci* 8: 476-83, 2005.

14. **Bailey MJ, Beremand PD, Hammer R, Bell-Pedersen D, Thomas TL, and Cassone VM.** Transcriptional profiling of the chick pineal gland, a photoreceptive circadian oscillator and pacemaker. *Mol Endo* 17: 2084-2095, 2003.

15. **Balsalobre A, Damiola F and Schibler, U.** A serum shock induces circadian gene expression in mammalian tissue culture cells. *Cell* 93: 929-937, 1998.

16. **Balsalobre A, Brown SA, Marcacci L, Tronche F, Kellendonk C, Reichardt HM, Schutz G and Schibler, U.** Resetting of circadian time in peripheral tissues by glucocorticoid signaling. *Science* 289: 2344-2347, 2000.

17. **Bell-Pedersen D, Cassone VM, Earnest DJ, Golden SS, Hardin PE, Thomas TL, and Zoran MJ.** Circadian rhythms from multiple oscillatorsL lessons from diverse organisms. *Nat RevGen.* 1-13, 2005.

18. **Bercovich B, Stancovski I, Mayer A, Blumenfeld N, Laszlo A, Schwartz AL, and Ciechanover A.** Ubiquitin-dependent degradation of certain protein substrates in vitro requires the molecular chaperone Hsc70. *J Biol Chem* 272: 9002-9010, 1997.

19. **Bunning E and Chandrashekaran MK.** Pfeffer's view on rhythms. *Chronobiol* 2: 160-167, 1975.

20. **Carbajo-Perez E, Carbajo S, Orfao A, Vicente-Villardon JL, and Vazquez R.** Circadian variation in the distribution of cells throughout the different phases of the cell cycle in the anterior pituitary gland of adult male rats as analysed by flow cytometry. *J Endocrinol* 129: 329-333, 1991.

21. **Castel M, Belenky M, Cohen S, Ottersen OP and Storm-Mathisen J.** Glutamate-like immunoreactivity in retinal terminals of the mouse suprachiasmatic nucleus. *Eur J Neurosci* 5: 368-381, 1993.

22. **Castel M, Belensky M, Cohen S, Wagner S., and Schwartz WJ.** Light-induced c-fos expression in the mouse suprachiasmatic nucleus: immunoelectron microscopy reveals co-localization in multiple cell types. *Eurp. J. Neuroscience* 9: 1950-1960, 1997.

23. **Ceriani MF, GreJB, Yanovsky M, Panda S, Straume M, and Kay SA.** Genome-wide expression analysis in Drosophila reveals genes controlling circadian behavior. *J Neurosci* 22: 9305-9319, 2002.

24. **Cheng MY, Bullock CM, Li C, Lee AG, Bermak JC, Belluzzi J, Weaver DR, Leslie FM, Zhou QY.** Prokineticin 2 transmits the behavioural circadian rhythm of the suprachiasmatic nucleus. *Nature* 417: 405-10, 2002.

25. **Colwell, CS.** Rhythmic coupling among cells in the suprachiasmatic nucleus. *J Neurobiolog* 43: 379-88, 2000.

26. **Correa A, Lewis ZA, Greene AV, March IJ, Gomer RH, and Bell-Pedersen D.** Multiple oscillators regulate circadian gene expression in *Neurospora*. *Proc Natl Acad Sci USA* 100: 13597-13602, 2003.

27. **Crosio C, Cermakain N, Allis CD, and Sassone-Corsi P.** Light induces chromatin modification in cells of the mammalian circadian clock. *Nat Neurosci* 3: 1241-7, 2000.

28. **Cutler DJ, Haraura M, Reed HE, Shen S, Sheward WJ, Morrison CF, Marston HM, Harmar AJ, Piggins HD.**The mouse VPAC2 receptor confers suprachiasmatic nuclei cellular rhythmicity and responsiveness to vasoactive intestinal polypeptide in vitro. *Eur J Neurosci* 17: 197-204, 2003.

29. **Dahlquist KD, Salomonis N, Vranizan K, Lawlor SC, and Conklin BR.** GenMAPP, a new tool for viewing and analyzing microarray data on biological pathways. *Nat Genet* 31: 19-20, 2002.

30. **Ding JM, Chen D, Weber ET, Faiman LE, Rea MA, and Gillette, MU.** Resetting the biological clock: mediation of nocturnal circadian shifts by glutamate and NO. *Science* 266: 1713-1717, 1994.

31. **Doniger SW, Salomonis N, Dahlquist KD, Vranizan K, Lawlor SC, Conklin BR.** MAPPFinder: using Gene Ontology and GenMAPP to create a global gene-expression profile from microarray data. *Genome Biol* 4: R7, 2003.

32. **Duffield GE, Best JD, Meurers BH, Bittner A, Loros JJ, and Dunlap JC.** Circadian programs of transcriptional activation, signaling and protein turnover revealed by microarray analysis of mammalian cells. *Cur Biol* 12: 551-557, 2002.

33. **Duffield, GE.** DNA microarray analyses of circadian timing: the genomic basis of biological time. *J Neuroendo* 15: 991-1002, 2003.

34. **Earnest DJ and Sladek CD.** Circadian vasopressin release from perifused rat suprachiasmatic explants in vitro: effects of acute stimulation. *Brain Res* 422: 398-402, 1987.

35. **Earnest DJ, DiGiorgio S, and Olschowka JA**. Light induces expression of fos-related proteins within gastrin-releasing peptide neurons in the rat suprachiasmatic nucleus. *Brain Res* 627: 205-209, 1993.

36. **Earnest DJ, Liang FQ, DiGiorgio, S, Gallagher M, Harvey B, Earnest B, and Seigel G.** Establishment and characterization of adenoviral E1A immortalized cell lines derived from the rat suprachiasmatic nucleus. *J Neurobiol* 39: 1-13, 1999a.

37. **Earnest DJ, Liang FQ, Ratcliff M, and Cassone VM.** Immortal time: circadian clock properties of rat suprachiasmatic cell lines. *Science* 283: 693-695, 1999b.

38. **Edmunds LN.** *Cellular and Molecular Bases of Biological Clocks: Models and Mechanisms for Circadian Timekeeping*. New York: Springer-Verlag, 1988.

39. **Enright JT.** Temporal precision in circadian systems: a reliable neuronal clock from unreliable components? *Science* 209: 1542-1545, 1980.

40. **Foster RG.** Shedding light on the biological clock. *Neuron.* 20: 829-832, 1998.

41. **Gannon RL and Rea MA**. Glutamate receptor immunoreactivity in the rat suprachiasmatic nucleus. *Brain Res* 622: 337-342, 1993.

42. **Gladstone Institutes. GenMAPP Archives.** *Gene Archives and GenMAPPs.* http://www.GenMAPP.org, 2003.

43. **Gillette MU.** Cellular and biochemical mechanisms underlying circadian rhythms in vertebrates. *Curr Opin Neurobiol* 7: 797-804, 1997.

44. **Gillette MU and Reppert SM.** The hypothalamic suprachiasmatic nuclei: circadian patterns of vasopressin secretion and neuronal activity in vitro. *Brain Res Bull* 19: 135-139, 1987.

45. **Golden SS, Canales SR.** Cyanobacterial circadian clocks - timing is everything. *Nature Rev Microbiol* 1: 191-199, 2003.

46. **Grima B, Lamouroux A, Chelot E, Papin C, Limbourg-Bouchon B, and Rouyer F.** The F-box protein slimb controls the levels of clock proteins period and timeless. *Nature* 420: 178-82, 2002.

47. **Grundschober C, Delaunay F, Puhlhofer A, Triqueneaux G, Laudet V, Bartfai T, and Nef P.** Circadian regulation of diverse gene products revealed by mRNA expression profiling of synchronized fibroblasts. *J Biol Chem* 276: 46751-8, 2001.

48. Hamada T, LeSauter J, Lokshin M, Romero MT, Yan L, Venuti JM, Silver R. Calbindin influences response to photic input in suprachiasmatic nucleus. *J Neurosci* 23: 8820-6, 2003.

49. Hanafy KA, Krumenacker JS, and Murad F. NO, nitrotyrosine, and cyclic GMP in signal transduction. *Med Sci Monit* 7**:** 801–819, 2001.

50. Hannibal J, Ding JM, Chen D, Fahrenkrug J, Larsen PJ, Gillette MU, Mikkelsen JD. Pituitary adenylate cyclase-activating peptide (PACAP) in the retinohypothalamic tract: a potential daytime regulator of the biological clock. *J Neurosci* 17: 2637-44, 1997.

51. Hannibal J, Jamen F, Nielsen HS, Journot L, Brabet P, Fahrenkrug J. Dissociation between light-induced phase shift of the circadian rhythm and clock gene expression in mice lacking the pituitary adenylate cyclase activating polypeptide type 1 receptor. *J Neurosci* 21: 4883-90, 2001.

52. Hannibal J, Moller M, Ottersen OP, and Fahrenkrug J. PACAP and Glutamate are co-stored in the retinohypothalamic tract. *The Jorn of Comp. Neurology* 418: 147-155, 2000.

53. Harley CW, Farrell RC, and Rusak B. Daily variation in the distribution of glycogen phosphorylase in the suprachiasmatic nucleus of syrian hamsters. *J Comp Neurol* 435: 249–58, 2001.

54. Harmar AJ, Marston HM, Shen S, Spratt C, West KM, Sheward WJ, Morrison CF, Dorin JR, Piggins HD, Reubi JC, Kelly JS, Maywood ES, Hastings MH. The VPAC(2) receptor is essential for circadian function in the mouse suprachiasmatic nuclei. *Cell* 109: 497-508, 2002.

54a. **Harrington ME, Hoque S, Hall A, Golobek D, Biello S.** Pituitary adenylate cyclase activating peptide phase shifts circadian rhythms in a mannersimilar to light. *J Neurosci* 19: 6637-42, 1999.

55. Hattar S, Liao H-W, Takao M, Berson DM, and Yau K-W. Melanopsin-containing retinal ganglion cells: architecture, projections, and intrinsic photosensitivity. *Science* 295: 1065-9, 2002.

56. Heid CA, Stevens J, Livak KJ, and Williams PM. Real time quantitative PCR. *Genome Res* 6: 986-994, 1996.

57. Herzog ED and SchwartzWJ. A neural clockwork for encoding circadian time. *J Appl Physiol.* 92: 401-8, 2002.

58. Hille B. Potassium channels and chloride channels. In: *Ionic Channels of Excitable Membranes*, edited by Sinauer HB. Sunderland, MA: Sinauer, 1992, p 130-135.

59. Hollnagel A, Oehlmann V, **Heymer J, Rüther U, and Nordheim A.** *Id* Genes are direct targets of bone morphogenetic protein induction in embryonic stem cells**.** *J Biol Chem* 274: 19838-19845, 1999.

60. Holmes RP and Assimos DG. Glyoxylate synthesis, and its modulation and influence on oxalate synthesis. *J Urol* 160: 1617-1624, 1998.

61. Honma S, Nakamura W, Shirakawa T, and Honma K. Diversity in the circadian periods of single neurons of the rat suprachiasmatic nucleus depends on nuclear structure and intrinsic period. *Neurosci Lett* 358: 173-6, 2004.

62. **Hurst WJ, Mitchell JW, and Gillette MU.** Synchronization and phase-resetting by glutamate of an immortalized SCN cell line. *Biochem Biophys Res Comm* 298: 133-43, 2002.

63. **Inouye ST and Kawamura H.** Persistence of circadian rhythmicity in a mammalian hypothalamic "island" containing the suprachiasmatic nucleus. *Proc Natl Acad Sci USA* 76: 5962-6, 1979.

64. **Johnson CH, Elliot JA, and Foster R.** Entrainment of circadian programs. *Chronobiol Int.* 20: 174-774, 2003.

65. **Johnson RF, Moore RY, and Morin LP.** Loss of entrainment and anatomical plasticity after lesions of the hamster retinohypothalamic tract. *Brain Res* 460: 297-313, 1988a.

66. **Johnson RF, Morin LP, and Moore RY.** Retinohypothalamic projections in the hamster and rat using cholera toxin. *Brain Res.* 462: 301-12, 1988b.

67. **Kita Y, Shiozawa M, Jin W, Majewski RR, Besharse JC, Greene AS, and Jacob HJ.** Implications of circadian gene expression in kidney, liver and the effects of fasting on pharmacogenomic studies. *Pharmacogenetics* 12: 55-65, 2002.

68. **Kleiber J, Kalousek F, Swaroop M, and Rosenberg LE.** The general mitochondrial matrix processing protease from rat liver: structural characterization of the catalytic subunit. *Proc Natl Acad Sci USA* 87: 7978-82, 1990.

69. **Klein DC, Moore RY, and Reppert SM.** *Suprachiasmatic Nucleus: The Mind's Clock*. New York: Oxford Univ. Press, 1991.

70. **Ko HW, Jiang J, and Edery I.** Role of *Slimb* in the degradation of *Drosophila* protein phosphorylated by doubletime. *Nature* 240: 673-678, 2002.

71. **Kornhauser JM, Nelson DE, Mayo KE, and Takahashi JS.** Photic and circadian regulation of c-fos gene expression in the hamster suprachiasmatic nucleus. *Neuron* 5: 127-134, 1990.

72. **Kozak M.** How do eukaryotic ribosomes select initiation regions in messenger RNA? *Cell.* 15: 1109-23, 1978.

73. **Kramer A, Yang FC, Snodgrass P, Li X, Scammell TE, Davis FC, Weitz CJ.** Regulation of daily locomotor activity and sleep by hypothalamic EGF receptor signaling. *Science* 294: 2511-5, 2001.

74. **Kriegsfeld LJ, Demas GE, Lee, SE, Dawson TM, Dawson VL, and Nelson RJ.** Circadian locomotor analysis of male mice lacking the gene for neuronal nitric oxide synthase (nNOS-/-). *J Biol Rhythms* 14: 20-27, 1999.

75. **Kriegsfeld LJ, Drazen DL, and Nelson RJ.** Circadian organization in male mice lacking the gene for endothelial nitric oxide synthase (eNOS-/-). *J Biol Rhythms* 16: 142-148, 2001.

76. **Kriegsfeld LJ and Silver R.** The regulation of neuroendocrine function: Timing is everything. *Hormones and Behavior* 29: 557-74, 2006.

77. **Krumenacker JS and Murad F.** NO-cGMP signaling in development and stem cells. *Molecular Genetics and Metabolism* 87: 311-14, 2006.

78. **Kurosawa G and Iwasa Y.** Temperature compensation in circadian clock models. *Journal of Theoretical Biology* 233: 453-68, 2005.

79. **La Fleur SE, Kalsbeek A, Wortel J, Buijs RM.** A suprachiasmatic nucleus generated rhythm in basal glucose concentrations. *J Neuroendocrinol.* 11: 643-52, 1999.

80. **Lambert LE, Whitten JP, Baron BM, Cheng HC, Doherty, NS, and McDonald IA.** Nitric oxide synthesis in the CNS endothelium and macrophages differs in its sensitivity to inhibition by arginine analogues. *Life Sci* 48: 69-75, 1991.

81. **Lavialle M, and Servière J.** Circadian fluctuations in GFAP distribution in the Syrian hamster suprachiasmatic nucleus. *NeuroReport* 4: 1243-1246, 1993.

82. **Lee CK, Klopp RG, Weidruch R, and Prolla TA.** Gene expression profile of aging and its retardation by caloric restriction. *Science* 285: 1390-1393, 1999.

83. **Lehman MN, Silver R, Gladstone WR, Kahn RM, Gibson M, and Bittman EL.** Circadian rhythmicity restored by neural transplant. Immunocytochemical characterization of the graft and its integration with the host brain. *J Neurosci* 7: 1626-38, 1987.

84. **LeSauter J, Lehman MN, Silver R.** Restoration of circadian rhythmicity by transplants of SCN "micropunches".*J Biol Rhythms.* 11: 163-71, 1996.

85. **LeSauter J and Silver R.** Localization of a suprachiasmatic nucleus subregion regulating locomotor rhythmicity. *J Neurosci* 19: 5574-85, 1999.

86. **Liu Y, Tsinoremas NF, Johnson CH, Lebedeva NV, Golden SS, Ishiura M, Kondo T.** Circadian orchestration of gene expression in cyanobacteria. *Genes Dev* 9: 1469-78, 1995.

87. **Long MA, Jutras MJ, Connors BW, Burwell RD.** Electrical synapses coordinate activity in the suprachiasmatic nucleus. *Nat Neurosci* 8: 61-6, 2005.

88. **Lowenstein CJ and Snyder SH.** Nitric oxide, a novel biologic messenger. *Cell* 70: 705-707, 1992.

89. **Lovenberg TW, Baron BM, de Lecea L, Miller JD, Prosser RA, Rea MA, Foye PE, Racke M, Slone AL, Siegel BW, Danielson PE, Sutcliffe JG, and Erlander MG.** A novel adenyl cyclase-activating serotonin receptor (5-HT^7) implicated in the regulation of mammalian circadian rhythms. *Neuron* 11: 449-458, 1993.

90. **Lui C and Reppert, SM.** GABA synchronizes clock cells within the suprachiasmatic circadian clock. *Neuron* 25. 123-128, 2000.

91. **Matsuo T, Yamaguchi S, Mitsui S, Emi A, Shimoda F, and Okamura H.** Control mechanism of the circadian clock for timing of cell division in vivo. *Science* 302: 255-259, 2003.

92. **McCallum CD, Do H, Johnson AE, and Frydman J.** The interaction of the chaperonin tailless complex polypeptide 1 (TCP1) ring complex (TRiC) with ribosome-bound nascent chains examined using photo-cross-linking. *J Cell Biol* 149: 591-602, 2000.

93. **McDonald MJ and Rosbash M.** Microarray analysis and organization of circadian gene expression in Drosophila. *Cell* 107: 567-578, 2001.

94. **McGowan KM, Long SD, and Pekala PH.** Glucose transporter gene expression: regulation of transcription and mRNA stability. *Pharmacol Ther* 66: 465-505, 1995.

94a. **Medanic M and Gillette MU.** Serotonin regulates the phase of the rat suprachiasmatic circadian pacemaker in vitro only during the subjective day. *J Physiol* 450: 629-42, 1992.

95. **Meijer JH and Schwartz WJ.** In search of the pathways for light-induced pacemaker resetting in the suprachiasmatic nucleus. *J Biol Rhythms* 18: 235-249, 2003.

96. **Meijer JH, Watanabe K, Detari L, and Schaap J.** Circadian rhythm in light response in suprachiasmatic nucleus neurons of freely moving rats. *Brain Res* 741: 352-55, 1996.

97. **Meijer JH, van der Zee EA and Dietz M.** Glutamate phase shifts circadian activity rhythms in hamsters. *Neurosci Lett* 86: 177-183, 1988.

98. **Menger GJ, Kim L, Thomas T, Cassone VM, and Earnest DJ.** Circadian profiling of the transcriptome in immortalized rat SCN cells. *Physiol Genomics* 21: 370-81, 2005.

98a. **Menger GJ, Allen GC, Neuendorff N, Nahm SS,Thomas TL, Cassone VM, and Earnest DJ.** Circadian profiling of the transcriptome in NIH/3T3 fibroblasts: comparison with rhythmic gene expression in SCN2.2 cells and the rat SCN. *Physiol Genomics* Epub. 2007.

99. **Mikkelsen JD, Larsen PJ, Mick G, Vrang N, Ebling FJP, Maywood ES, Hastings MH, and Moller M.** Gating of retinal inputs through the suprachiasmatic nucleus: Role of excitatory neurotransmitters. *Neurochem. Int* 27: 263-272, 1995.

100. **Minc-Golomb D, Yadid G, Tsarfaty I, Resau JH, Schwartz JP.** In vivo

expression of inducible nitric oxide synthase in cerebellar neurons. *J Neurochem.* 66: 1504-9, 1996.

101. Mirande M, and Waller JP. Molecular cloning and primary structure of cDNA encoding the catalytic domain of rat liver aspartyl-tRNA synthetase. *J Biol Chem* 264: 842-847, 1989.

102. Mitome M, Shirakawa T, Oshima S, Nakamura W, Oguchi H. Circadian rhythm of nitric oxide production in the dorsal region of the suprachiasmatic nucleus in rats. *Neurosci Lett* 303: 161-4, 2001.

103. Mizzen LA, Chang C, Garrels JI, and Welch WJ. Identification, characterization, and purification of two mammalian stress proteins present in mitochondria, grp 75, a member of the hsp 70 family and hsp 58, a homolog of the bacterial groEL protein. *J Biol Chem* 264: 20664-75, 1989.

104. Moore RY. Organization and function of a central nervous system circadian oscillator: the suprachiasmatic hypothalamic nucleus. *Fed Proc* 42: 2783-9, 1983.

105. Moore RY and Eichler VB. Loss of a circadian adrenal corticosterone rhythm following suprachiasmatic lesions in the rat. *Brain Res* 42: 201-6, 1972.

106. Moore RY, Speh JC, Leak RK. Suprachiasmatic nucleus organization. *Cell Tissue Res* 309: 89-98, 2002.

107. Mori T, Binder B, and Johnson, CH. Circadian gating of cell division in cyanobacteria growing with average doubling times of less than 24 hours. *Proc Natl Acad Sci USA* 93: 10183-10188, 1996.

108. Munekawa K, Tamada Y, Iijima N, Hayashi S, Ishihara A, Inoue K, Tanaka M, Ibata Y. Development of astroglial elements in the suprachiasmatic nucleus

of the rat: with special reference to the involvement of the optic nerve. *Exp Neurol.* 166: 44-51, 2000.

109. National Library of Medicine and National Institutes of Health. *Tools for Data Mining*, at National Center for Biotechnology Information (NCBI): http://www.ncbi.nlm.nih.gov/, July 2003-December 2006.

110. Newman GC, Hospod FE, Patlak CS, and Moore RY. Analysis of in vitro glucose utilization in a circadian pacemaker model. *J Neurosci* 12: 2015-2021, 1992.

111. Niethammer M, Kim E, and Sheng M. Interaction between the C terminus of NMDA receptor subunits and multiple members of the PSD-95 family of membrane-associated guanylate kinases. *J Neurosci* 16: 2157-2163, 1996.

112. Oess S, Icking A, Fulton D, Govers R, Muller-Esterl W. Subcellular targeting and trafficking of nitric oxide synthases. *Biochem J.* 396: 401-9, 2006.

113. Onishi H, Yamaguchi S, Yagita K, Ishida Y, Dong X, Kimura H, Jing Z, Ohara H, Okamura H. Rev-erbalpha gene expression in the mouse brain with special emphasis on its circadian profiles in the suprachiasmatic nucleus. *J Neurosci Res* 68: 551-7, 2002.

114. Panda S, Antoch MP, Miller,BH, Su AI, Schook AB, Straume M, Schultz G, Kay SA, Takahashi JS, and Hogenesch JB. Coordinated transcription of key pathways in the mouse by the circadian clock. *Cell* 109: 307-320, 2002.

115. Panda S, Sato TK, Castrucci AM, Rollag MD, DeGrip WJ, Hogenesch JB, Provencio I, and Kay SA. Melanopsin (Opn4) requirement for normal light-induced circadian phase shifting. *Science* 298: 2213-6, 2002.

116. Pellerin L and Magistretti PJ. Neuroenergetics: calling upon astrocytes to satisfy hungry neurons. *Neuroscientist* 10: 53-62, 2004.

117. Peterson PK, Hu S, Anderson WR, and Cao CC. Nitric oxide production and neurotoxicity mediated by activated microglia from human versus mouse brain. *J Infect Dis.* 170: 457-60, 1994.

118. Pickard GE, Smith BN, Belenky M, Rea MA, Dudek FE, Sollars PJ. 5-HT1B receptor-mediated presynaptic inhibition of retinal input to the suprachiasmatic nucleus. *J Neurosci* 19: 4034-45, 1999.

119. Pickard GE. Bifurcating axons of retinal ganglion cells terminate in the hypothalamic suprachiasmatic nucleus and the intergeniculate leaflet of the thalamus. *Neurosci Lett* 55(2): 211-7, 1985.

120. Pittendrigh CS. Temporal organization: reflections of a Darwinian clock-watcher. *Ann Rev Physiol* 55: 16-54, 1993.

121. Pittendrigh CS and Caldarola PC. General homeostasis of the frequency of circadian oscillations. *Proc Natl Acad Sci USA*.70: 2697-701, 1973.

122. Pittendrigh CS. *Circadian systems: general perspective*. Pacific Grove, CA. Hopkins Marine Station. Stanford University. 1981.

123. Pittendrigh CS. On temperature independence in the clock system controlling emergence in Drosophila. *Proc Natl Acad Sci USA.* 40: 1018-29, 1954.

124. Pittendrigh CS. Circadian rhythms and the circadian organization of living systems. *Cold Spring Harb Symp Quant Biol.* 25: 159-84, 1960.

125. Preitner N, Damiola F, Lopez-Molina L, Zakany J, Duboule D, Albrecht U, Schibler U. The orphan nuclear receptor REV-ERBalpha controls circadian

transcription within the positive limb of the mammalian circadian oscillator. *Cell.* 110: 251-60, 2002.

126. Prosser RA, Dean RR, Edgar DM, Heller HC, and Miller JD. Serotonin and the mammalian circadian system: I. *In Vitro* phase shifts by serotonergic agonists and antagonists. *J Biol Rhythms* 8: 1-16, 1993.

127. Pruitt KD and Maglott DR. RefSeq and LocusLink: NCBI gene-centered resources. *Nucleic Acids Res* 29: 137-140, 2001.

128. Quintero JE, Kuhlman SJ, McMahon DG. The biological clock nucleus: a multiphasic oscillator network regulated by light. *J Neurosci.* 23: 8070-6, 2003.

129. Ralph MR, Foster RG, Davis FC, and Menaker M. Transplanted suprachiasmatic nucleus determines circadian period. *Science* 247: 975-978, 1990.

130. Rea MA, Glass JD, and Colwell CS. Serotonin modulates photic responses in the hamster suprachiasmatic nuclei. *J Neurosci* 14: 3635-3642, 1994.

131. Reppert SM and Weaver DR. Molecular analysis of mammalian circadian rhythms. *Ann Rev Physiol* 63: 647-676, 2001.

132. Reppert SM and Weaver DR. Coordination of circadian timing in mammals. *Nature* 418: 935-941, 2002.

133. Resendez E Jr, Wooden SK, and Lee AS. Identification of highly conserved regulatory domains and protein-binding sites in the promoters of the rat and human genes encoding the stress-inducible 78-kilodalton glucose-regulated protein. *Mol Cell Biol* 8: 4579-84, 1988.

134. Ruby NF, Brennan TJ, Xie X, Cao V, Franken P, Heller HC, and O'Hara BF. Role of Melanopsin in circadian responses to light. *Science.* 298: 2211-3, 2002.

135. Rutter J, Reick M, and McKnight SL. Metabolism and the control of circadian rhythms. *Ann Rev Biochem* 71: 307-331, 2002.

136. Schaffer, Landgraf J, Accerbi M, Simon V, Larson M, and Wisman E. Microarray analysis of diurnal and circadian-regulated genes in Arabidopsis. *Plant Cell* 13: 113-123, 2001.

137. Schwartz WJ. SCN metabolic activity in vitro. In *Suprachiasmatic Nucleus: The Mind's Clock*, edited by Klein, DC, Moore, RY, and Reppert, SM. New York: Oxford Univ. Press, 1991, p. 144-156.

138. Schwartz WJ, Zimmerman P. Lesions of the suprachiasmatic nucleus disrupt circadian locomotor rhythms in the mouse. *Physiol Behav.* 49: 1283-7, 1991.

139. Shearman LP, Zylka MJ, Weaver DR, Kolakowski LF, Jr., and Reppert SM. Two period homologs: circadian expression and photic regulation in the suprachiasmatic nuclei. *Neuron* 19: 1261-1269, 1997.

140. Shen H, Watanabe M, Tomasiewicz H, and Glass JD. Genetic deletions of NCAM and PSA impair circadian function in the mouse. *Physiol Behav* 73: 185-193, 2001.

141. Shirakawa S, and Moore RY. Glutamate shifts the phase of the circadian neuronal firing rhythm in the rat suprachiasmatic nucleus *in vitro*. *Neurosci Lett* 178: 47-50, 1994.

142. Silver R, Lehman MN, Gibson M, Gladstone WR, Bittman. Dispersed cell suspensions of fetal SCN restore circadian rhythmicity in SCN-lesioned adult hamsters. *Brain Res* 525: 45-58, 1990.

143. Silver R, LeSauter J, Tresco PA, and Lehman MN. A diffusible coupling signal from the transplanted suprachiasmatic nucleus controlling circadian locomotor rhythms. *Nature* 382: 810-3, 1996.

144. Simmons ML and Murphy S. Induction of nitric oxide synthase in glial cells. *J Neurochem.* 59: 897-905, 1992.

145. Snodgrass-Belt P, Gilbert JL, Davis FC. Central administration of transforming growth factor-alpha and neuregulin-1 suppress active behaviors and cause weight loss in hamsters. *Brain Re.*1038: 171-82, 2005.

146. Stephan FK and Zucker I. Circadian rhythms in drinking behavior and locomotor activity of rats are eliminated by hypothalamic lesions. *Proc Natl Acad Sci USA*. 69: 1583-6, 1972.

147. Storch KF, Lipan O, Leykin I, Viswanathan N Davis FC, Wong WH, and Weitz CJ. Extensive and divergent circadian gene expression in liver and heart. *Nature* 417: 78-83, 2002.

148. Sumi Y, Yagita K, Yamaguchi S, Ishida Y, Kuroda Y, Okamura H. Rhythmic expression of ROR beta mRNA in the mice suprachiasmatic nucleus. *Neurosci Lett.* 320: 13-6, 2002.

149. Ueda HR, Chen W, Adachi A, Wakamatsu H, Hayashi S, Takasugi T, Nagano M, Nakahama K, Suzuki Y, Sugano S, Iino M, Shigeyoshi Y, and

Hashimoto S. A transcription factor response element for gene expression during circadian night. *Nature* 418: 534-539, 2002a.

150. Ueda, HR, Matsumoto, A, Kawamura, M, Iino, M, Tanimura, T, and Hashimoto, S. Genome-wide transcriptional orchestration of circadian rhythms in Drosophila. *J Biol Chem* 277: 14048-14052, 2002b.

151. van den Pol AN, Hermans-Borgmeyer I, Hofer M, Ghosh P and Heinemann S. Ionotropic glutamate-receptor gene expression in hypothalamus: Localization of AMPA, kainate, and NMDA receptor RNA with in situ hybridization. *J Comp Neurol* 343: 428-444, 1994.

151a. van den Pol AN. *Suprachiasmatic Nucleus: The Mind's Clock,* edited by Klein DC, Moore RY, and Reppert SM. New York: Oxford Univ. Press, 1991, p. 17-50.

152. van Esseveldt KE, Lehman MN, and Boer GJ. The suprachiasmatic nucleus and the circadian time-keeping system revisited. *Brain Res Brain Res Rev.* 33: 34-77, 2000.

153. Vannucci SJ and Simpson IA. Developmental switch in brain nutrient transporter expression in the rat. *Am J Physiol Endocrinol Metab* 285: E1127-E1134, 2003.

154. Vernet D, Bonavera JJ, Swerdloff RS, Gonzalez-Cadavid NF, Wang C. Spontaneous expression of inducible nitric oxide synthase in the hypothalamus and other brain regions of aging rats. *Endocrinology* 139: 3254-61, 1998.

155. Wang D, Kranz-Eble P, and De Vivo DC. Mutational analysis of GLUT1 (SLC2A1) in Glut-1 deficiency syndrome. *Hum Mutat* 16: 224-231, 2000.

156. Wang J, Yang X, Zhou P, and Han H. Cloning of mouse genomic ribosomal protein L6 and analysis of its promoter. *Biochemica et Biophysica Acta* 1576: 219-224, 2002.

157. Watanabe A, Hamada T, Shibata S, and Watanabe S. Effects of nitric oxide synthase inhibitors on N-methyl-D-aspartate-induced phase delay of circadian rhythm of neuronal activity in the rat suprachiasmatic nucleus in vitro. *Brain Res* 646: 161-164, 1994.

158. Welsh DK, Logothetis DE, Meister M, Reppert SM. Individual neurons dissociated from rat suprachiasmatic nucleus express independently phased circadian firing rhythms. *Neuron* 14: 697-706, 1995.

159. Welsh DK, Yoo-S-H, Lui AC, Takahashi JS, and Kay SA. Bioluminescence of individual fibroblasts reveals persistent, independently phased circadian rhythms of clock gene expression. *Curr Biol* 14: 2289-95, 2004.

160. Yamazaki S, Numano R, Abe M, Hida A, Takahashi R, Ueda M, Block GD, Sakaki Y, Menaker M, and Tei H. Resetting central and peripheral circadian oscillators in transgenic rats. *Science* 288: 682-685, 2000.

161. Yan L and Silver R. Resetting the brain clock: time course and localization of mPER1 and mPER2 protein expression in suprachiasmatic nuclei during phase shifts. *Eur J Neurosci.* 19: 1105-9, 2004.

162. Yoo SH, Yamazaki S, Lowrey PL, Shimomura K, Ko CH, Buhr ED, Siepka SM, Hong HK, Oh WJ, Yoo OJ, Menaker M, Takahashi JS. PERIOD2::LUCIFERASE real-time reporting of circadian dynamics reveals

persistent circadian oscillations in mouse peripheral tissues. *Proc Natl Acad Sci USA.* 101: 5339-46, 2004.

163. Young MW. Life's 24-hour clock: molecular control of circadian rhythms in animal cells. *Trends Biochem Sci* 25: 601-606, 2000.

164. Zylka MJ, Shearman LP, Weaver DR, Reppert SM. Three period homologs in mammals: differential light responses in the suprachiasmatic circadian clock and oscillating transcripts outside of brain. *Neuron* 20: 1103-10, 1998.

APPENDIX

Table A.1. ***Functional categorization of circadian regulated genes in SCN2.2 cells (secondary expression criteria).***

GenBank ID	Locus Link ID	Gene descriptor	Phase group
Category 1 - Energetics (11)			
X73653	**84027**	Glycogen synthase kinase 3 beta	**III**
AA684929	**NF**	Similar to NADH-ubiquinone oxidoreductase	**III**
X59737	**29593**	Ubiquitous mitochondrial creatine kinase (*Ckmt1*)	**III**
AI070142	**24624**	Propionyl coenzyme A carboxylase, beta polypeptide	**I**
U28975	**116509**	Glycine transporter 1 (*Glyt1*)	**I**
X80395	**60422**	Acetylcholine transporter (vesicular) / solute carrier family 18, member 3 (*Slc18a3*)	**II**
AF031234	**NF**	Ileal sodium-dependent bile acid transporter	**III**
L32601	**171516**	20 alpha-hydroxysteroid dehydrogenase (*2α-Hsd*)	**III**
AA818403	**LOC299564**	Similar to cytochrome P450 4F5 (*Cyp4f5*)	**III**
J05035	**24950**	Steroid 5-alpha-reductase (*Srd5a1*)	**IV**
AA892232	**81759**	Renin-binding protein (*Renbp*)	**II**
Category 2 - Cellular and Systems-level Communication (54)			
D28512	**25731**	Synaptotagmin 3 (*Syt3*)	**II-III**
AF044201	**246274**	Neural membrane protein 35 / lifeguard (*Lfg*)	**II**
AB003991	**25012**	Synaptosomal-associated protein (*Snap25*)	**III**
U26402	**54309**	Synaptotagmin 5 (*Syt5*)	**IV-I**
X17184	**50592**	Glutamate receptor, ionotropic, AMPA1(*Gria1*)	**I**
S94371	**29629**	Glutamate receptor, ionotropic, AMPA4 (*Gria4*)	**I**
X74835	**54240**	Cholinergic receptor, nicotinic, delta polypeptide (*Chrnd*)	**II**
D00833	**25674**	Glycine receptor, alpha 1 subunit (*Glra1*)	**III**
U31815	**24239**	Voltage-dependent channel, alpha 1C subunit (*Cacna1c/Rob2*)	**I**

Table A.1 continued

AF061266	**89821**	Transient receptor protein 1 (*Trrp1*)	**IV**
X83581	**29719**	Inwardly-rectifying channel, subfamily J, member 16 (*Kcnj16*)	**II**
AJ007628	**114032**	Voltage-gated channel, subfamily H, member 4 (*Kcnh4*)	**II**
U75210	**117018**	Voltage-gated channel, subfamily H, member 2 (*Kcnh2*) / Erg *(r-erg*)	**II-IV**
M31433	**24766**	Voltage-gated, type 2, alpha 1 polypeptide (*Scn2a1*)	**II**
Z36944	**60586**	Putative chloride channel (similar to Mm *Clcn4-2*)	**II**
AB013112	**65054**	Aquaporin 9 (*Aqp9*)	**III**
X92070	**25041**	Purinergic receptor P2X-like 1 (*P2rxl1*)	**II**
L40030	**94203**	Placenta growth factor (*Pgf*)	**I**
D90219	**114593**	Natriuretic peptide precursor, C-type (*Nppc*)	**I**
X55183	**29183**	Amphiregulin (*Areg*)	**I**
M23643	**25569**	Thyrotropin-releasing hormone (*THR*)	**II**
K01701	**25504**	Neurophysin / oxytocin (*Oxt*)	**II**
L00111	**24241**	Calcitonin / calcitonin-related polypeptide, alpha (*Calca*)	**II**
X58294	**54231**	Carbonic anhydrase 2 (*Ca2*)	**II-III**
X56551	**29348**	Fibroblast growth factor 7 (*Fgf7*)	**II-III**
M12579	**25194**	Gonadotropin-releasing hormone 1 (*Gnrh1*)	**IV-I**
L10072	**25689**	5-hydroxytryptamine (serotonin) receptor 5A (*Htr5a*)	**II**
M84009	**25432**	Dopamine receptor D4 (*Drd4*)	**II**
AF041244	**25593**	Orexin receptor-1 / hypocretin receptor 1 (*Hcrtr1*)	**I**
U04738	**25555**	Somatostatin receptor subtype 4 (*Sstr4*)	**II**
L02842	**25449**	Follicle stimulating hormone receptor (*Fsh-r*)	**II**
D43778	**24182**	Angiotensin II type 2 receptor (*Agtr2*)	**II**
E12742	**LOC305384 OR 12425**	Similar to cholecystokinin-A receptor / cholecystokinin A receptor (*Cckar*)	**III**
AF091574	**65140**	Olfactory receptor 41 (*Ol41*)	**III**
AF091576	**LOC315571**	Similar to olfactory receptor MOR171-5 / HFL-VN1	**III**
X89701	**LOC302957**	Similar to olfactory receptor-like protein 5 / TPCR13	**III**
AA848831	**116744**	Endothelial differentiation G-protein-coupled receptor, 2 (*Edg2*)	**III**

Table A.1 continued

AB009463	**89787**	Low density lipoprotein receptor-related protein 3 (*Lrp3*)	**III**
AI639289	**266806**	Rab6 interacting protein 2 (*Elks*)	**III**
AF064868	**79146**	Brain-enriched guanylate kinase-associated (*BEGAIN*)	**III**
M82826	**24592**	Neurofibromatosis protein type I (*NF1*)	**III**
M18332	**25522**	Protein kinase C, zeta (*Prkcz*)	**II**
L36088	**25237**	Serine-threonine kinase receptor / activin a rec. type II-like 1 (*Acvrl1*)	**II**
D86556	**29660**	Pregnancy upregulated non-ubiquitously expressed CaM kinase (*Pnck*)	**II**
X96488	**60352**	SAP kinase / mitogen-activated protein kinase 12 (*Mapk12/Erk-6*)	**II**
U21954	**171287**	Eph receptor A7 (*Epha7*)	**III**
U48596	**116667**	MAP kinase kinase kinase 1 (*MEKK1/Map3K1*)	**III**
M31809	**24675**	Protein phosphatase 3, catalytic subunit, beta (*Ppp3cb*)	**I**
AJ011035	**85240**	Phospholipase C beta (*Plcb2*)	**III**
U73458	**29714**	Protein tyrosine phosphatase, receptor-type, N polypeptide 2 (*Ptprn2*)	**I**
AA892207	**LOC292426**	Similar to zinc finger Krab	**I**
U01146	**54278**	Nuclear receptor subfamily 4, group A, member 2	**I**
AI234969	**54254**	Gata-binding protein 4 (*Gata4*)	**II**
L13202	**29203**	Forkhead box D3 (*Foxd3*)	**II**

Category 3 - Protein Dynamics (5)

J00778	**24691**	Pancreatic trypsin (*Prss1*)	**II**
AA892512	**LOC361205**	Similar to LECT2	**I**
X59608	**Close to LOC287438**	Similar to DNA directed RNA polymerase II subunit	**I**
U30813	**LOC315406**	Aspartyl-tRNA synthetase (pseudogene)	**III**
AA875646	**246303**	Hypothetical RNA binding protein RDA288 (*Rda288*)	**III**

Table A.1 continued

Category 4 - Cellular Development (7)

U24174	**114851**	Cyclin-dependent kinase inhibitor 1A (*Cdkn1a*)	**I**
AB000216	**171440**	Ankyrin repeat protein (*Cca3*)	**I**
U73586	**24361**	Fanconi anemia group C (*Fancc*)	**III**
U08290	**94270**	Neuronatin alpha (*Nnat-alpha*)	**I**
AI070026	**24452**	Homeobox gene A11 / Homeo box A2 (*Hoxa2*)	**II**
M31076	**24827**	Transforming growth factor alpha (*Tgfa*)	**IV-I**

Category 5 - Defense and Detoxification (12)

U09815	**24256**	Carcinoembryonic antigen (*CGM3*)	**I**
X62325	**LOC290188**	TcRValphaT48a2 / T cell receptor V-alpha J-alpha	**I**
M23889	**24820**	T-cell receptor beta chain (*Tcrb*)	**I-II**
L37971	**NF**	T-cell receptor alpha-chain (*Tcra*)	**II**
S79523	**29259**	Lymphocyte selectin / L-selectin (*Sell*)	**II**
L07398	**LOC314510**	Similar to immunoglobulin heavy chain	**III**
AF006619, D83661, S71597, and U03699	**24599**	Inducible nitric oxide synthase (*iNos/Nos2*)	**I-III**
Z69594	**25259**	Glycoprotein 5 (*Gp5*)	**IV-I**
X57565	**63867**	UDP-glucuronosyltransferase 2A1 (*Ugt2a1*)	**II**
AA818499	**298423**	Lauric acid omega-hydroxylase / cytochrome P-450, 4a3 (*Cyp4a3*)	**III**
X62086	**25642**	Cytochrome P450, subfamily 3A, polypeptide 3 (*Cyp3a3*)	**III**
AF072865	**50551**	Thioredoxin reductase (*TrxR2*)	**IV-I**

Category 6 - Cytoskeleton and Adhesion (10)

M92074	**29248**	Troponin I, type 3 (*Tnni3*)	**I**
L24776	**117557**	Tropomyosin 3 (*Tmp3*)	**II-III**
AF075250	**29605**	Myosin heavy chain polypeptide 13 (*Myh13*)	**III**
AA799508	**64862**	Microtubule-associated proteins 1A/1B light chain 3 (*Mpl3*)	**IV**

Table A.1 continued

S79214	**25681**	Procollagen type X (*Col10a1*)	**II**
X06564	**24586**	Neural cell adhesion molecule 1 (*Ncam1*)	**III**
X63722	**25361**	Vascular cell adhesion molecule 1 (*Vcam1*)	**III-IV**
X71466	**81686**	Matrix metalloproteinase 2 (*Mmp2*)	**II**
X02601	**171045**	Matrix metalloproteinase 3 (*Mmp3*)	**II**

ESTs and Genes with Unknown Function (32)

AA800680	**LOC311794**	Similar to ankyrin-repeat protein Nrarp	**I**
AA799678	**54702**	EGL nine homolog 3 (*Egln3*)	**I**
M31032	**192266**	Glutamine/glutamic acid-rich protein (*Grp-Ca*)	**II**
M19357	**301472**	Gamma-F-crystallin, gamma 4-1 (*Crygf*)	**III**
AA799552	**LOC303472**	Similar to ankyrin-repeat protein Nrarp	**I**
AA800218	**LOC304496**		**I**
AA894318	**EST**		**I**
AI639028	**EST**		**I**
AI639525	**EST**		**I**
H31747	**EST**		**I**
AA874978	**Close to LOC315114**		**I**
AA892526	**EST**		**I**
AA800717	**LOC300670**		**I-II**
AA874877	**EST**		**II**
AA892561	**EST**		**II**
AA893192	**close to 170847**		**II**
AI639027	**LOC310568**		**II**
AI639201	**LOC305631**		**II**
AI639422	**Close to LOC289234**		**II**

Table A.1 continued

H33301	**EST**	**II**
H33448	**LOC296361**	**II**
AA875255	**LOC305540**	**II-III**
AA859718	**LOC306328**	**III**
AI638972	**EST**	**III**
AI639305	**LOC289479**	**III**
H31982	**EST**	**III**
D84482	**Close to LOC301336**	**III**
U34897	**LOC310146**	**III**
AA893366	**Close to LOC293171**	**III**
U31866	**Close to LOC305204**	**III**
AA944973	**LOC302035**	**IV**

Functional categorization of circadian-regulated genes in SCN2.2 cells. Similar to Table 1, the GenBank, Locus Link ID, functional category/cluster and Phase Group assignment are listed for unique genes and ESTs that surpassed secondary expression criteria and showed rhythmic patterns of mRNA expression.

Table A.2. ***Functional categorization of circadian-regulated genes in the rat SCN (stringent expression criteria).***

GenBank ID	Locus Link ID	Gene descriptor	Phase group
Category 1 - Energetics (34)			
Cluster 1 - Glucose metabolism and mitochondrial energy transduction (7)			
J01436	**NF**	Cytochrome B	**III**
L25387	**60416**	Phosphofructokinase C (*PFK-C/Pfkp*)	**I**
L11694	**24645**	Phosphoglucomutase 1 (*Pgm1*)	**I-II**
K00750	**25309**	Cytochrome c, somatic (*Cycs*)	**I**
J01435	**26196**	ATP synthase 8, mitochondrial (*mt-Atp8*)	**I-II**
AI171506	**24552**	Malic enzyme 1 (*Me1*)	**II**
M27467	**54322**	Cytochrome oxidase subunit Vic (*Cox6c*)	**III**
Cluster 2 - Lipid and fatty acid metabolism (4)			
U02096	**80841**	Fatty acid binding protein 7, brain (*Fabp7*)	**II**
J02585	**246074**	Stearoyl-Coenzyme A (CoA) desaturase 1 (*Scd1*)	**I**
D90109	**25288**	Long chain fatty acid coenzyme A (CoA) ligase (*Facl2*)	**I-III**
X57988	**29534**	Peroxisomal membrane protein 3 (*Pxmp3*)	**I**
Cluster 3 - Transporters (3)			
D63834	**25027**	Monocarboxylate transporter (*Mct1/Slc16a1*)	**I**
S68135	**58971**	Glucose transporter / solute carrier family 2, member 1 / (*Glut 1/Slc2a1*)	**IV**
AA800202	**25391**	Similar to bicarbonate transporter related protein 1 (*Slc4 11*)	**I**

Table A.2 continued

Cluster 4 - Miscellaneous metabolism (20)

M95768	**81652**	Di-N-acetylchitobiase (*Ctbs*)	**I**
M95591	**29580**	Farnesyl diphosphate farnesyl transferase 1 (*Fdft1*)	**III**
M84719	**25256**	Flavin-containing monooxygenase 1 (*Fmo1*)	**III**
L34262	**29411**	Palmitoyl-protein thioesterase (*Ppt*)	**I**
M26686	**25604**	Protein-L-isoaspartate (D-aspartate) O-methyltransferase (*Pcmt1*)	**I-III**
M19533	**25518**	Peptidylprolyl isomerase A (*Ppia*)	**I**
S77494	**24914**	Lysyl oxidase (*Lox*)	**II**
S72505	**LOC360447**	Glutathione S-transferase	**I**
U07971	**81660**	L-arginine:glycine amidinotransferase (*Gatm*)	**I**
J03481	**64192**	Quinoid dihydropteridine reductase	**I**
L19998	**83783**	Sulfotransferase family 1A, phenol-preferring, member 1 (*Sult1a1*)	**IV**
U81186	**84013**	Smooth muscle-specific 17beta-hydroxysteroid dehydrogenase type 3 (*Hsd17b12*)	**I**
U83880	**25062**	Glycerol-3-phosphate dehydrate dehydrogenase (*mtGPDH/Gpd2*)	**I-II**
X78949	**64475**	Prolyl 4-hydroxylase alpha subunit (*P4ha1*)	**I**
X08056	**25257**	Guanidinoacetate methyltransferase (*Gamt*)	**IV**
Y12178	**24268**	Bilitranslocase / Ceruloplasmin (*Cp*)	**III**
X16554	**29562**	Phosphoribosylpyrophosphate synthetase subunit I (*Prps1*)	**I**
AI177004	**29637**	Hmgc synthase 1 (Hmgcs1)	**I**
M10934	**25703**	Retinol-binding protein / retinol binding protein 4, plasma (*RBP/Rbp4*)	**II**
AF043642	**83624**	Matrin cyclophilin (M*atrin-cyp/Ppig*)	**III**

Table A.2 continued

Category 2 - Cellular and Systems-level Communication (64)

Cluster 1 - Neurotransmission (15)

Glutamatergic metabolism and signaling (6)			
M61099	**24414**	Metabotropic glutamate receptor 1 (*Grm1*)	**I**
M92076	**24416**	Metabotropic glutamate receptor 3 (*Grm3*)	**I**
M83561	**29559**	Glutamate receptor, ionotropic, kainate 1 (*Grik1*)	**I**
U08259	**24411**	N-methyl-D-aspartate receptor NMDAR2C subunit (*Grin2c*)	**III**
AF093267 and AF093268	**29546**	Homer1 and splice variant 1b, neuronal immediate early gene, 1 (*Homer1*)	**I-III/I**
X63744	**29483**	Glutamate transporter (*Glut-1*) / solute carrier family 1, member 3 (*Slc1a3*)	**I**
Synaptic function and maintenance (4)			
M64780	**25592**	Agrin (*Agrn*)	**I**
AB003991	**25012**	SNAP-25A	**I**
L20821	**81803**	Syntaxin 4 (*Stx4a*)	**I**
AF007758	**29219**	Synuclein 1, alpha (*Snca*)	**I**
Miscellaneous neurotransmission (5)			
M63901	**25719**	7B2 protein / Secretory granule neuroendocrine, protein 1 (*Sgne1*)	**I**
M22254	**24766**	Sodium channel, voltage-gated, type II, alpha polypeptide (*Scn2a1*)	**I**
U01344	**116631**	A-2 arylamine N-acetyltransferase 1 (*Nat1*)	**I-III**
U78090	**245960**	Potassium channel regulator 1	**I**
M86621	**25399**	Dihydropyridine-sesitive L-type calcium channel alpha-2 subunit (*Cacna2d1*)	**II**

Cluster 2 - Extracellular factors (2)

M62641	**24659**	Pro-melanin-concentrating hormone (*Pmch*)	**IV**
S49491	**29237**	Proenkephalin related sequence (*Penk-rs*)	**III**

Table A.2 continued

Cluster 3 - G-protein coupled receptors and associated proteins (10)

M64236	**24807**	Tachykinin receptor 1 / Substance P receptor (*Tacr1/SPR*)	**IV-I**
U12568	**64664**	ADP-ribosylation factor-like protein 3 (*Arl3/Rard3*)	**I**
AF076619	**58844**	Growth factor receptor bound protein 14 (*Grb14*)	**I-II**
AF091563	**309574**	Olfactory receptor gene (*Olr1687/QIL-LD1*)	**III-IV**
L12380	**64310**	ADP-ribosylation factor 1 (*Arf1*)	**I**
AJ001320	**29365**	Multiple PDZ domain protein (*Mpdz*)	**II**
U76206	**171108**	G protein-coupled receptor 105 (*Gpr105*)	**I**
X57764	**50672**	Endothelin receptor type B (*Ednrb*)	**I**
X55812	**25248**	Cannabinoid receptor 1, brain (*Cnr1*)	**I**
X52311	**117180**	Unr protein (*Unr*)	**I-III**

Cluster 4 - Cytosolic signaling factors and transducers (21)

M83298	**117104**	Caldesmon 1 / protein phosphatase 2, regulatory subunit B, alpha (*Ppp2r2a*)	**I**
L36088	**25237**	Activin receptor like kinase 1 / activin A receptor type II-like 1 (*Acvrl1*)	**III**
U26397	**80849**	Inositol polyphosphate 4-phosphatase (*Inpp4a*)	**I**
U48288	**25228**	A-kinase anchoring protein (*Akap11*)	**I**
D84346	**58823**	NCK-associated protein 1 (*Nckap1*)	**I**
U15734	**29218**	Reticulocalbin 2 / Taipoxin-associated calcium binding protein-49 (*Rcn2*)	**I**
U17901	**116645**	Phospholipase A-2-activating protein (*Plap/Plaa*)	**I**
U16655	**140693**	Phospholipase C delta-4 (*Plcd4*)	**IV**
AF095927	**64538**	Protein phosphatase 2C (*Ilkap*)	**III**
AF012714	**29688**	Multiple inositol polyphosphate histidine phosphatase 1 (*Minpp1*)	**I**
D45920	**84587**	130kDa-Ins(1,4,5)P3 binding protein	**I**

Table A.2 continued

D17521	**84360**	Protein kinase C-regulated chloride channel / chloride channel 3 (*Clcn3*)	**I**
D28560	**84050**	Ectonucleotide pyrophosphatase/phosphodiesterase 2 (*Enpp2*)	**I-III**
X58828	**117063**	Protein-tyrosine phosphatase, non-receptor type 2 (*Ptpn2*)	**I-III**
X16043	**NF**	Phosphatase 2A catalytic subunit isotype alpha	**I**
U38376	**24653**	Cytosolic phospholipase A2 (*Pla2g4a*)	**IV**
AF080435	**64013**	Phosducin-like protein (*Pdcl*)	**IV-I**
X16044	**24673**	Ppp2cb: protein phosphatase 2a, catalytic subunit, beta isoform	**I-II**
AJ000347	**64473**	3(2),5-bisphosphate nucleotidase (Bpnt1)	**I**
M93017	**170699**	Rat alternatively spliced mRNA / ATPase, Ca++-sequestering (*Atp2c1*)	**I-II**

Cluster 5 - Nuclear factors (16)

E-box and immediate early factors (6)

U17254	**79240**	Nuclear receptor subfamily 4, group A, member 1 (*Nr4a1/Ngfi-B*)	**I-II**
AF023087 and U75397	**24330**	Nerve growth factor induced factor A (*Ngfi-A*/*Egr1*)	**III**
U78102	**114090**	Krox-20 / early growth response 2 (*Egr2*)	**III-IV**
U09228	**84382**	NE Deaconess E-box binding factor / transcription factor 4 (*Tcf4*)	**III**
X96437	**294235**	Immediate early response 3 (*Ler3/PRG1*)	**IV**
AA875032	**NF**	Fos-related antigen, exon 4	**I**

Other nuclear factors (10)

M65251	**29721**	HIV type 1 enhancer-binding protein 2 (*Hivep2*)	**I**
U30381	**58820**	Zinc finger binding protein 148 (*Znf148*)	**I**
U48247	**64353**	LIM domain-containing protein / enigma homolog (*Enh*)	**II-III**
L23148	**24370**	Inhibitor of DNA-binding 1, splice variant 1d1	**III**
U67082	**25165**	KRAB-zinc finger protein KZF-1 / zinc finger protein 386 (*Znf386*)	**I**
M63282	**25389**	Leucine zipper protein / Activating transcription factor 3 (*Atf3*)	**III**
X59993	**312440**	Putative zinc finger protein / jumonji domain containing 1A (*Jmjd1a*)	**I**
L26292	**114505**	Kruppel-like factor (*Klf4*)	**I-II**

Table A.2 continued

L06804	**117555**	Myristoylated alanine-rich protein kinase C substrate / LIM homeobox protein 2 (*Lhx2*)	**III**

Category 3 - Protein Dynamics (28)

Cluster 1 - Degradation and synthesis (18)

M29358	**29304**	Ribosomal protein S6 (*Rps6*)	**I**
U30485 and AI009682	**116483**	Aspartyl-tRNA synthetase (Dars)	**I**
U64705	**303831**	Protein synthesis initiation factor 4AII	**I**
U11071	**LOC298510**	Polyadenylate-binding protein-related protein mRNA, 3' end.	**III**
AF096835	**29702**	Eukaryotic translation initiation factor 2 alpha kinase 3 (*Eif2ak3*)	**II-III**
AB022014	**116722**	Proteasome (prosome, macropain) 26S subunit, non-ATPase (*Psmd10*)	**I-II**
D21800	**29676**	Proteasome (prosome, macropain) subunit, beta type 3 (*Psmb3*)	**IV**
D30804	**29674**	Proteasome (prosome, macropain) subunit, alpha type 7 (*Psma7*)	**II**
D90258	**NF**	Proteasome subunit RC8	**I**
L14684	**114017**	Mitochondrial elongation factor G (*Gfm*)	**I**
AF000899	**245922**	Nucleoporin p58 (*p58/p45*)	**I-III**
X96426	**25435**	Eukaryotic elongation factor-2 kinase (*Eef2k*)	**I**
Y00826	**58958**	Integral membrane glycoprotein gp210 / nuclear pore protein (*Pom210*)	**I-III**
X82396	**64529**	Cathepsin B (*Ctsb*)	**II**
X67859	**81783**	Sjogren syndrome antigen B (*Ssb*)	**I**
AA859882	**29545**	Ubiquitin carboxyl-terminal hydrolase 1 (*Uchl1*)	**IV-I**
AA849648	**79449**	Ribosomal gene L21 (*Rpl21*)	**III**
M58340	**83840**	Ribosomal protein S6 kinase, polypeptide 1 (*Rps6kb1*)	**I**

Cluster 2 - Protein sorting and trafficking (2)

J03583	**54241**	Clathrin, heavy polypeptide (*Hc*)	**I**
U75400	**60384**	Coatomer beta subunit beta 2 (*Copb2*)	**I-II**

Table A.2 continued

Cluster 3 -Protein modification and folding (8)

X82021	**81800**	Heat shock related protein / suppression of tumorigenicity 13 (*St13*)	**I**
U95727	**84026**	DnaJ (Hsp40) homolog, subfamily A, member 2 (*Dnaja2*)	**I**
U68562	**63868 OR 25462**	Chaperonin 60 (*Hsp60*) and chaperonin 10 (*Cpn10/Hspe1*)	**I**
AF006617	**29734**	Stress 70 protein chaperone, microsome-associated, 60kD human homolog (*Stch*)	**I**
S78556	**NF**	75 kda glucose regulated protein	**I**
AI236601	**Close to LOC288444**	Similar to Heat shock protein (*Hsp105*)	**I-III**
L11319	**65166**	Signal peptidase complex (18kD) (*Spc18*)	**I**
L18889	**29144**	Calnexin (*Canx*)	**III-IV**

Category 4 - Cellular Development (17)

Cluster 1 - Cell cycle (1)

AF030091	**114121**	Cyclin L1 (*Ccnl1*)	**I**

Cluster 2 - DNA/chromatin related (5)

M64986	**25459**	High mobility group box 1 (*Hmgb1*)	**I**
D45254	**64530**	Cellular nucleic acid binding protein (*Cnbp*)	**I**
H33461	**117520**	Oxidation resistance 1 (*Oxr1*)	**I**
U95920	**81740**	Pericentriolar material (*Pcm1*)	**I**
AA964849	**25591**	ADP-ribosyltransferase 1 (*Adprt*)	**III**

Cluster 3 - Growth and differentiation (11)

L13619	**64194**	Growth response protein / insulin induced gene 1 (*Cl-6/Insig1*)	**I**
U03414	**93667**	Neuronal olfactomedin-related ER localized protein (*D2Sut1e/Olfm1*)	**III**

Table A.2 continued

D82074	**29458**	BHF-1 / Neurogenic differentiation 1 (*Neurod1*)	**III**
Y07704	**65190**	Best5 protein (*Best5*)	**III**
U95178	**79128**	Disabled homolog 2 (*Dab2*)	**I**
X62322	**29143**	Epithelin 1 and 2 / Granulin (*Grn*)	**III**
AI014163	**29596**	Interferon related developmental regulator 1 (Ifrd)	**I**
D89983	**58961**	Ornithine decarboxylase antizyme inhibitor (Oazi)	**I-III**
AF017437	**29364**	Integrin-associated protein / CD47 antigen (Rh-related antigen, integrin-associated signal transducer) (*Cd47*)	**III**
D88250	**192262**	Serine protease / complement component 1 (*C1s*)	**II**

Category 5 - Defense and Detoxification (10)

M76740	**24573**	Intestinal mucin / mucin 3 (*Muc3*)	**III**
M81642	**25439**	Coagulation factor II / thrombin receptor (*F2r*)	**II-III**
M86564	**29222**	Prothymosin alpha (*Ptma*)	**I**
U41803	**64476**	Hypertension-related protein / mitofusin 2 (*Mfn2*)	**I-III**
S79676	**25166**	Interleukin-1 beta-converting enzyme / caspase 1 (*Casp1*)	**IV-I**
AF087944	**60350**	Monocyte differentiation antigen CD14	**I-II**
D10926	**29436**	Tissue factor pathway inhibitor (*Tfpi*)	**I**
AF029240	**365527**	MHC class Ib RT1.S3 (RT1.S3) / RT1 class I, M6, gene 2	**II**
L26268	**29618**	B-cell translocation gene 1, anti-proliferative (*Btg1*)	**I**
U90829	**84019**	APP-binding protein 1 (*Appbp1*)	**I**

Category 6 - Cytoskeletal and Adhesion (10)

S85184		Cathepsin L proenzyme	**III**
U18314	**25359**	Lamina associated polypeptide 2 / thymopoietin (*LAP2/Tmpo*)	**I**
U09357	**25613**	Protein tyrosine phosphatase zeta/beta (*Ptprz1*)	**I**
AF104362	**83717**	Osteoadherin / osteomodulin (*Omd*)	**I-II**

Table A.2 continued

AF097593	**83501**	Cadherin 2 (*Cdh2*)	**I**
AJ012603	**57027**	A disintegrin and metalloproteinase domain 17 (*Adam17*)	**II**
D90401	**26955**	Afadin (*Af6*)	**IV**
M88469	**64456**	F-spondin (*Sponf*)	**I**
X70369	**84032**	Pro alpha 1 collagen type III (*Col3a1*)	**I-III**
M23697	**25692**	Plasminogen activator, tissue (*Plat*)	**I**

ESTs and Genes with Unknown Function (138)

AA799442	**EST**	**I**
AA799466	**EST**	**III**
AA799594	**EST**	**IV**
AA799621	**EST**	**I**
AA799889	**EST**	**I**
AA799899	**EST**	**IV**
AA799971	**LOC313369**	**I**
AA800156	**LOC310071**	**I-III**
AA800184	**EST**	**I**
AA800200	**LOC298426**	**II**
AA800551	**EST**	**I**
AA800693	**Close to 83578**	**I**
AA800701	**EST**	**I**
AA800708	**LOC295310**	**II**
AA800738	**EST**	**IV**
AA800749	**EST**	**III**
AA800782	**LOC294082**	**II**
AA800808	**EST**	**I**
AA800853	**LOC305302**	**II**

Table A.2 continued

AA800948	**EST**		**IV**
AA818226	**EST**		**III**
AA849648	**EST**		**III**
AA859652	**EST**		**I-II**
AA859702	**EST**		**I-II**
AA859954	**EST**		**I**
AA859996	**LOC305436**		**II**
AA860030	**EST**		**I-III**
AA860047	**EST**		**I**
AA866383	**EST**		**I**
AA874943	**EST**		**I**
AA875032	**EST**		**I**
AA875190	**EST**		**I**
AA875198	**EST**		**I**
AA875206	**114590**	Ubiquilin 1 (*Ubqln1*)	**I-III**
AA875233	**EST**		**III**
AA875598	**EST**		**III**
AA891035	**EST**		**I**
AA891580	**EST**		**II**
AA891634	**EST**		**I**
AA891681	**EST**		**I**
AA891734	**EST**		**I**
AA891824	**EST**		**I-III**
AA891834	**EST**		**I**
AA891851	**EST**		**I**
AA891872	**EST**		**I**
AA892027	**EST**		**IV**

Table A.2 continued

AA892056	**EST**		**I**
AA892083	**EST**		**III**
AA892094	**EST**		**I**
AA892128	**EST**		**III**
AA892306	**EST**		**I**
AA892367	**EST**		**III**
AA892390	**EST**		**I-II**
AA892548	**EST**		**I**
AA892554	**EST**		**I**
AA892557	**EST**		**I-II**
AA892559	**EST**		**III**
AA892598	**LOC294523**	Similar to hypothetical protein MGC46970	**II**
AA892638	**EST**		**I-III**
AA892820	**EST**		**IV-I**
AA892828	**EST**		**I**
AA892859	**EST**		**I-II**
AA892860	**EST**		**I**
AA892863	**close to LOC295922**		**I**
AA893330	**EST**		**I**
AA893436	**EST**		**III**
AA893602	**EST**		**IV-I**
AA893673	**EST**		**II**
AA893853	**EST**		**II**
AA894101	**EST**		**I**
AA894193	**EST**		**I**
AA894259	**LOC304206**		**IV-I**
AA894282	**EST**		**I**

Table A.2 continued

AA894321	**EST**	**III**
AA925473	**EST**	**I**
AA925717	**EST**	**III**
AA943331	**EST**	**III**
AA945169	**EST**	**II**
AA946040	**EST**	**IV**
AA946439	**EST**	**II-III**
AA955859	**EST**	**II**
AA957961	**EST**	**III**
AA963449	**Close to Cyp51**	**I**
AA998683	**EST**	**IV**
AI010357	**EST**	**I**
AI010580	**EST**	**I**
AI012275	**EST**	**I**
AI012595	**EST**	**I**
AI029805	**EST**	**III**
AI102868	**EST**	**IV**
AI103671	**EST**	**I-III**
AI103838	**EST**	**IV**
AI170685	**EST**	**I**
AI170776	**EST**	**I**
AI171090	**EST**	**III**
AI171268	**EST**	**III**
AI171630	**EST**	**I**
AI176170	**EST**	**I-II**
AI177404	**EST**	**I**
AI227887	**EST**	**I**

Table A.2 continued

AI229497	**EST**	**IV**
AI230572	**EST**	**III**
AI230602	**EST**	**III**
AI231354	**EST**	**I-II**
AI231807	**EST**	**I-III**
AI233225	**EST**	**I**
AI233365	**EST**	**III**
AI234604	**EST**	**I**
AI236484	**EST**	**I**
AI237592	**EST**	**I**
AI638985	**EST**	**I**
AI639015	**EST**	**I-II**
AI639039	**EST**	**III**
AI639044	**EST**	**III**
AI639076	**EST**	**III**
AI639097	**EST**	**III-IV**
AI639128	**EST**	**II**
AI639148	**LOC292262**	**IV**
AI639149	**EST**	**II**
AI639161	**EST**	**II**
AI639187	**EST**	**III**
AI639324	**EST**	**I**
AI639410	**EST**	**I**
AI639413	**LOC307334**	**IV-I**
AI639429	**EST**	**III**
AI639448	**EST**	**III**
AI639521	**EST**	**I**

Table A.2 continued

H31323	**EST**		**II**
H33426	**EST**		**II**
H33629	**EST**		**I**
M13100	24540	Long interspersed repetitive DNA sequence LINE3 (*Lre3*).	**I**
M91235	**NF**	Rat VL30 element mRNA.	**I**
U48828	**NF**	Retroviral-like ovarian specific transcript 30-1 mRNA.	**I-II**
U49058	245924	CTD-binding SR-like protein rA4	**I**
U61729	286988	Proline rich protein 2 (*Pnrc1*)	**I**
X52817	**NF**	C1-13 gene product	**IV-I**
X60351	**NF**	Alpha B-crystallin (ocular lens tissue)	**IV**
AB008538	**79559**	Activated leukocyte cell adhesion molecule (*Alcam*)	**I**

Functional categorization of circadian-regulated genes in the rat SCN. Listed are the GenBank, Locus Link ID, functional category/cluster and Phase Group assignment for genes and ESTs that surpassed stringent expression criteria and displayed circadian profiles of mRNA expression in the rat SCN.

Table A.3. ***Genes with circadian profiles common to NIH/3T3 cells and Rat-1 or Rat 3Y1 fibroblasts.***

Gene descriptor (symbol)	Rat-1 (**32**)	Rat 3Y1 (**47**)
Period 2 (*Per2*)	**X**	**X**
Cryptochrome 1 (*Cry1*)	**X**	**X**
Brain and muscle ARNT-like protein (*Bmal1* or *Mop3)*	**X**	
Annexin XI (*Anxa11*)	**X**	**X**
Cell-division kinase 4 (*Cdk4*)		**X**
Ubiquitin-like 4 *(*Ubl4*)*	**X**	
Histone *H2a*(A)-613, *H2a*(B)-613, and *H2b*-613 (H2b) genes		**X**
Immunoglobulin kappa chain V-region *(Iak-V28*)		**X**
RAN GTPase activating protein 1 (*Rangap1*)		**X**
Voltage-dependent, L type, alpha 1C calcium channel (*Cacna1c*)		**X**

Genes with circadian expression profiles in NIH/3T3 cells and in rat-1 or 3Y1 fibroblasts. The gene descriptor and symbol are listed for rhythmic genes identified in NIH/3T3 cells that correspond to functionally similar or homologous genes with rhythmic patterns observed in rat-1 (**32**) or rat 3Y1 fibroblasts (**47**).

Table A.4. ***Functional categorization of temporal profiles of gene expression in NIH/3T3 cells***

GenBank ID	Gene descriptor (symbol)	Phase Group
Category 1 - Energetics		
Cluster 1 - Glucose Metabolism and Electron Transport Chain		
Rhythmic (N=2)		
***X13586**	2,3-bisphosphoglycerate mutase (*Bpgm*)	**I**
***AF058955**	ATP-specific succinyl-CoA synthetase beta subunit (*Scs*)/	**IV**
	succinate-Coenzyme A ligase, ADP-forming (*Sucla2*)	
NIH/3T3-specific non-rhythmic genes (N=1)		
D50430	Glycerol-3-phosphate dehydrogenase (*Gdm1*)	
Cluster 2 - Lipid and fatty acid metabolism		
Rhythmic (N=3)		
X13135	Fatty acid synthase (*Fasn*)	**I**
†M21285	Stearoyl-coenzyme A desaturase 1 (*Scd1*)	**I**
†U15977	Mus musculus long chain fatty acyl CoA synthetase (*Facl*)	**I**
NIH/3T3-specific non-rhythmic genes (N=1)		
L42293	Acyl-coenzyme A/cholesterol acyltransferase (*Soat1*)	
Cluster 3 - Transporters		
Rhythmic (N=4)		
***U17132**	Zinc transporter 1 (*Znt1/Slc30a1*)	**I**
AF035526	Kanadaptin/solute carrier family 4 (anion exchanger), member 1, adaptor protein (*Slc4a1ap*)	**I**
U74079	Solute carrier (sodium/hydrogen exchanger), isoform 3 regulator 1 (*Slc9a3r1*)	**I**
***U13838**	ATPase, H+ transporting, V1 subunit B, isoform 2 (*Atp6v1b2*)	**IV**

Table A.4 continued

NIH/3T3-specific non-rhythmic genes (N=5)		
X67056	Glycine transporter (*Glyt1*)	
L23755	Solute carrier family 19 (sodium/hydrogen exchanger), member 1 (*Slc19a1*)	
X66119	5-hydroxytryptamine (serotonin) transporter (*Slc6a4*)	
AB015800	*Octn2* solute carrier family 22 (organic cation transporter), member 5 (*Slc22a5*)	
M21247	Uncoupling protein 1 (mitochondrial, proton carrier) (*Ucp1*)	

Cluster 4 - Miscellaneous metabolism		
Rhythmic (N=8)		
X61172	Mouse mRNA for alpha-mannosidase II	**I**
X07888	3-hydroxy-3-methylglutaryl coenzyme A reductase, exon 2 (*Hmgcr*)	**I**
U12961	NAD(P)H menadione oxidoreductase 1, dioxin inducible (*Nqo1*)	**II**
L42996	Nuclear-encoded mitochondrial acyltransferase	**I**
U52524	Hyaluronan synthase 2 (*Has2*)	**I**
K01515	Hypoxanthine guanine phosphoribosyl transferase (*Hprt*)	**I**
M35970	Mouse tumor metastatic process-associated protein (*NM23*/*Nme1*)	**I-IV**
Z23077	S-adenosylmethionine decarboxylase, pseudogene 1/Amd-ps1	**I**
NIH/3T3-specific non-rhythmic genes (N=9)		
U20257	Class IV alcohol dehydrogenase (*Adh3*)	
X98055	Glutathione S-transferase theta (*Gstt1*)	
AF074926	Heparan sulfate N-deacetylase/N-sulfotransferase 1 (*Ndst1*)	
M34141	Prostaglandin-endoperoxide synthase 1 (*Ptgs1*)	
M81483	Calmodulin dependent phosphatase catalytic subunit (*Ppp3cb*)	
AB001607	Prostacyclin synthase (*Ptgis*)	
AF001871	GRP1 Pleckstrin homology, Sec7 and coiled-coil domains 3 (*Pscd3/Grp1/AI648983*)	

Table A.4 continue

U18975	Beta-1,4 N-acetylgalactosaminyltransferase (*Galgt1*)	
AF031467	Branched-chain amino acid aminotransferase (*Bcat2*)	

Category 2 - Cellular Communication		
Cluster 1 - Neurotransmission		
Glutamatergic metabolism and signaling (1 rhythmic, 0 non-rhythmic)		
Rhythmic (N=1)		
***U95053**	Glutamate cysteine ligase/gamma-glutamylcysteine synthetase (*Gclm*)	**I**
NIH/3T3-specific non-rhythmic genes (N=0)		

Synaptic function and maintenance		
Rhythmic (N=0)		
NIH/3T3-specific non-rhythmic genes (N=1)		
D38375	Syntaxin 3D-2 (*Stx3*)	

Miscellaneous neurotransmission		
Rhythmic (N=1)		
U17869	Voltage-dependent, L type, alpha 1C calcium channel (*Cacna1c*)	**I**
NIH/3T3-specific non-rhythmic genes (N=6)		
Z49916	Chloride channel 4-2 (*Clcn4-2*)	
X82655	Acetylcholine receptor beta 2 neural (beta 2-subunit)	
Y09585	Serotonin 4L receptor (*Htr4*)	
U37249	Arylamine N-acetyltransferase stable form (*Nat2*)	
AF051947	T-type calcium channel alpha-1 subunit (*Cacna1h*)	
X94908	Serotonin 1D receptor (*5-HT1D*)	

Table A.4 continued

Rhythmic (N=1)		
***Z22703**	Fibroblast growth factor 7 (*Fgf7*)	**I**
NIH/3T3-specific non-rhythmic genes (N=4)		
X72307	Hepatocyte growth factor (*Hgf*)	
X55573	Brain-derived neuroptrophic factor (*Bdnf*)	
X99572	c-fos induced growth factor (*Figf*)	
AF004874	Latent TGF-beta binding protein-2 (*Ltbp2*)	

Cluster 3 - G-protein coupled receptors and associated proteins		
Rhythmic (N=5)		
U08110	RAN GTPase activating protein 1 (*Rangap1*)	**I**
L32752	Mouse (clone M2) GTPase (*Ran*)	**I**
U10551	GTP binding protein (gene overexpressed in skeletal muscle)	**I**
L38444	Mus musculus (clone U2) T-cell specific GTPase (*Tgtp*)	**II**
***D87901**	ADP-ribosylation factor 4 (*Arf4*)	**I**
NIH/3T3-specific non-rhythmic genes (N=8)		
U08354	Melanocortin-5 receptor (*Mc5r*)	
D49956	8-oxo-dGTPase (*Mth1*)	
L08075	Phosducin (*Rpr1*)	
AB004879	M-Ras (*M-Ras*)	
AF019371	CCK-B/gastrin receptor (*Cckbr*)	
D86563	Rab 4 (*Rab4a*)	
U33005	Tbc1 (*Tbc1d1*)	
AB004315	RGS4 Regulator of G-protein signaling 4 (*Rgs4*)	

Table A.4 continued

Cluster 4 - Cytosolic signaling factors and transducers		
Rhythmic (N=25)		
AF086905	Mus musculus protein kinase (*Chk2*)	**II**
M96163	Mus musculus (clone 2) serum inducible kinase (*SNK*)	**I**
***X13664**	Neuroblastoma ras oncogene (*Nras*)	**I**
X76850	Mus musculus mRNA for MAP kinase-activated protein kinase 2	**I**
X63440	Protein tyrosine phosphatase, non-receptor type 12 (*Ptpn12*)	**III**
AF039574	Serine/threonine kinase 2 (*Slk*)	**I**
U68171	Phosphodiesterase 7A (*Pde7a*)	**IV**
***D37801**	Protein tyrosine phosphatase, receptor type D (*Ptpn21*)	**I**
***AF006201**	Mus musculus prostaglandin F2 alpha receptor regulatory protein (*Ptgfrn*)	**IV**
U84411	Mus musculus protein tyrosine phosphatase (PRL-1)	**I**
AB020202	Mus musculus mRNA for adenylate kinase isozyme 2	**I**
U73478	Acidic nuclear phosphoprotein 32	**III**
AJ223071	Mus musculus mRNA for serine/threonine kinase protein, long-form	**III**
***L02526**	Protein kinase, mitogen activated, kinase 1/*p45*	**I**
U43585	Mus musculus kinase suppressor of ras-1 (KSR1)	**I**
AF043326	Mus musculus N-myristoyltransferase 1 (*Nmt1*)	**I**
AF033663	PRP4 pre-mRNA processing factor 4 homolog B (yeast)/pre-mRNA protein kinase (*Prpf4b*)	**I**
U34973	Phosphoserine/threonine/tyrosine interaction protein (*Styx*)	**I**
U02313	MAST205 protein kinase/microtubule associated serine/threonine kinase 2 (*Mast2*)	**I**
AI180687	Phosphodiesterase 4B, cAMP specific (*Pde4b*)	**I**
AV336804	Mus musculus cDNA/3' end of protein kinase C, theta (*Prkcq*)	**II**
AI838337	Mus musculus cDNA/polynucleotide kinase 3'- phosphatase (*Pnkp*)	**I**
U65986	Annexin XI (*Anxa11*)	**I**
L21671	Epidermal growth factor receptor pathway substrate 8 (*Eps8*)	**I**

Table A.4 continued

AV007820	Mus musculus cDNA/S100 calcium binding protein A13 (*S100a13*)	**IV**
NIH/3T3-specific non-rhythmic genes (N=13)		
D17433	Prostaglandin F receptor (*Ptgfr*)	
AF059029	Calcium/calmodulin-dependent protein kinase II delta (*Camk2d*)	
M63801	Connexin 43 (*Gja1*)	
M80739	Protein tyrosine phosphatase, non-receptor type 2 (*Ptpn2*)	
X82288	Protein-tyrosine-phosphatase (*Ptprs*)	
AF099988	Ste-20 related kinase SPAK (*Stk39*)	
AB012393	Inositol 1,4,5 trisphosphate receptor type2 (*Itpr2*)	
X84896	ATP receptor (*P2rx1*)	
AJ009823	P2X7 receptor subunit (*P2rx7*)	
X77731	Deoxycytidine kinase (*Dck*)	
AF000236	RDC1 orphan chemokine receptor (*Cmkor1*)	
X70764	Serine/threonine protein kinase (*Emk*)	
AF039601	Betaglycan transforming growth factor, beta receptor III (*Tgfbr3*)	

Cluster 5 - Nuclear factors		
E-box and immediate early factors		
Rhythmic (N=8)		
***U10325**	Aryl hydrocarbon receptor nuclear translocator (*Arnt*)	**I**
X61800	CCAAT/enhancer binding protein (*C/EBP-delta*)	**I**
M60285	CAMP responsive element modulator	**I**
†U16322	Transcription factor 4 (*Tcf4*)	**I**
M94087	Activating transcription factor 4 (*Atf4*)	**I**
X67644	Cyclic AMP inducible gene 3/immediate early response 3 (*Ier3*)	**I, I-IV**

Table A.4 continued

AF036893	Mus musculus circadian clock protein period homolog 2 (Drosophila) (*Per2*)	**I**
†M28845	Early growth response 1 (*Egr-1*)	**I**
NIH/3T3-specific non-rhythmic genes (N=3)		
AF017128	Fos-related antigen 1 (*fra-1*)	
X12761	Jun oncogene (*Jun*)	
M61007	CCAAT/enhancer binding protein (C/EBP), beta (*Cebpb*)	

Other nuclear factors		
Rhythmic (N=14)		
AB000777	Cryptochrome 1 (photolyase-like) (*Cry1*)	**I**
X95504	Mus musculus mRNA for zinc finger protein	**I**
AB023485	Mus musculus mRNA for transcription factor CA150b	**I**
M36146	Zinc finger protein 35	**I**
U46186	Zinc finger protein 93	**III**
AB000490	Nuclear receptor subfamily 5, group A, member 1 (*Nr5a1*)	**III**
U53228	RAR-related orphan receptor alpha (*Rora / sg, ROR1, ROR2, ROR3, Nr1f1*)	**I**
X17459	Recombining binding protein suppressor of hairless (Drosophila) (Rbpsuh-rs3)	**I**
M34476	Retinoic acid receptor, gamma (*Rarg*)	**I**
AF050182	Mus musculus Period 3 (*Per3*)	**I**
X74040	Forkhead box C2 (*Foxc2*)	**I**
Y12293	Mus musculus lun gene, exon 1/forkhead box F2 (*Foxf2*)	**I**
U20282	Transcription factor 20 (*Tcf20*)	**III**
AA794509	Mus musculus cDNA/reduced expression 2 (*Rex2*)	**I**
NIH/3T3-specific non-rhythmic genes (N=10)		
L13204	HNF-3/fork-head homolog-4 (*Foxj1*)	

Table A.4 continued

Z23066	Mi protein (*Mitf*)
X66223	Retinoid X receptor-alpha (*Rxra*)
M60909	Retinoic acid receptor-alpha (*Rara*)
M57966	HNF-3/fork-head homolog-1 (*Tcf1*)
X60136	Trans-acting transcription factor 1 (*Sp1*)
AB013097	Brain finger protein (*Zfp179*)
D90174	Nuclear factor I/A (*Nfia*)
L00039	Myelocytomatosis oncogene (*c-myc*)
X16995	Nuclear receptor subfamily 4, group A, member 1 (*Nr4a1*)

Category 3 - Protein dynamics		
Cluster 1 - Degradation and synthesis		
Rhythmic (N=15)		
X54327	Mus musculus mRNA for glutamyl-prolyl-tRNA synthetase (*Eprs*)	**I**
U39473	Mus musculus histidyl-tRNA synthetase mRNA (*Hars*)	**I**
U20619	Mus musculus serine-rich RNA polymerase suppressor protein1 (SRP1)	**I**
X91656	Splicing factor, arginine/serine-rich 3 (*SRp20*)	**I**
J04761	Ubiquitin-like 4 (*Ubl4*)/solute carrier family 10 (sodium/bile acid cotransporter family) (*Slc10a3*)	**I**
Y13071	Proteasome (prosome, macropain) 26S subunit, non-ATPase, 14 (*Psmd14*)	**I**
U11274	Heterogeneous nuclear ribonucleoprotein D (*Hnrpd*)	**I**
X98511	Splicing factor, arginine/serine-rich 2 (SC-35) (*Sfrs2*)	**I**
L00993	Sjogren syndrome antigen B (*Ssb*)	**IV**
AF061503	Bop1 protein (*Bop1*) and heat shock transcription factor I (*Hsf1*)	**I**
AB007139	Proteaseome (prosome, macropain) 28 subunit, 3 (*Psme3*)	**I**

Table A.4 continued

AA690583	Splicing factor proline/glutamine rich (polypyrimidine tract binding protein associated) (*Sfpq*)	**I**
AF060490	TLS-associated protein TASR-2/FUS interacting protein (serine-arginine rich) 1(*Fusip1*)	**I**
AW121031	Mus musculus cDNA/nucleolar protein family A, member 2 (*Nola2*)	**I**
J04620	Primase p49 subunit/(*Prim1*)	**I**
NIH/3T3-specific non-rhythmic genes (N=4)		
U58280	Second largest subunit of RNA polymerase I (*Rpo1-2*)	
U12620	Dipeptidyl peptidase IV (*CD26*)	
AF091998	Calpain Lp82 (*Capn3*)	
M27347	Elastase 1 (*Ela1*)	

Cluster 2 - Protein sorting and trafficking		
Rhythmic (N=7)		
D17577	Kinesin heavy chain member 1B (*Kif1b*)	**I**
AF020771	Mus musculus importin alpha Q1 mRNA/karyopherin alpha 4	**I**
X14971	Adaptor protein complex AP-2, alpha 1 subunit (*Ap2a1*)	**I**
AW123408	KDEL (Lys-Asp-Glu-Leu) endoplasmic reticulum protein retention receptor 2 (*Kdelr2*)	**I**
U91933	Adaptor-related protein complex 3, sigma 2 subunit (*Ap3s2*)	**II**
U78315	Hermansky-Pudlak syndrome 1 homolog (human) (*Hps1*)	**II**
AF043120	Coatomer protein complex, subunit beta 2 (beta prime) (*Copb2*)	**I**
NIH/3T3-specific non-rhythmic genes (N=2)		
AF003999	Golgi SNARE GS15 (*Bet1l*)	
AF076681	Eukaryotic translation initiation factor 2 alpha kinase 3 (*Eif2ak3*)	

Table A.4 continued

Cluster 3 - Protein modification and folding		
Rhythmic (N=4)		
U08215 AA919208 &	Mus musculus Hsp70-related NST-1 (*hsr.1*)	**I**
D85904	Heat shock protein 4 (Hspa4/*Hsp70*)	**I**
D50264	Phosphatidylinositol glycan, class F (*Pigf*)	**III**
***U73820**	UDP-N-acetyl-alpha-D-galactosamine:polypeptide N-acetylgalactosaminyltransferase 1 (*Galnt1*)	**IV**
NIH/3T3-specific non-rhythmic genes (N=2)		
M60320	Protein-L-isoaspartate (D-aspartate) O-methyltransferase1/protein carboxyl methyltransferase (*Pcmt1*)	
U35646	Puromycin-sensitive aminopeptidase (*Psa*)	

Category 4 - Cellular Development		
Cluster 1 - Cell Cycle		
Rhythmic (N=5)		
AA791962	Mus musculus cDNA/ similar to D-type G1 cyclin catalytic subunit/ cyclin-dependent kinase 4 (*Cdk4*)	**II**
AJ223087	Mus musculus mRNA for Cdc6-related protein	**I**
AF016583	Mus musculus checkpoint kinase 1 homolog (*Chk1/Chek1*)	**I**
U42385	SMC2 structural maintenance of chromosomes 2-like 1 (yeast) (*Smc2l1*)	**I**
D83745	B-cell translocation gene 3 (*Btg3*)	**I**
NIH/3T3-specific non-rhythmic genes (N=1)		
U09968	Cyclin-dependent kinase inhibitor (*p27kip1*)	

Table A.4 continued

Cluster 2 - Maintenance of DNA and chromatin		
Rhythmic (N=10)		
AF006602	Mus musculus histone deacetylase (mHDA1)	**I**
AF012710	Mus musculus centromere protein A (*Cenp-a*) gene, promoter region and partial cds	**III**
L32751	Lipopolysaccharide response/Ran, member RAS oncogene family	**I**
D87973	Imprinted and ancient (*Impact*)	**I**
X12944	HMG-17 chromosomal protein/binding domain 2 (*Hmgn2*)	**II**
U62673	Mus musculus histone *H2a(A)-613*, histone *H2a(B)-613*, and histone *H2b-613* (*H2b*) genes	**IV**
X67668	High mobility group box 2 (*Hmgb2*)	**I**
U25691	Helicase, lymphoid specific (*Hells*)	**I**
D26089	Mini chromosome maintenance deficient 4 homolog (*S. cerevisiae*) (*Mcm4*)	**I**
AB028920	A kinase anchor protein 8	**I**
NIH/3T3-specific non-rhythmic genes (N=1)		
X12521	Transition protein 1 (*Tnp1*)	

Cluster 3 - Growth and differentiation		
Rhythmic (N=9)		
Y00208	Homeo box A5 (*Hoxa5*)	**I**
X55318	Homeo box C9 (*Hoxc9*)	**II**
L06864	Epidermal growth factor receptor (*EGFR*)	**III**
X96639	Exostoses (multiple) 1 (*Ext1*)	**I**
U88327	Suppressor of cytokine signalling-2 (*SOCS-2*)	**I**
M12379	Mouse Thy-1.2 glycoprotein/thymus cell antigen 1, theta (*Thy1*)	**I**
K02245	Proliferin (*Plf*)	**I-II**

Table A.4 continued

D31967	Jumonji, AT rich interactive domain 2 (*Jarid2*)	**I**
AF014117	GDNF receptor/glial cell line derived neurotrophic factor family receptor alpha 1 (*Gfra1*)	**I**
NIH/3T3-specific non-rhythmic genes (N=13)		
AB010557	Pax4 (*Pax4*)	
D49921	Glial cell line-derived neurotrophic factor (*Gdnf*)	
L35049	Bcl2-like (*Bcl2l*)	
D85028	Semaphorin 3A (*Sema3a*)	
AB018194	BIT/Signal-regulatory protein alpha (*Sirpa/Ptpns1*)	
U59746	Bcl-w (*Bcl2l2*)	
AF017255	Persyn Synuclein, gamma (*Sncg*)	
Z21858	pS2m/trefoil factor 1 (*Tff1*)	
AB010152	p73H/transformation related protein 63 (*Trp63*)	
U94331	Osteoprotegerin (*Tnfrsf11b*)	
AF047389	Dominant megacolon mutant Sox-10 protein (*Sox10*)	
Z12171	Putative homeotic protein/Dlk1-like protein (*Dlk1*)	
L12447	Insulin-like growth factor binding protein 5 (*Igfbp5*)	

Category 5 - Defense and Detoxification		
Rhythmic (N=21)		
M57999	Nuclear factor of kappa light chain gene enhancer in B-cells (*Nfkb1*)	**I**
***U92565**	Small inducible cytokine subfamily D, 1	**I**
AF100927	Mus musculus apoptosis-inducing factor AIF (*Aif*)	**I**
V00835	Metallothionein 1 (*Mt1*)	**IV**
Y13090	Mus musculus mRNA for caspase-12	**IV**

Table A.4 continued

D89613	Cytokine inducible SH2-containing protein (*Cish*)	**I**
***AF029215**	Antigen identified by monoclonal antibody MRC OX-2 (*Mox2*)	**IV**
D64162	Retinoic acid early transcript gamma (Rae-123) cell surface protein (*Raet1c*)	**II**
M63695	CD1d1 antigen (*Cd1d1*)	**I-II**
***U27267**	Small inducible cytokine B subfamily, member 5/chemokine (C-X-C motif) ligand 5 (*Cxcl5*)	**I**
D63679	Decay accelerating factor 1 (*Daf1*)	**I**
U10094	Killer cell lectin-like receptor, subfamily A, member 7	**IV**
X00246	Set 1 repetitive element for a class I MHC complex/histocompatibility 2, D region locus 1 (*H2-D1*)	**II**
***U81052**	Defender against cell death 1 (*Dad1*)	**I**
***J04596**	GRO1 oncogene/chemokine (C-X-C motif) ligand 1 (*Cxcl1*)	**I**
U35623	Myeloid cell leukemia sequence 1 (*Mcl1*)	**I**
U44088	Pleckstrin homology-like domain, family A, member 1 (*Phlda1*)	**I**
M18237	Mouse Ig kappa chain V-region/similar to immunoglobulin light chain variable region	**III**
AF071179	Formyl peptide receptor, related sequence 1 (*Fpr-rs1*)	**I**
AW045202	Thioredoxin domain containing 7	**I**
***AB027565**	Thioredoxin reductase 1 (*Txnrd1*)	**I**
NIH/3T3-specific non-rhythmic genes (N=7)		
M20658	Interleukin 1 receptor, type I (*Il1r1*)	
U38261	Extracellular superoxide dismutase (*Sod3*)	
M27960	Interleukin 4 receptor, alpha (*Il4ra*)	
AF036907	Linker for activation of T cells (*Lat*)	
AF027707	Apoptosis activator (*Mtd/Bok*)	
X81627	Lipocalin 2 (*Lcn2*)	

Table A.4 continued

AJ009840	Cathepsin E protein, exon 1

Category 6 - Cytoskeletal elements and Adhesion		
Rhythmic (N=14)		
X52046	Procollagen, type III, alpha 1 (*Col3a1*)	**III**
U20365	Actin, gamma 2, smooth muscle, enteric (*Actg2*)	**I**
X66084	Hyaluronic acid receptor/CD44 antigen (*Cd44*)	**I**
***U12884**	Mus musculus C57BL/6 vascular cell adhesion molecule-1 truncated form T-VCAM-1 (*Vcam-1*)	**I**
L07921	Iduronate 2-sulfatase (*Ids*)	**III**
U14135	Integrin alpha V (*Cd51/Itgav*)	**IV**
J04181 & M12481	Actin, beta, cytoplasmic (*Actb*)	**I**
L18880	Vinculin (*Vcl*)	**I**
Z19543	h2-Calponin 2 (*Cnn2*)	**I**
J03520	Plasminogen activator, tissue (*Plat*)	**III**
M32490	Insulin-like growth factor binding protein 10/cysteine rich protein 61 (*Cyr61*)	**III**
D88793	Cysteine rich protein/cysteine and glycine-rich protein 1 (*Csrp1*)	**I**
M62470	Thrombospondin 1 (*Thbs1*)	**I**
AW123707	Mus musculus cDNA/par-3 (partitioning defective 3) homolog (*C. elegans*) (*Pard3*)	**I**
NIH/3T3-specific non-rhythmic genes (N=7)		
X72795	Gelatinase b (*Mmp9*)	
D78265	Pancortin-4 (*Olfm1*)	
U07890	Epidermal surface antigen (*Flot2*)	
U90435	Flotillin (*Flot1*)	

Table A.4 continued

AB020886	Ssecks A kinase anchor protein (*Gravin*) 12 (*Akap12*)	
X83506	Utrophin (*Utrn*)	
L31397	Dynamin (*Dnm*)	

Category 7 - Unknown and ESTs		
Rhythmic (N=166)		
L36829	Mus Musculus alpha A-crystallin-binding protein I (*alphaA-CRYBP1*) gene	**I-IV**
AW046227	UI-M-BH1-ala-a-08-0-UI.s1 Mus musculus cDNA	**III**
AI643885	Mus musculus cDNA	**IV**
AI838853	Mus musculus cDNA	**I**
AI131982	Mus musculus cDNA	**II**
Z31360	Mus musculus (Balb/C) P/L01 mRNA	**IV**
Z83956	Similar to spermidine synthase/Mus musculus spermidine synthase pseudogene	**I**
U95783	Mus musculus endogenous provirus Imposon1 envelope gene	**III**
U17961	Similar to SRC associated in mitosis, 68 kDa	**IV**
AW046194	Mus musculus cDNA	**I**
AI854432	Mus musculus cDNA	**I**
X14206	Poly (ADP-ribose) polymerase/model, pseudogene, not transcribed	**IV**
AA871791	Abhydrolase domain containing 5 (*Abhd5*)	**I**
AW046850	Mus musculus cDNA	**III**
AW048189	Mus musculus cDNA	**I**
AI843655	Mus musculus cDNA	**I**
AI788543	Mus musculus cDNA	**I**
AI197507	Mus musculus cDNA	**I**

Table A.4 continued

D73368	Musculus domesticus adult thymus Mer protein/enhancer of rudimentary homolog (*Drosophila*) (*Erh*)	**I**
U88588	Cerebellar degeneration-related 2 (*Cdr2*)	**I**
U70210	TR2L/amyloid beta (A4) precursor protein-binding, family B, member 2 (*Apbb2*)	**I**
AF034580	Mus musculus TSG118.1 (*Tsg118*)	**II**
AW046579	Mus musculus cDNA	**I**
AA738776	Mus musculus cDNA/paraspeckle protein 1 (*Pspc1*)	**I**
AW124334	Mus musculus cDNA	**I**
AW122523	Mus musculus cDNA	**I**
AI837786	Mus musculus cDNA	**I**
AW123286	Mus musculus cDNA	**III**
AA388099	Mus musculus cDNA/DNA segment, Chr 7, Wayne State University 128, expressed (*D7Wsu128e*)	**I**
AW123729	Mus musculus cDNA	**I**
AW050153	Mus musculus cDNA	**I**
AA110657	Mus musculus cDNA	**I**
AI850624	Mus musculus cDNA	**I**
AI507524	Mus musculus cDNA	**I**
AI645050	Mus musculus cDNA	**IV**
AW046694	Mus musculus cDNA	**IV**
AI852578	Mus musculus cDNA	**IV**
AA863742	Mus musculus cDNA	**IV**
AI563623	Mus musculus cDNA	**I**
AW121972	Mus musculus cDNA	**I**
AW046889	Mus musculus cDNA	**I**

Table A.4 continued

AI551347	Mus musculus cDNA	**II**
AI851421	Mus musculus cDNA	**I**
AI837625	Mus musculus cDNA	**I**
***AI852641**	Mus musculus cDNA	**I**
AI850638	Mus musculus cDNA	**I**
AW122811	Mus musculus cDNA	**I**
AI846961	Mus musculus cDNA	**I**
AI838249	Mus musculus cDNA	**I**
AI839901	Mus musculus cDNA	**I**
AI845987	Mus musculus cDNA	**IV**
AW121695	Mus musculus cDNA	**I**
AI839417	Mus musculus cDNA	**I**
AI839803	Mus musculus cDNA	**I**
AA646966	Mus musculus cDNA	**I**
***AI846851**	Mus musculus cDNA	**I**
AA645537	Mus musculus cDNA	**I**
AA667100	Mus musculus cDNA	**III**
AW123347	Mus musculus cDNA	**I**
AW060526	Mus musculus cDNA	**IV**
AW061073	Mus musculus cDNA	**I**
AA796214	Mus musculus cDNA/spindlin (*Spin*)	**I**
AW123983	Mus musculus cDNA	**I**
AW124904	Mus musculus cDNA	**II**
AI853347	Mus musculus cDNA	**I**

Table A.4 continued

AA709728	Mus musculus cDNA	**I**
AW121924	Mus musculus cDNA	**I**
AV171460	Mus musculus cDNA	**IV**
AV229143	Mus musculus cDNA	**IV**
AV232133	Mus musculus cDNA	**II**
AV025111	Mus musculus cDNA	**IV**
AV295044	Mus musculus cDNA	**III**
AV322550	Mus musculus cDNA	**IV**
AV305832	Mus musculus cDNA	**IV**
AV374868	Mus musculus cDNA	**I**
AV334573	Mus musculus cDNA	**I**
AV290470	Mus musculus cDNA	**I**
AA867778	Mus musculus cDNA	**I**
***AW123542**	Mus musculus cDNA	**I**
AI891475	Mus musculus cDNA	**I**
AI842259	Mus musculus cDNA	**I**
AW045233	Mus musculus cDNA	**I**
AI847564	Mus musculus cDNA	**I**
***AI845584**	Mus musculus cDNA	**I**
***AW122310**	Mus musculus cDNA	**I**
AW122897	Mus musculus cDNA	**IV**
AI840579	Mus musculus cDNA/expressed sequence AW550801	**I**
AW107884	Mus musculus cDNA	**I**
AA763918	Mus musculus cDNA	**I**
AI837493	Mus musculus cDNA	**III**

Table A.4 continued

AW060546	Mus musculus cDNA	**I**
AW045204	Mus musculus cDNA	**I**
AW123852	Mus musculus cDNA	**II**
AI661370	Mus musculus cDNA	**I**
AW046443	Mus musculus cDNA	**II**
AW125190	Mus musculus cDNA	**III**
AI837311	Mus musculus cDNA	**I**
AI845886	Mus musculus cDNA	**I**
AW122551	Mus musculus cDNA	**I**
AI849615	Mus musculus cDNA	**I**
AW123801	Mus musculus cDNA	**I**
AA666464	Mus musculus cDNA	**I**
AW122851	Mus musculus cDNA	**I**
***AW046181**	Mus musculus cDNA	**I**
AI843119	Mus musculus cDNA	**I**
AI847879	Mus musculus cDNA	**I**
AW122860	Mus musculus cDNA	**I**
AW124520	Mus musculus cDNA	**I**
AI852534	Mus musculus cDNA	**I**
AW120683	Mus musculus cDNA	**I**
AI850113	Mus musculus cDNA	**I**
AA959180	Mus musculus cDNA	**II**
AI849067	Mus musculus cDNA	**I**
AW124224	Mus musculus cDNA	**I**
AI843709	Mus musculus cDNA	**I**

Table A.4 continued

AW124044	Mus musculus cDNA	**I**
AI836083	Mus musculus cDNA	**I**
AI850362	Mus musculus cDNA	**I**
AW045974	Mus musculus cDNA	**I**
AI835784	Mus musculus cDNA	**I**
AI853476	Mus musculus cDNA	**I**
AI850546	Mus musculus cDNA	**I**
AI843210	Mus musculus cDNA	**I**
AI848453	Mus musculus cDNA	**I**
AI843417	Mus musculus cDNA	**I**
AI851104	Mus musculus cDNA	**I**
AW121624	BC018507: cDNA sequence BC018507	**I**
AW046661	Mus musculus cDNA	**I**
AI838452	Mus musculus cDNA	**I**
AI847050	Mus musculus cDNA	**I**
AA623426	Mus musculus cDNA	**IV**
AI844374	Mus musculus cDNA	**I**
AI843046	Mus musculus cDNA	**I**
AJ130975	Mus musculus cDNA/similar to Ariadne-2 protein homolog (ARI-2) (Triad1 protein) (*HT005*)	**I**
AF093821	Synaptotagmin binding, cytoplasmic RNA interacting	**I**
AA869927	Mus musculus cDNA	**I**
AW050287	Mus musculus cDNA	**I**
AW120722	Mus musculus cDNA	**I**
AW124889	Mus musculus cDNA	**I**
AW061228	Mus musculus cDNA	**II**

Table A.4 continued

AI846519	Mus musculus cDNA	**I**
AW046449	Mus musculus cDNA	**I**
AI854281	Mus musculus cDNA	**I**
AA716963	Mus musculus cDNA	**I**
AI648831	Mus musculus cDNA	**I**
AI854020	Mus musculus cDNA	**I**
AA153773	Mus musculus cDNA	**I**
AV381276	Mus musculus cDNA	**IV**
AI835630	Mus musculus cDNA	**I-II**
AI849453	Mus musculus cDNA	**I**
AI835520	Mus musculus cDNA	**I-II**
AI851081	Mus musculus cDNA	**I**
AI844751	Mus musculus cDNA	**I**
AA638002	Mus musculus cDNA	**I**
AW046160	Mus musculus cDNA	**I**
AI838293	Mus musculus cDNA	**I**
AI842649	Mus musculus cDNA	**I**
AW123507	Mus musculus cDNA	**I**
AI841320	Mus musculus cDNA	**IV**
AI451564	Mus musculus cDNA	**IV**
AI854285	Mus musculus cDNA	**I**
AW124318	Mus musculus cDNA	**III**
AA881294	Mus musculus cDNA	**I**
AI849333	Mus musculus cDNA	**I-II**
AI840458	Mus musculus cDNA	**II**
AI848623	Mus musculus cDNA	**I**

Table A.4 continued

NIH/3T3-specific non-rhythmic genes (N=19)	
AW122331	Mus musculus cDNA
AI847619	Mus musculus cDNA (also AI846570)
AI849354	Mus musculus cDNA
AI841159	Mus musculus cDNA, (*Lcn2*)
AI117848	Mus musculus cDNA
AW121844	Mus musculus cDNA, (*Itm2b*)
AA711915	Mus musculus cDNA, 9130211I03Rik
AV345565	Mus musculus cDNA, 3' end (*Adarb1*)
AI839886	Mus musculus cDNA, (*Apbb1*)
AI851821	G protein beta subunit-like (*Gbl-pending*)
Y18298	CUG triplet repeat, RNA binding protein 2 (*Cugbp2*)
X73580	Secretin (*Sct*)
U55060	Beta-galactoside binding lectin (*Lgals9*)
AF087695	Veli 3/Lin-7 homolog C (*C. elegans*) (*Veli3-pending*)
U36384	Twist-related bHLH protein Dermo-1, (*Twist2*)
AW047343	Mus musculus cDNA (*Dbp*)
AA007891	Mus musculus cDNA
AF039563	Retinoblastoma binding protein (*Rbbp9*)
M77497	Cytochrome P-450 naphthalene hydroxylase (*Cyp2f2*)

Functional categorization of rhythmic (**bold**) genes in NIH/3T3 fibroblasts and of NIH/3T3-specific non-rhythmic (regular) genes. Listed are the GenBank ID, gene descriptor and functional category/cluster assignment for annotated genes and ESTs or genes of unknown function that surpassed expression criteria in NIH/3T3 fibroblasts. Rhythmic genes only expressed in NIH/3T3 cells are denoted by * whereas genes with rhythmic patterns in NIH/3T3 cells, SCN2.2 cells, and the rat SCN are indicated by †.

VITA

Name: Gus John Menger III

Address: Center for Research on Biological Clocks, Department of Biology, Texas A&M University
College Station, Texas 77843

E-mail Address: gmenger@mail.bio.tamu.edu

Education: B.S. Biology, Southwest Texas State University, 1998

Selected Publications:

Menger GJ, Koke JR, and Cahill GM. Diurnal and Circadian Retinomotor Movements in Zebrafish. *Visual Neuroscience* 22: 203-9, 2005.

Menger GJ, Lu K, Thomas T, Cassone VM, Earnest DJ. Circadian profiling of the transcriptome in immortalized rat SCN cells. *Physiological Genomics* 21(3): 370-81, 2005.

Menger GJ, Allen GC, Neuendorff N, Nahm SS,Thomas TL, Cassone VM, and Earnest DJ Circadian Profiling of the Transcriptome in NIH/3T3 Fibroblasts: Comparison with Rhythmic Gene Expression in SCN2.2 Cells and the Rat SCN. *Physiol Genomics* 2007.